Manipulation of Mammalian Cells by Femtosecond Laser Irradiation

HE, Hao

A Thesis Submitted in Partial Fulfillment
of the Requirements for the Degree of
Doctor of Philosophy
in
Electronic Engineering

The Chinese University of Hong Kong

August 2010

ProQuest LLC.
789 East Eisenhower Parkway
P.O. Box 1346
Ann Arbor, MI 48106 - 1346

飛秒激光對哺乳動物細胞的操控

賀號

電子工程課程

哲學博士論文

香港中文大學

2010 年 8 月

ABSTRACT OF THESIS ENTITLED:

Manipulation of Mammalian Cells by Femtosecond Laser Irradiation

Submitted by HE Hao

For the degree of Doctor of Philosophy in Electronic Engineering

at The Chinese University of Hong Kong in December 2010

Biophotonics is an exciting and fast-expanding frontier which involves a fusion of advanced photonics and biology. It has not only developed many novel methodologies for biomedical research, but also achieved significant results as an independent field. Aided with femtosecond (fs) laser technologies, important progresses have been made on manipulating, imaging, and engineering of biological samples from single molecules to tissues in the last 10 years. The laser beam of ultra-short pulses at near-infrared band enjoys a lot of advantages: high nonlinear efficiency, low absorption by biological samples, high spatial and temporal resolution with tight confinement, low photo-toxicity, non-invasive, and ease of control. In this thesis, we report new findings from cell manipulation by fs laser, including transfection, cell-cell fusion, and induction of apoptosis in cells, which are detailed as follows:

1. Transfection is a key technique in cell and molecular biology with many important biochemical applications. We selected a fiber fs laser at 1554 nm, an instrument widely used in optical communication research, as the excitation source. Our results demonstrated that the fs laser could perforate the cell membrane and the hole would close in sub-second interval after the laser exposure. We determined the

safe exposure duration by detecting if there was any sign of mitochondrial depolarization at 1.5 hours after photoporation. Furthermore, we had successfully transfected HepG2 cells with a plasmid DNA containing the GFP gene, whose fluorescence could still be detected 24 hours after exposure. The transfection efficiency was as high as 77.3%. We also observed the proliferation of the transfected cells after 48 hours.

2. Cell-cell fusion is a powerful tool for the analysis of gene expression, chromosomal mapping, monoclonal antibody production, and cancer immunotherapy. One of the challenges of *in vitro* cell fusion is to improve the fusion efficiency without adding extra chemicals while maintaining the cells alive and healthy. We show here that targeted human cancer cells could be selected by an optical tweezer and fused by a finely focused fs laser beam at 1554 nm with a high fusion efficiency. The result confirmed that human cells could be fused exclusively by fs laser pulses, and this is the first time human cells are fused together all-optically. Mixing of cytoplasm in the fused cells was subsequently observed, and cells from different cell lines were also fused. Based on these, we firstly developed the method of optical cell-cell fusion.

3. Failure in the induction of apoptosis or programmed cell death is one of the major contributions to the development of cancer and autoimmune diseases. Here we used a fs laser as a novel method to provide a direct apoptosis trigger to observe dynamic changes at subcellular level during apoptosis. First, we examined the effect of fs laser irradiation on the creation of reactive oxygen species (ROS) in exposed

cells, which could trigger programmed cell death. By controlling the mitochondria electron transport chain (ETC), we investigated the mechanism of ROS generation by the fs pulses, including thermal effect and direct free electron liberation. Second, we induced apoptosis to targeted cells by the fs laser and found that the nuclear envelope (NE) formed tubular or tunnel-like structures (nuclear tubules – NT) inside the nucleus. The average number of NTs in each cell with laser treatment was significantly larger than in the control. Besides, the development of a NT was observed since its inception and it eventually merged with another one to form a larger NT. Meanwhile, mitochondria and tubulin were found inside the NT, and the NT formation always occurred after an upsurge of cellular Ca^{2+} concentration. More DNA fragmentation were also found in the region around the NTs. Based on this, we propose that NTs are developed during apoptosis and mitochondria migrate into the nucleus through the NTs to release death signals to trigger DNA fragmentation. Third, we used the fs laser to induce Ca^{2+} in cells in the form of a slow release, and firstly discovered that most Ca^{2+} was stored in the cytoplasm, and could diffuse into the nucleus after the optical trigger. Using fast confocal scanning, we obtained the path way of Ca^{2+} diffusion after the trigger in different cases. Our findings thus provide a new method of regulating the rate of apoptosis.

摘要

光子生物學是一門由高級光學和生物學的交叉的，令人振奮和快速擴展的前沿科學。它不僅為生物醫學研究開發出了很多新方法，而且作為一門獨立學科，也取得了令人矚目的結果。在過去的 10 年裏，通過飛秒雷射技術的輔助，在從單分子到組織量級的成像、操控、和生物工程領域取得了一系列進展。近紅外波段的超短脈衝具備很多優點：高非線性效率，生物樣品對它的低吸收率，高空間和時間解析度，低毒性，潔淨，非侵入，和可控。在本文中，我們報導了一些細胞操控的新發現，包括用飛秒鐳射產生的轉基因，細胞融合，和細胞凋亡。以下是它們的詳細介紹：

1 轉基因是讓原本無法穿透細胞膜的分子，如 DNA，穿越細胞膜而在細胞內表達相應蛋白質的一個過程。它是細胞生物學和分子生物學的一項核心技術，具有很多重要的生物醫學應用。我們採用了在光通信領域廣泛使用的波長在 1554nm 的光纖飛秒雷射器，作為激發源。我們的結果表明，這種飛秒鐳射可以在細胞膜上開孔，而細胞膜也可以在曝光後一秒之內再次恢復。我們通過對線粒體的膜電壓的測量來決定了安全的曝光時間。此外，我們成功地把綠色螢光蛋白 GFP 的 DNA 轉基因到人體肝癌細胞 HepG2 中，並在曝光之後的 24 小時後檢測到了 GFP 的表達。轉基因的效率達到了 77.3%。我們也觀測到了轉基因細胞在 48 小時後的繁殖。

2 細胞融合是一種分析基因表達，染色體定位，單克隆抗體生成，和癌症免疫治療的有力的工具。在體外細胞融合的一個難點是如何提高融合效率，而

同時不引入多餘的化學藥物，並保持細胞活性和健康。我們發現，人體癌症細胞可以被光鑷自由挑選移動，然後被波長為 1554nm 的飛秒光融合，融合效率相對較高。我們的結果表明，人體細胞可以僅由飛秒鐳射來產生融合，而這也是人體細胞第一次由全光技術融合。我們也觀察到了融合之後細胞的細胞質之間的混合。此外，我們也做到了不同株之間的細胞交叉融合。在此基礎上，我們系統地做出了全光細胞融合的方法。

3 細胞凋亡的失敗是癌症和自免疫疾病的主要原因之一。我們使用飛秒鐳射作為一種激發細胞凋亡並在小於細胞的尺度上觀測細胞凋亡變化動態的新方法。首先，我們測量了飛秒鐳射在被曝光的細胞中產生活性氧化物（ROS）的效果，而 ROS 可以出發細胞凋亡。通過控制線粒體的電子傳輸鏈，我們研究了飛秒光產生 ROS 的機理，包括熱效應和直接產生自由電子。其次，我們用飛秒光來觸發細胞凋亡，發現細胞核的核膜在細胞核內形成了管狀或通道狀結構。在鐳射處理過的細胞中，核管的平均數量顯著高於未被處理的對照組。此外，核管的動態發展過程也被觀測到，並且記錄了它與另一個核管融合而形成一個更大核管的過程。同時，線粒體和微管蛋白也在核管中被發現。而在核管的形成過程總是在細胞內鈣離子濃度的顯著上升之後。在核管周圍的區域裏，更多的 DNA 碎片也被發現。在此基礎上，我們提出核管是在凋亡過程中形成，線粒體會通過核管遷移到細胞核中來釋放 DNA 碎片的信號。第三，我們使用飛秒鐳射來觸發細胞的鈣離子的緩慢增長，首次發現鈣離子主要儲存於細胞質中，並且在光激發後可以擴散到細胞核中。使用快速共聚焦掃描，我們獲得了鈣離子擴散的路徑。我們的發現提供了一個研究細胞凋亡過程的新方法。

Acknowledgements

It is very difficult to overstate my gratitude to those people who have been helping me so much during my 4-year PhD study in the Chinese University of Hong Kong. I want to take this opportunity to present my sincere thanks to them.

At first, I want to express my special thanks to my supervisor, Prof. K.T. Chan, who shared with me a lot of his expertise and research insight. I really appreciate his great ideas, helpful suggestions, constant encourages, and supports to me. He taught me a lot on researches and the way of thinking as a PhD. His passion on research encouraged me to work on Biophotonics, and we worked hard together to build a research platform and got many results. He gave me a lot of useful suggestions, analyzed problems we faced, and aimed the direction we should go. He becomes for me the role model of a successful researcher in the field.

I really want to thank Prof. S.K. Kong as much as possible. Without his supports and helps, I would not have got understood so much on biology. It is really my fortune to work in Prof. Kong's lab for 4 years. Prof. Kong shared with me his expertise on biochemistry and a lot of experimental supports. He teaches me a lot on cell biology, and we have many useful discussions on my researches, where many ideas are created. Prof. Kong is very kind, nice, and patient and I have passed a quite happy 4-year period with him.

I want to thank Prof. H.P. Ho for his kind helps and supports to me for supporting me with the confocal microscope. Without that I would have not been able to do a lot of experiments.

I wish to express my appreciation to Prof. J.F. Wang from the Dept. of Physics, and Prof. B. Zheng from the Dept. of Chemistry for their helpful suggestions and their kind collaborations with our group.

I want to thank Prof. L. Jin (Shenzhen Institutes of Advanced Technology) for his kind helps to me when I know nothing about Biophotonics. He taught me a lot on microscope and research techniques. I also want to give my special thanks to Prof. M.L. Hu from Tianjin University. He is very kind and helped us to build up a new fiber laser for my further research. He had a lot of wonderful discussions with me and taught me a lot on lasers and research methods.

I want to thank Prof. D.P. Tsai from National Taiwan University for his kind support for my visit to his lab. It is happy for me to work there and we had some good discussions. I studied a lot from his group and hope we can have a good collaboration.

I would like to express my thanks to Ms. L.C. Ho. She helped and taught me a lot during my lab period. I want to thank Dr. Y.H. Luo, Dr. K.J. Chen, Mr. Z.X. Zhang, Miss. M.Y. Chen, and Mr. Z.L. Ma for their helps to me in our group. Especially I want to thank Miss J.J. Liu for her great help on the fs laser maintenances. Besides, I want to thank Dr. C.M. Sun, Dr. X.Lin, Dr. T. Yang, Mr. X. Chen, Mr. Y.H. Dai, Mr. J.B. Du, Mr. L.K. Cheng, Mr. L. Wang, Mr. C. Wong, Mr. K. Lei, and all other members in our lab.

I would like to thank Dr. Y.K. Suen, Dr. K.Y. Lee, Ms. Irene Lau, Ms. W. Qian, Ms. Alice Yang and all other members in the lab of Prof. Kong. They gave me great helps for the biological technical support. Special thanks to Ms. Lau for her cells every week. I also want to thank Mr. H.J. Chen from the Dept. of Physics for his kind fabrication of gold nanorods for me.

Besides, I want to thank all the friends in the Chinese University of Hong Kong.

Finally, I want to thank my parents. They encourage and support me all the time. With their deep love, I can finish my PhD study and now thank them by this thesis.

Thank you all!

Table of Contents

List of Tables and Figures

List of Abbreviations

CW	continuous wave
DHE	dihydroethidium bromide
ER	endoplasmic reticulum
ETC	mitochondrial electron transport chain
FI	fluorescence intensity
FS	femtosecond
GFP	green fluorescence protein
GNR	gold nanorod
MMP	mitochondrial membrane permeabilization
MPI	Multi-photon ionization
NA	numerical aperture
NE	nuclear envelope
NIR	near infrared
NT	nuclear tubule
RI	refractive index
SESAM	semiconductor saturable absorber mirror
SM	single mode
SPM	self-phase modulation
TBPW	time-bandwidth product

Chapter 1: Introduction

1.1 Introduction to Biophotonics

Biophotonics is a fast developing science combining with photonics and biology, which has been being applied in many fields such as biology, biochemistry, molecular biology, medicine, agriculture, and environmental science. It is not only research tools and methodologies of biology, but an independent field attracting more and more attentions all over the world. With great progresses of laser technologies in last 20 years, significant results have been made, and a lot of fields have been developed in this science, as shown in Fig. 1-1 [1].

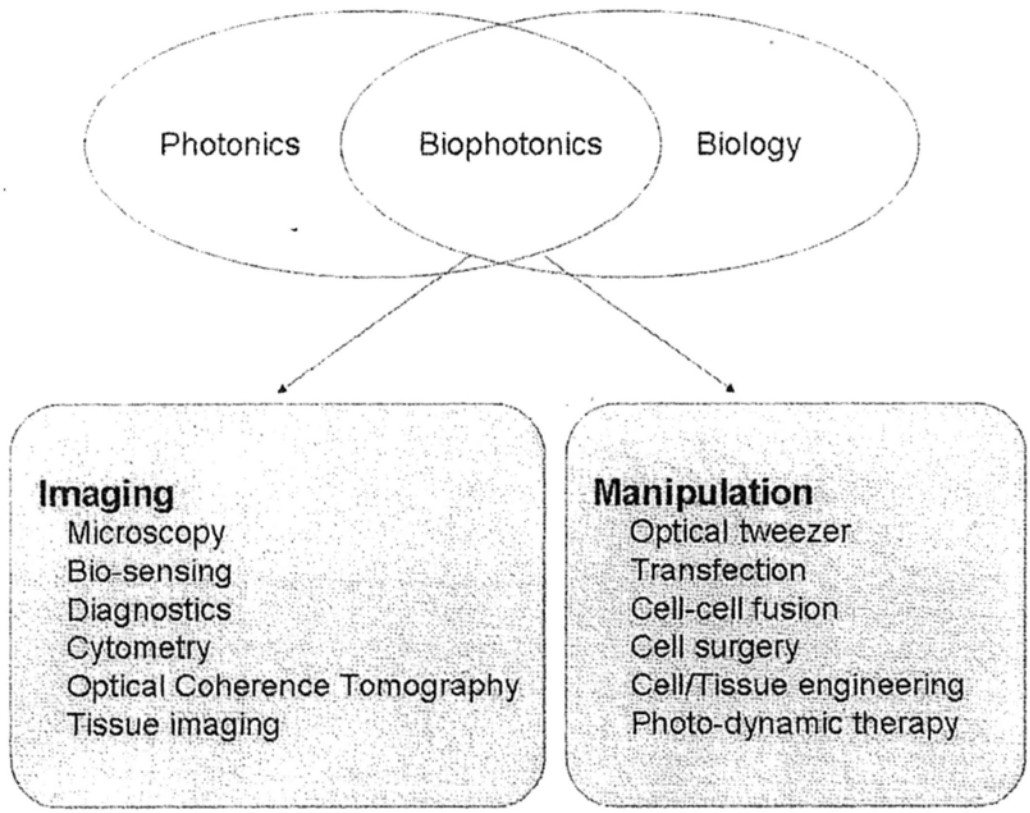

Fig. 1-1. The contents of Biophotonics: Imaging and Manipulation.

Generally speaking, Biophotonics can be divided into two directions, imaging and manipulation. A lot of imaging methods have been developed and used for many years. Based on normal trans-illuminating microscope and aided by lasers, inverted, fluorescent, confocal scanning [2], and near field microscopes [3] have been quite widely used for daily researches. Fluorescence is the most important bridge between the micro- and real world. Almost all imaging methods are based on the fluorescence excitation and detection. Total internal reflection fluorescence (TIRF) [4], fluorescence resonance energy transfer (FRET) [5], fluorescence recovery after photo-bleaching (FRAP) [6], fluorescence coherence spectroscopy (FCS) [7], fluorèscence lifetime imaging microscopy (FLIM) [8] and cytometry [9] are direct fluorescent imaging methods. Cytometry has been quite developed and widely used in biology and bio-statistics.

With pulsed lasers, especially femtosecond (fs) lasers, multi-photon microscopy (MPM) [10] and some other nonlinear imaging methods like second harmonic generation (SHG) [11] are more and more important optical imaging method to get the ultra high resolution at both space and time dimension. Some far-field optical imaging methods can even get the resolution at tens of nanometers or single molecule level, such as STORM and STED [12, 13].

Imaging for cancer diagnostic is also very attractive, which is mainly based on special fluorescence spectrum. Auto-fluorescence imaging (AFI) [14] and Raman spectrum of some cancer cells [15] have been measured and the differences with normal cells have been confirmed in laboratories. Coherent anti-Stokes Raman

scattering (CARS) [16] has been developing very fast as a nonlinear diagnostic method. Since photons in the near infrared (NIR) range have a much better propagation property in tissue, such methods by NIR lasers are developing very fast for in vivo tissue imaging. Optical coherence tomography (OCT) [17] is another very important method for tissue imaging, and it can reach the deepest distance in tissue.

Optical imaging method is the 'eye' for human to observe biological samples, and manipulation is the 'hand' to operate on them. Arthur Ashkin pioneered the field of laser-based optical trapping in 1980s [18, 19]. In a series of seminal papers, he demonstrated that optical forces could displace and levitate micron-sized dielectric particles in both water and air. It has come to be known when Ashkin and co-workers employed optical trapping in a wide-ranging series of experiments from the cooling and trapping of neutral atoms to manipulating live bacteria and viruses. Optical tweezers were developed quite fast to control, trap, and move particles like cells, polymer beads, and even single macro molecules (such as DNA) [20]. A lot of techniques have been combined with optical tweezers, especially holography, which can control the distribution of laser beam intensity.

After controlling of the targeted cells, pulsed lasers, especially the fs lasers, have been used to operate on cells like scissors, knives, and injectors [21]. Surgeries at the level of micron can be done under microscope with no invasive contact with cells [22]. Transfection [23], cell-cell fusion [24], and sub-cellular operations [25] have been developing very fast, providing lots of alternative methods to the

traditional biological engineering. The lasers also work as special stimulations to biological samples, to research sub-cellular dynamics instead of chemical and mechanical stimuli [26]. In the field of cancer researches, lasers play now not only a role of diagnostics, but also supplying methods of therapy, for example, photodynamic therapy is a very promising method [27]. Fundamental biological researches such as gene engineering [28], apoptosis (programmed cell death) [29], and anti-body analyzing [30], also involve lasers more and more. Biophotonics has been attracting attentions all over the world and making progresses at every moment.

1.2 Optical manipulation of mammalian cells

Traditionally, there are a lot of methods to manipulate cells, mostly by mechanical equipments [31], chemicals [32], and biological approaches [33]. For example, micro-manipulator has been used to control and move cells for many years, which needs a very sharp tip or a couple of metal tip to trap cells. Indeed, such a setup is very expensive, complicated, huge, and difficult to operate. What is the worse is that the tip needs mechanical contact with cells [34]. Possible contamination and mechanical harm to cells are two severe problems.

A. Ashkin and his co-workers introduced optical tweezer, which originally is used to trap and cool atoms, to manipulate cells in media [18]. By focusing a single laser beam onto the targeted cell, it can be trapped in the laser focus. The trapping force is formed by the momentum change of photons, which needs to conditions: 1) the object has a different refractive index (RI) with the media; 2) the laser intensity has a radial gradient distribution. The resulting force will point to the maximum intensity spot, the center of the laser focus. The principle of optical tweezer can be simply demonstrated by Fig. 1-2 [19].

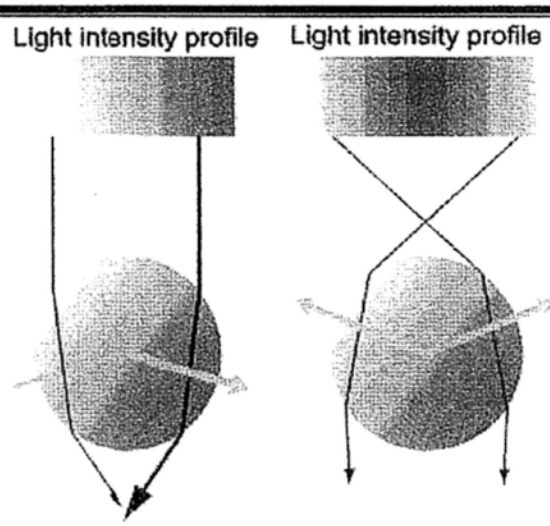

Fig. 1-2. The principle of optical tweezers. If a transparent bead is illuminated by a parallel beam of light with an intensity gradient increasing from left to right [19]. Two representative rays of light of different intensities (represented by black lines of different thickness) from the beam are shown. The refraction of the rays by the bead changes the momentum of the photons, equal to the change in the direction of the input and output rays. Conservation of momentum dictates that the momentum of the bead changes by an equal but opposite amount, which results in the forces depicted by gray arrows. The net force on the bead is to the right, in the direction of the intensity gradient, and slightly down. However, to form a stable trap, the light must be focused, producing a three-dimensional intensity gradient. In this case, the bead is illuminated by a focused beam of light with a radial intensity gradient. Two representative rays are again refracted by the bead but the change in momentum in this instance leads to a net force towards the focus. Gray arrows represent the forces. The lateral forces balance each other out and the axial force is balanced by the scattering force (not shown), which decreases away from the focus. If the bead moves in the focused beam, the imbalance of optical forces will draw it back to the equilibrium position.

Technically, considering the small difference of RI between cells and water, the numerical aperture (NA) of the objective should be very high, usually larger than 1 [35]. The laser power has also a requirement, depending on different cells. However, if the laser power is too high, optical harm to cells is also a problem.

Lasers also have side effects on cells. When the wavelength is short, like, the visible range, the energy of photons is relatively high, very easy to be absorbed by proteins in cells to cause harm. The absorption spectrum by some important proteins in cells is shown as in Fig. 1-3 (a) [36]. The scattering of visible or even ultra violet (UV) is also very large, according to Rayleigh's law, promoting photon absorption. In the contrast, if the wavelength is as long as in the IR range, such as 1600 nm, there will be little cellular scattering and absorption, but the absorption by water will be quite high and the thermal effect will affect cells a lot, as shown in Fig. 3 (b). And thus, the NIR range in 700-1100 nm, which has very little absorption coefficient of water and very low photon energy, resulting in quite transparence to both cells and water, is called the "optical window". Most interactions between the laser beam and cells can be thus confined inside the laser focus to prevent cells from photo-damage.

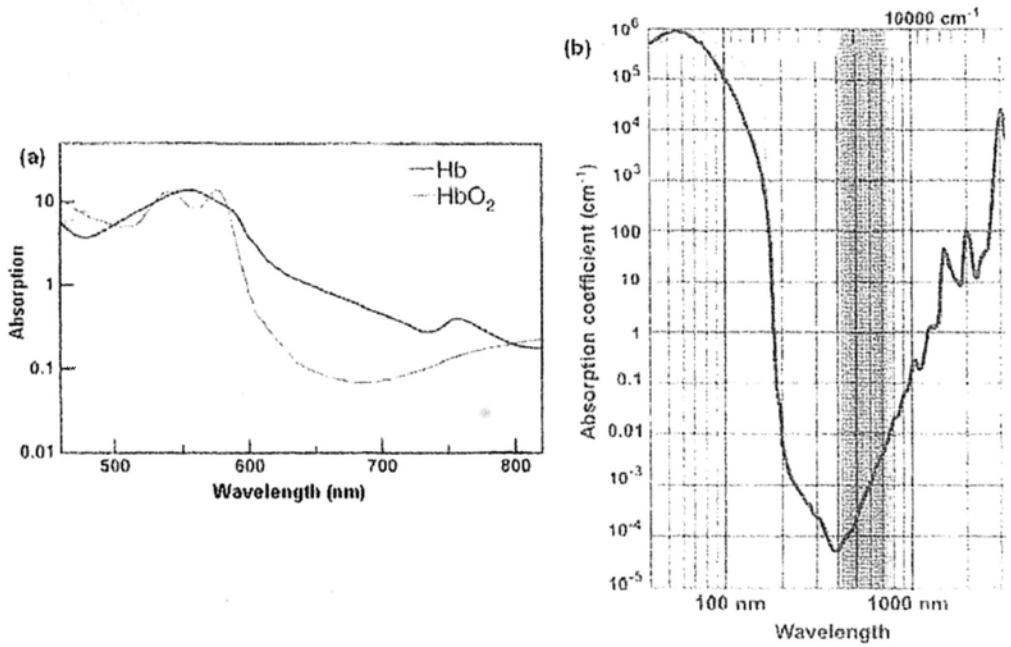

Fig. 1-3. Absorption spectrum of biological materials. (a) The absorption spectrum of Hb and HbO2, which are important proteins in cells. (b) The absorption spectrum of water.

Continuous wave (CW) lasers in such a range thus are relatively safe to cells when they illuminate cells to trap and move them for seconds. However, since the CW laser power works at only some hundreds mW, the application is quite limited except tweezers, and at that power level, the thermal effect of the laser beam is a severe problem to cells. The temperature in the focus can reach tens of degrees and diffuse away and influence an area in hundreds of microns. To get higher photon density with compromising to the mean power, pulsed lasers were considered to extend the interaction between photons and cells while produce little harm to them. But pulses longer than about 10 μs a stationary temperature distribution similar to that produced by continuous-wave (cw) irradiation evolves around the laser focus [37]. It was demonstrated that pulsed laser microdissection relies on plasma

formation supported by linear absorption, and that this is associated with violent mechanical effects (shock-wave emission and cavitation bubble formation) reaching well beyond the region of energy deposition [38, 39]. Pulse energies in the microjoule range typical for nanosecond laser microbeams, which means, the photon density in the focus at the peak of the pulse is around $10^7 \sim 10^{10}$ W cm^{-2}, can therefore severely affect the cell viability.

With the advent of fs laser technology, due to the ultra-short pulse, if the NA of the objective is large enough (usually >1), the photon density at the peak of the pulse can reach a level of more than 10^{12} W cm^{-2}, and thus most interactions are based on nonlinear absorption [40]. Then, fs pulses exhibit a much weaker dependence on the absorption coefficient of the target material but mostly relative with the optical parameters of the laser itself, if which is high enough to introduce the nonlinear absorption. In this way, the laser effects are very finely confined in the focal volume, whose spatial extent is below the optical diffraction limit [41] as shown in Fig. 1-4.

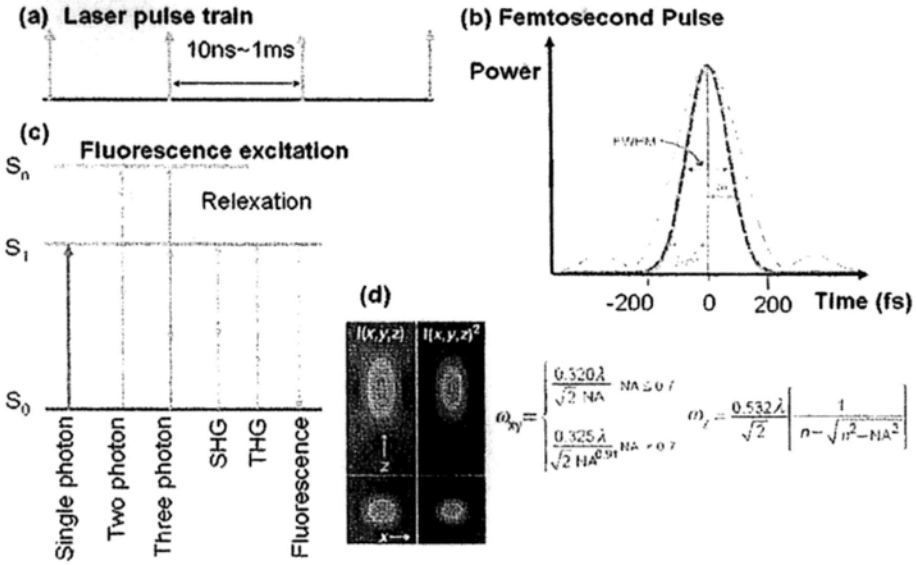

Fig.1-4. Femtosecond laser pulses for fluorescence excitation. (a) Typical fs pulse train. (b) Typical fs pulse. Dashed red line: original intensity distribution of a pulse. Solid red line: square of the original intensity distribution. (c) fluorescence excitation by several methods. (d) spatial optical intensity distribution after focus.

Inside the fs pulse, the ultra-high power (>10^{12} W cm^{-2}) can excite electrons in most molecules directly to be free. Such plasma-formation can thus work as a kind of optical knife to operate on cells. This has been demonstrated in chromosomes [42], various other cell organelles [43, 44], small organisms [45, 46], and even tissues [47, 48]. And when the beam is focus on cell membrane, the pulses can open the membrane by disrupting the lipid, resulting free molecule exchange between the cytoplasm and the environment. Thus, optical transfection and cell-cell fusion can be performed based on this effect [23]. Currently, fs lasers have been one of the most important tools of Biophotonics, and now widely used for both imaging and manipulation of cells, making quite a lot of significant results. Such ultra-short

pulses provide a lot of advantages: high nonlinear efficiency, low absorption by biological samples, high spatial and temporal resolution and confinement, low photo-toxicity, clean, non-invasive, and controllable.

1.3 Organization of the thesis

The structure of this thesis is arranged as follows:

In Chapter 1, a simple introduction of Biophotonics is introduced. The structure of Biophotonics is analyzed, and a brief introduction to the application is also given. The concept of manipulation is explained, and advantages of fs lasers at NIR range is briefly presented for the following works.

In Chapter 2, some basic concepts and structures of mammalian cells are described, following by the working principle of fs laser. Interactions between fs pulses and cells are analyzed with details. The nonlinear process of multi-photon absorption is analyzed with a simplification that the materials in cells are treated as H_2O molecules. Properties of the fs pulses, including plasma formation, thermal effects, and implication confinement are briefly explained.

In Chapter 3, the development of transfection is introduced, and different methods of transfection are compared. We developed an optical transfection approach by a fiber fs laser at 1554 nm. Our results demonstrated that the fs laser could perforate cell membrane and the hole would close in sub-second interval after the laser exposure. We determined the safe exposure duration by detecting if there was any sign of mitochondrial depolarization at 1.5 hours after photoporation. Furthermore, we had successfully transfected HepG2 cells with a plasmid DNA containing the GFP gene, whose fluorescence could still be detected 24 hours after

exposure. The transfection efficiency was as high as 77.3%. nanorods, automatic transfection.

Chapter 4 presents the further work, cell-cell fusion, based on the same mechanism of fs pulses and cell membrane, but with much more complicated interactions between membrane and the control of multi-cells. We show here that targeted human cancer cells could be selected by an optical tweezer and fused by a finely focused fs laser beam at 1554 nm with a high fusion efficiency. This is the first time human cells are fused together all-optically. Mixing of cytoplasm in the fused cells was subsequently observed, and cells from different cell lines were also fused. Based on these, we propose the mechanism of such a process.

However, fs lasers can harm cells during such processes, and can work as a kind of apoptosis stimulation. In Chapter 5, we used a fs laser as a novel method to provide a direct apoptosis trigger to observe dynamic changes at subcellular level during apoptosis. First, we examined the effect of fs laser irradiation on the creation of reactive oxygen species (ROS) in exposed cells, which can trigger programmed cell death. By controlling the mitochondria electron transport chain (ETC), we investigated the mechanism of ROS generation by the fs pulses, including thermal effect and direct free electron liberation. Second, we induced apoptosis to targeted cells by the fs laser and found that the nuclear envelope (NE) forms tubular or tunnel-like structures inside the nucleus. The average number of NTs in each cell with laser treatment is significantly larger than the control. Besides, the development of a NT was observed and it eventually merged with another one to

form a larger NT. Meanwhile, mitochondria and tubulin were found inside the NT, and the NT formation always occurs after an upsurge of cellular Ca^{2+} concentration. More DNA fragmentation were also found in the region around the NTs. Based on this, we propose that NTs are developed during apoptosis and mitochondria migrate into the nucleus through the NTs to release death signals to trigger DNA fragmentation. Third, we induced subcellular Ca^{2+} release by femtosecond laser exposure in Ca^{2+}-free media and PBS with Ca^{2+} channels in cell membrane blocked, and observed its propagation by confocal scanning. It was found Ca^{2+} store volume in cytoplasm is significantly more than in nucleus, and Ca^{2+} will diffuse into nucleus after trigger. Ca^{2+} release inside nucleus can also influence Ca^{2+} in cytoplasm. Our findings thus provide a new method of regulating the rate of apoptosis.

Chapter 6 gives a summary on the whole work. Potential and current applications of related techniques are introduced, and some important works from other groups are also introduced. Then we propose some future works based on current results.

References

1. P. N. Prasad, Biophotonics, New York: Wiley-Interscience, 2003.
2. G. Bkaily, P. Pothier, P. D'Orléans-Juste, M. Simaan, D. Jacques, D. Jaalouk, F. Belzile, G. Hassan, C. Boutin, G. Haddad, and W. Neugebauer. The use of confocal microscopy in the investigation of cell structure and function in the heart, vascular endothelium and smooth muscle cells, Molecular and Cellular Biochemistry, 1997, 172(1): 171-194.
3. B. Hecht, B. Sick, U. P. Wild, V. Deckert, R. Zenobi, O. J. F. Martin, and D. W. Pohl. Scanning near-field optical microscopy with aperture probes: Fundamentals and applications, Journal of Chemical Physics, 2000, 112(18): 7761-7774.
4. D. Axelrod. Total internal reflection fluorescence microscopy in cell biology, Traffic, 2001, 2(11): 764-774.
5. Elizabeth A Jares-Erijman & Thomas M Jovin, FRET imaging Nature biotechnology, 21, pp1387 - 1395 2003
6. Eric A.J. Reits and Jacques J. Neefjes, From fixed to FRAP: measuring protein mobility and activity in living cells, NATURE CELL BIOLOGY, 3, E145, 2001.
7. Keith M. Berland, Peter T. C. So, and Enrico Gratton, Two-Photon Fluorescepce Correlation Spectroscopy: Method and Application to the Intracellular Environment, Biophysical Journal Volume 68 February 1995 694-701

8. Erik B. van Munster and Theodorus W. J. Gadella, Fluorescence Lifetime Imaging Microscopy (FLIM), Advances in Biochemical Engineering/Biotechnology, 95, 143-175, 2005

9. Dr. Z. Darzynkiewicz, S. Bruno, G. Del Bino, W. Gorczyca, M. A. Hotz, P. Lassota, F. Traganos, Features of apoptotic cells measured by flow cytometry, Cytometry Part A, Volume 13 Issue 8, Pages 795 - 808. 2004

10. WR Zipfel, RM Williams, WW Webb, Nonlinear magic: multiphoton microscopy in the biosciences, Nature Biotechnology, 21, 1369. 2003

11. L Moreaux, O Sandre, J Mertz, Membrane imaging by second-harmonic generation microscopy, J. Opt. Soc. Am. B, 17, 1685, 2000.

12. M. J. Rust, M. Bates, X. Zhuang, "Sub-diffraction-limit imaging by stochastic optical reconstruction microscopy (STORM)", Nature Methods 3, 793-795 (2006)

13. Katrin I. Willig, Silvio O. Rizzoli, Volker Westphal, Reinhard Jahn & Stefan W. Hell, STED microscopy reveals that synaptotagmin remains clustered after synaptic vesicle exocytosis, 440, 935, 2006.

14. Giovanni Bottiroli and Anna Cleta Croce, Autofluorescence spectroscopy of cells and tissues as a tool for biomedical diagnosis, Photochem Photobiol Sci. 2004; 3(11-12):189-210.

15. Zhiwei HUANG, Annette MCWILLIAMS, Harvey LUI, David I. MCLEAN, Stephen LAM and Haishan ZENG, NEAR-INFRARED RAMAN SPECTROSCOPY FOR OPTICAL DIAGNOSIS OF LUNG CANCER, Int. J.

Cancer: 107, 1047–1052 (2003)

16. A Zumbusch, GR Holtom, XS Xie, Three-Dimensional Vibrational Imaging by Coherent Anti-Stokes Raman Scattering, Phys. Rev. Lett. 82, 4142–4145. 1998.
17. D Huang, et. al, Optical coherence tomography, Science, 254, 1178-1181, 1991.
18. Ashkin, A., Dziedzic, J. M., Bjorkholm, J. E. & Chu, S. Observation of a single-beam gradient force optical trap for dielectric particles. Opt. Lett. 11, 288-290 (1986).
19. Ashkin, A. History of optical trapping and manipulation of small-neutral particle, atoms, and molecules. IEEE J. Sel. Top. Quantum Elec. 6, 841–856 (2000).
20. David G. Grier, A revolution in optical manipulation, NATURE, 424, 810. 2003
21. Berns, MW, Tadir, Y., Liang, H. & Tromberg, B. Laser scissors and tweezers. Methods Cell Biol. 55, 71–98 (1998).
22. K König, laser tweezers and multiphoton microscopes in life science, Histochemistry and Cell Biology, 114, 79-92, 2000
23. U. K. Tirlapur and K. Konig, "Targeted transfection by femtosecond laser," Nature **418**, 290-291 (2002).
24. Jixian Gong *et al.* Femtosecond laser-induced cell fusion, *Applied Physics Letters*, **92**, 093901 (2008)
25. Wataru Watanabe, Naomi Arakawa, Sachihiro Matsunaga, Tsunehito Higashi, Kiichi Fukui, Keisuke Isobe, and Kazuyoshi Itoh, Femtosecond laser disruption of subcellular organelles in a living cell, Optics Express, Vol. 12, Issue 18, pp.

4203-4213 (2004)

26. Uday K. Tirlapur, Karsten König, Christiane Peuckert, Reimar Krieg and Karl-J. Halbhuber, "Femtosecond Near-Infrared Laser Pulses Elicit Generation of Reactive Oxygen Species in Mammalian Cells Leading to Apoptosis-like Death," Experimental Cell Research, 263, 88-97 (2001).
27. THOMAS J DOUGHERTY. A Brief History of Clinical Photodynamic Therapy Development at Roswell Park Cancer Institute. Journal of Clinical Laser Medicine & Surgery. OCTOBER 1996, 14(5): 219-221.
28. Uchugonova Aisada; König Karsten; Bueckle Rainer; Isemann Andreas; Tempea Gabriel, Targeted transfection of stem cells with sub-20 femtosecond laser pulses. Optics express 2008;16(13):9357-6
29. Wihelma Echevarr, et al., Nature Cell Biology, 5, 440-446, 2003
30. Rika A. Furuta, Masao Nishikawa and Jun-ichi Fujisawa. Microbes and Infection, 8, 520-532 (2006).
31. M.R. Capecchi, "High efficiency transformation by direct microinjection of DNA into cultured mammalian cells", Cell, vol. 22, pp479–488 (1980)
32. David J. Stephens and Rainer Pepperkok, "The many ways to cross the plasma membrane", PNAS, vol. 98 pp4295–4298 (2001)
33. M.K. Chuah, D. Collen, T. VandenDriessche, "Biosafety of adenoviral vectors", Curr. Gene Ther. Vol. 3 pp527– 543 (2003)
34. Celis, J. E. Brookhaven Symp. Biol. Vol. **29**, pp178–196 (1978)
35. Keir C. Neuman and Steven M. Block, Optical trapping, Rev. Sci. Instrum., Vol.

75, 2787. 2004

36. George Zonios, Julie Bykowski and Nikiforos Kollias, Skin Melanin, Hemoglobin, and Light Scattering Properties can be Quantitatively Assessed In Vivo Using Diffuse Reflectance Spectroscopy, Journal of Investigative Dermatology (2001) 117, 1452–1457
37. A. Vogel, J. Noack, G. Hüttman, and G. Paltauf, Applied Physics B: Lasers and Optics 81, 1015 (2005).
38. V. Venugopalan, A. Guerra, K. Nahen, A. Vogel, Phys. Rev. Lett. 88, 078 103 (2002)
39. K. Lorenz, Mechanismen des Katapultierens biologischer Strukturenmit UV-Laserpulsen, Diploma Thesis, University of Applied Science Lübeck (2004)
40. J. Noack, A. Vogel, IEEE J. Quantum Electron. 35, 1156 (1999)
41. A. Vogel, J. Noack, K. Nahen, D. Theisen, S. Busch, U. Parlitz, D.X. Hammer, G.D. Nojin, B.A. Rockwell, R. Birngruber, Appl. Phys. B 68, 271 (1999)
42. K. König, I. Riemann, W. Fritsche, Opt. Lett. 26, 819 (2001)
43. A. Heisterkamp, I.Z. Maxwell, E. Mazur, J.M. Underwood, J.A. Nickerson, S. Kumar, D.E. Ingber, Opt. Express 13, 3690 (2005)
44. L. Sacconi, I.M. Tolic-Norrelyke, R. Antolini, F.S. Pavone, J. Biomed. Opt. 10, 014 002 (2005)
45. M.F. Yanik, H. Cinar, H.N. Cinar, A.D. Chisholm, Y. Jin, A. Ben-Yakar, Nature 432, 822 (2004)

46. W. Supatto, D. Dèbarre, B. Moulia, E. Brouz´es, J.-L. Martin, E. Farge, E. Beaurepaire, Proc. Natl. Acad. Sci. USA 102, 1047 (2005)

47. K. König, O. Krauss, I. Riemann, Opt. Express 10, 171 (2002)

48. I. Riemann, T. Anhut, F. Stracke, R. Le Harzic, K. König, Proc. SPIE 5695, 216 (2005)

Chapter 2: Biophotonics with Femtosecond Laser

2.1 Working principle of fs lasers

2.1.1 Ti: Sapphire laser

The Ti: sapphire laser has achieved a great deal of success in applications due to a variety of factors since the first report of a Kerr Lens mode- locked system in the early 1990s [1]. The operation of Ti: sapphire is generally limited to the 700–1000 nm, which is relatively highly penetrating into tissue but causes low amounts of damage by absorption of biological materials. When working for the nonlinear two-photon excitation geometry, it is readily absorbed by a wide range of common fluorophores and other materials. Thus Ti: sapphire lasers have been quite widely used for Biophotonics, especially for nonlinear imaging of biological samples.

The key principle of Ti: sapphire laser is Kerr Lens mode locking, which is based on spatial Kerr effect, resulting in self focusing of the beam. Consider a pulse propagating through a nonlinear material. The pulse will typically have a Gaussian spatial gain profile; hence, the centre of the beam will have a higher intensity than the edges. In the presence of the Kerr effect, the centre of the pulse will be subject to a greater nonlinear refractive index within the Kerr medium than the edges. The phase velocity of the wavefront will be less at the centre of the pulse than at the edges. Thus, in effect, a weak positive lens is induced within the medium and the

beam becomes focused, Fig. 2-1. This self-focusing or induced lens effect is known as a Kerr lens.

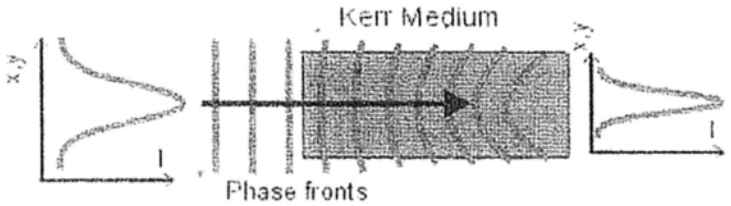

Fig. 2-1. The self-focusing of an intense laser beam propagating through a Kerr medium.

A typical structure of Ti:sapphire laser is shown as in Fig. 2-2. It has a wide gain bandwidth, capable of supporting many modes of oscillation simultaneously, between which mode beating occurs and produces self-amplitude modulation of the CW output. Primitive pulses can arise, from the modulation of the CW output, of sufficient intensity to induce the Kerr effect within the gain medium. The resulting Kerr lens and SPM change the spatial and spectral profile of the beam by self-focusing, thus changing the profile from that of the CW beam. The modulated beam profile can be made smaller than that of the CW beam by suitable configuration of the laser cavity elements. Then insertion of an aperture into the cavity causes increased losses to only the CW beam, thus favoring pulsed operation and allowing a train of pulses to build. The aperture used may be 'hard' or 'soft'. Hard-aperture mode locking uses a physical aperture to discriminate against the CW mode. Soft-aperture mode locking occurs when the laser is configured so that the pulsed mode experiences greater overlap with the pump beam in the laser crystal than the CW mode, and therefore experiences higher gain.

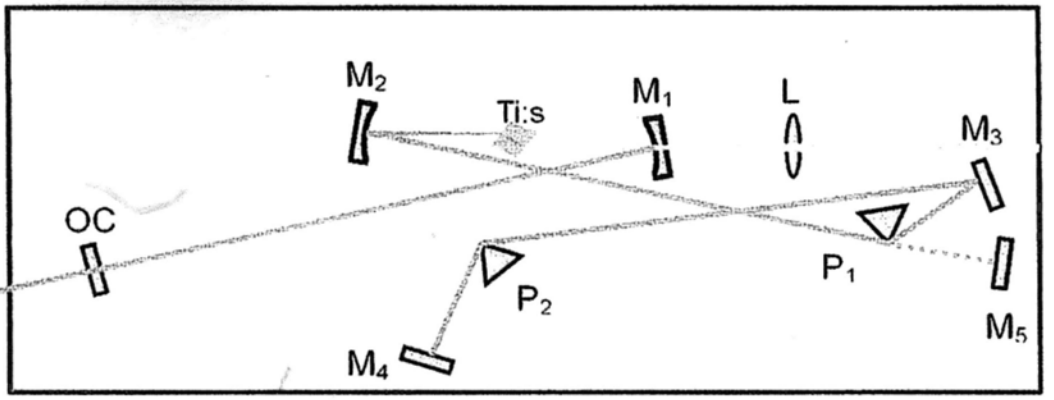

Fig. 2-2. Setup of Ti:sapphire oscillator with prism pair for dispersion compensation. L: focusing lens, to focus the pump laser to the crystal. M1, M2, plane-concave mirror to construct a cavity. M3, M4, M5, plane mirror. OC, Output coupler. P1, P2, Brewster angle cut prism dispersion compensation. The pumping laser from M1 into the cavity is usually a high power CW laser.

Kerr lens mode locking lasers require a primitive pulse of sufficient intensity to initiate the mode locked pulse sequence. This doesn't spontaneously occur from CW operation which means that Kerr lens mode locking is generally not self-starting. Some form of action is required to initiate Kerr lens mode locking, be it a genuine pulse or a noise spike. The easiest way to do this is to produce a sudden change in cavity length by tapping an end mirror, which causes an intense amplitude fluctuation to occur.

The output of Ti: sapphire laser is usually ranging from 700 nm to 1000 nm, with repetition rate around 40 to more than 80 MHz. The average power can be as high as some watts, with the pulse width only around 100 fs. Thus the peak power of each pulse is very high. The temporal and the spectral bandwidth of the pulse has a following relationship. The product of the pulse width and the spectral width (bandwidth) is called the time-bandwidth product (TBWP), which has a defined

minimum value. If the TBWP is equal to this minimum value, the pulses are transform-limited and assuming a Gaussian pulse shape, the temporal and spectral widths are related by the equation following:

$$\Delta t = \frac{0.44\lambda_0^{\ 2}}{c \cdot \Delta\lambda} \qquad (2\text{-}1)$$

where Δt is the pulse width, λ_0 is the peak wavelength of the spectrum, c is the light speed, and $\Delta\lambda$ is the spectral width. And it can be estimated and monitored the pulse width in this way. However, in the NIR region, all materials have positive dispersion, and thus the pulse is always positively chirped. When the pulses are propagating in optics, they will be thus broadened in temporal domain, but remain the same in spectral domain. In practical cases, negative dispersion needs to be added which is known as dispersion compensation [2].

2.1.2 Femtosecond fiber lasers

A further major growth area in recent years has been the development of fs fiber lasers. Such systems have advanced rapidly and are now capable of competing with the Ti: sapphire lasers discussed above. Intense ultra-short laser pulse generation from diode-pumped rare-earth-doped photonic crystal fiber lasers is a novel approach to achieve low-cost and compact femtosecond laser source, which is a promising work-horse on industry and scientific research.

Er- and Yb- doped fs fiber lasers have been developing for years. Er-doped lasers emitting pulses at 1550 nm are very widely used in optical communication.

They are relatively cheap, quite compact, and stable in different environments. Yb-doped fiber lasers have a very high efficiency of pumping-lasing conversion, more than 80%, and it is potential to develop high power lasers. Since in fiber lasers optical field is finely confined in single mode (SM) cores, which is only several microns, the nonlinear efficiency is much more higher than free-space lasers, and thus there are much more mode locking mechanisms than solid state lasers.

Er-doped fiber laser usually produce short pulses by soliton mode locking [3]. Considering the E field E(z, t) in the fiber propagating a length L, self phase modulation (SPM) can be clearly described as following equation

$$E(L,t) = E(0,t)\exp[i\phi(L,t)], \qquad (2\text{-}2)$$

where $\phi(L,t) = |E(o,t)|^2 (L_{eff} / L_{NL})$ is the phase, and $L_{eff} = [1-\exp(-\alpha L)]/\alpha$, α is the loss in the fiber. L_{NL} is the nonlinear length, related with the second order nonlinear refractive index of the media at the wavelength of the pulse, the peak power of the pulse, and the effective mode area. Thus, SPM produces pulses with consisting shape but changing phase related with the light intensity. In this way, the abnormal dispersion in fiber may get equality with SPM, and thus produce soliton. To ensure the soliton propagate stably in the fiber, the length of the soliton should be much lager than the amplification length, which is actually the length of the Er-doped fiber. This means, the phase change in such a fiber should meet the following condition:

$$\phi << 1 \qquad (2\text{-}3).$$

This is also a kind of limitation to the power of the soliton.

To trigger mode locking and make the fiber laser working stably, usually semiconductor saturable absorber mirror (SESAM) is widely used to remove the CW parts in fiber that have higher gain. SESAM can reflect light, and the larger the power of the inducing light is, the higher reflective index SESAM will be. When CW and pulsed beams illuminate on SESAM, photons can pump electrons in the semiconductor to conductive band. And when enough electrons are excited, SESAM is bleached, and the loss of the cavity is decreased, producing pulses with higher power. Usually, CW light can hardly bleach SESAM and is mostly absorbed by it. This is the mechanism of passive mode locking by SESAM. Besides, nonlinear polarization-rotation effect is also used to form pulses. The principle is as following: the linear polarization of incident pulses are firstly converted to circular/elliptical by a wave plate, and then coupled into the fiber. When pulses propagate in fiber, the nonlinear effect will form intensity-related polarization of the pulse. Another polarizer is put in the output of the fiber, working as a kind of loss modulation of the pulses. The photons that do not have that polarization will be removed by that polarizer. This role is the same as the aperture in the Kerr lens mode locking.

SESAM has two important time constants, intra-band thermalization, and inter-band transition. The semiconductor absorbs photons, exciting carriers from valence band to conductive band. Intra-band thermalization is the process of exciting electron transition to a sub-band, in around 100-200 fs. Inter-band transition is from the valence band to the conductive band, usually costing some ps

to hundreds of ps. These two constants are very important for mode locking, to form sub-ps pulses. A typical SESAM mode locked fiber laser setup is shown as in Fig. 2-3.

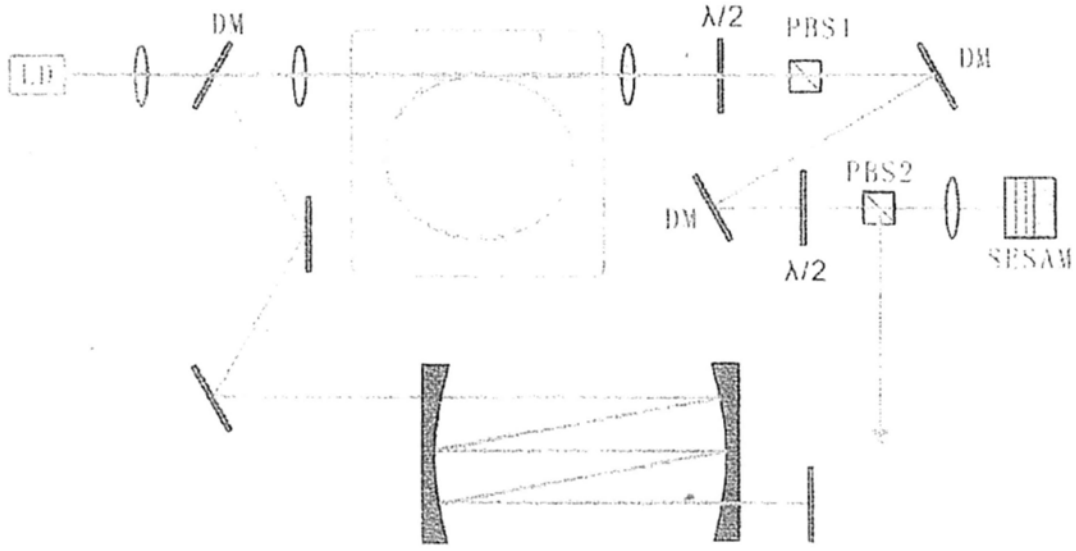

Fig. 2-3. Setup of a Yb-doped fiber laser with mode locked by SESAM. LD: laser diode for pumping. DM: dichroic mirror. PBS: polarization beam splitter. The Yb-doped fiber is in the orange box.

Fiber lasers have been developing very fast, and now combined with lots of other technologies, especially photonic crystal fiber to get a more broadened output range, higher power, and narrower pulses. Compared with Ti: sapphire lasers, they are more flexible, stable, and compact.

2.2 Introduction to mammalian cells

2.2.1 Cell structure

All most all living beings compose with cells. Although each kind of lives is quite different, the molecules inside cells are almost the same, which are mainly DNA, RNA, and proteins. Cells differentiate and also connect together to form tissues, which, then, integrate to be organs. The size of cells has a range from several microns to more than 0.1 mm. For mammalian cells, the size concentrates on around 5-20 μm. The structure of a mammalian cell is very complicated, as shown in Fig. 2-4. [4]

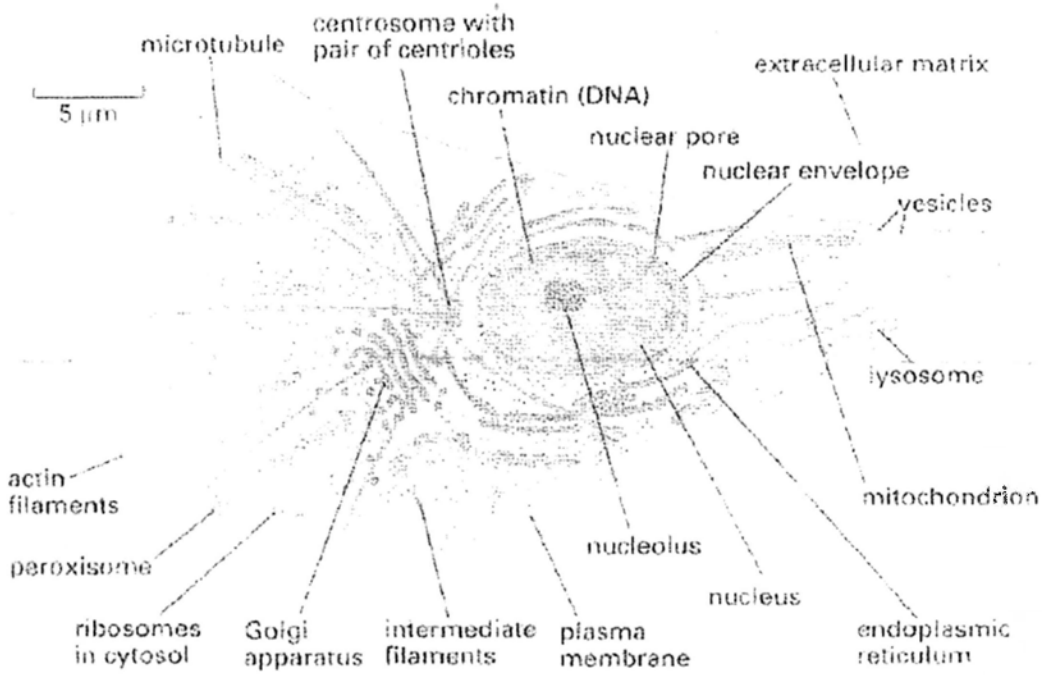

Fig. 2-4. Basic structure of a mammalian cell[4].

The cell is covered by plasma membrane, which is a kind of semi-permeable barrier defining the outline of the cell. The thickness is only around 5 nm. It is made from a bilayer of phospholipids, and cholesterol molecules inside provide rigidity of

such bilayer, without which, the lipid is only fluidic. The structure is shown as in Fig. 2-5. Besides, there are also a lot of proteins inside the membrane, and they form receptors, ion and other molecular channels, and enzymes to control transport and communication with the environment.

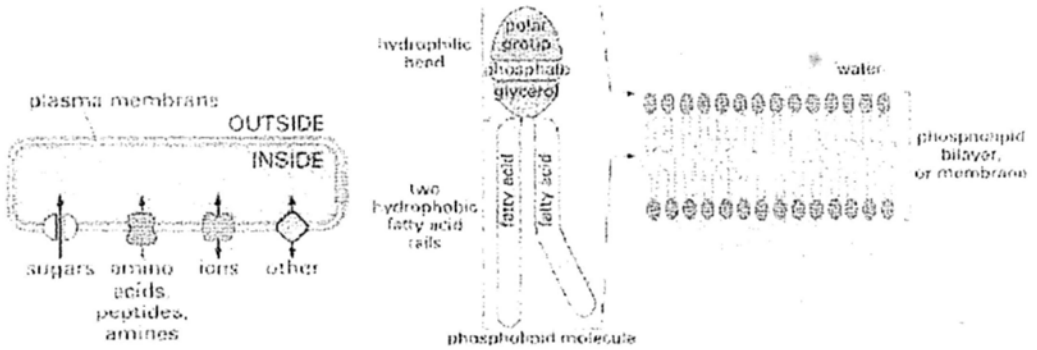

Fig. 2-5. Structure of the plasma membrane: double liplid [4].

Cytoskeleton is just behind membrane, which is mainly a network of protein filaments connecting with organelles. It provides cell shape, deformation, kinesis, transport, strength, and locomotion. What is more important, it can separate chromosomes during mitosis.

The central part of a mammalian cell is nucleus, which is the largest organelle, and its diameter is around 4-10 μm. Each cell has only one nucleus, with double layers of nuclear membrane. The structure is shown as in Fig. 2-6. Chromosomes with DNA are inside nucleus controlling genes. Usually, DNA molecules are combined with proteins and packaged in chromosomes. Besides, nucleolus is also inside nucleus, which can produce RNA. RNA is the bridge between genes in DNA and the synthesis of proteins. There are three kinds of RNA working for this process. First, messenger RNA (mRNA) can copy the information in DNA. This process is

called transcription, during which, the famous structure 'double helix' of DNA is unwound, and mRNA can exactly copy the gene from one single strand. After that, mRNA migrates into cytoplasm from nucleus, combining with ribosome. The RNA integrate with proteins to form ribosome in nucleolus is called rRNA. At last, some other RNA molecules transport special amino acid together to form proteins according to the information in mRNA. Those RNA binding with amino acids for transportation is called tRNA, and this process is called translation.

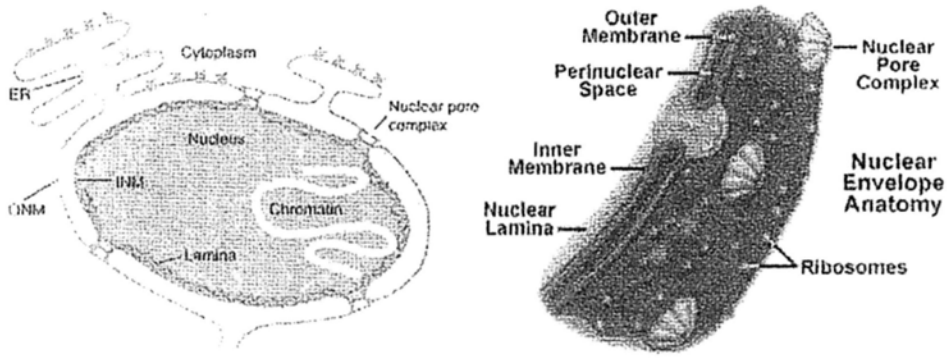

Fig. 2-6. Structure of nucleus and nuclear double membrane [4].

Since mRNA needs migrate from nucleus to cytoplasm, there should be some channels in the nuclear membrane, and they are called as nuclear pores. Actually, not only mRNA, but also a lot of ions and proteins can also diffuse through nuclear membrane. It is very important for the interaction between nucleus and cytoplasm.

As can be seen in Fig. 2-6, the nucleus membrane is connected with another complex network structure. It is called as endoplasmic reticulum (ER), composed by sheets, sacs, and tubes of membranes, as shown in Fig. 2-7. Its enclosing intracellular space is called lumen, which is very important to the 3D structure of folding proteins. ER has two types, rough ER and smooth ER. Rough ER is close to

nucleus, attached with a lot of ribosomes, working for the formation of proteins. Rough ER can transit to smooth ER, the site of synthesis of lipids and sugars.

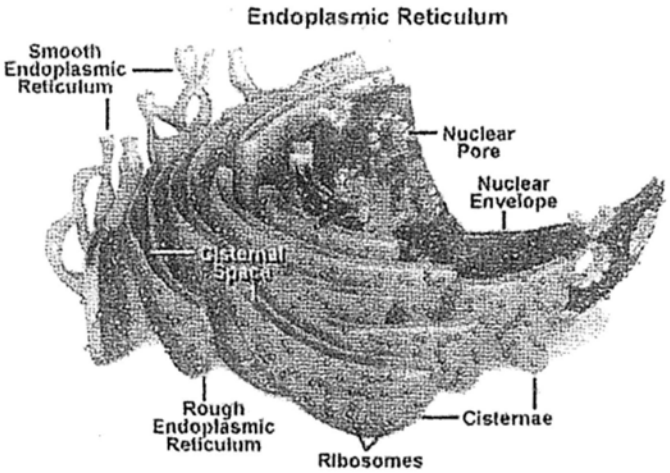

Fig. 2-7. Structure of ER, including rough ER and smooth ER [4].

Mitochondria are the power plant of the cell. There are many mitochondria inside cytoplasm, and their total volume is around 20% of the cell. Each mitochondrion is in a cylindrical shape, with a length of around 3-10 μm and diameter of 0.5-1.5 μm. It also has double membrane. The inner membrane convolute to form cristae, enlarging more area for enzymes attaching, producing energy by respiration. The structure is shown in Fig. 2-8. Besides the role of power plant, mitochondria have a lot of other functions. For example, they can modulate cellular ion concentration [5], and produce reactive oxygen species [6]. Mitochondria have their own DNA, RNA, and ribosome. The role of mitochondria in cellular processes remains something unclear.

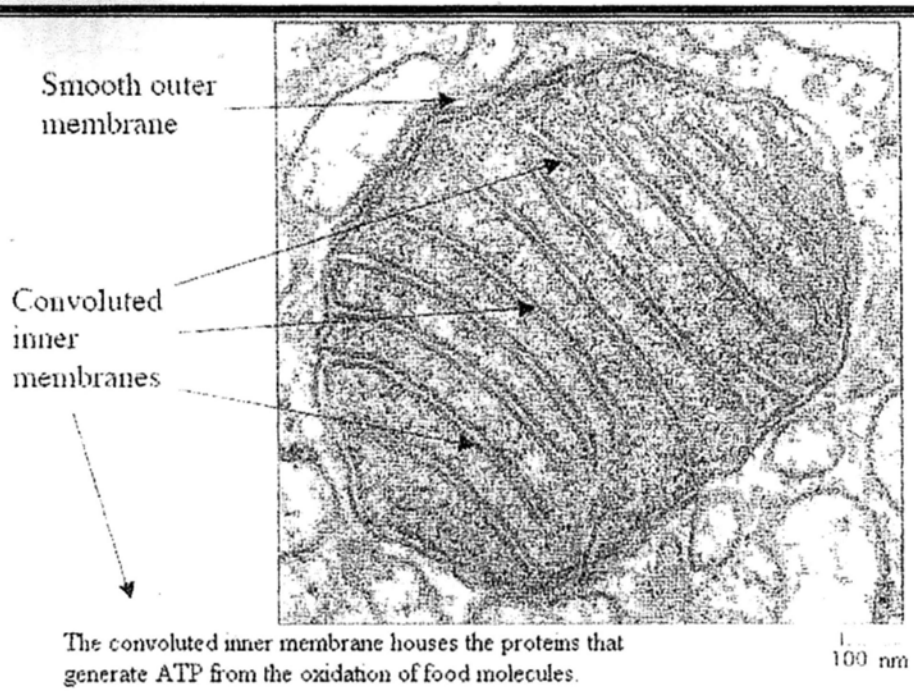

Fig. 2-8. Cross section of a mitochondrion in the electron microscopy [4].

Golgi apparatus is named from Camillo Golgi, who is the first scientist describing its structure. Golgi apparatus is stacked by some flattened sacs of membranes. It can ship proteins to other organelles by use of vesicles, and even transport proteins out of cells.

At last, lysosomes are very simple single membrane vesivcles, with a diameter around 0.2-0.5 μm. They contain enzymes in an acidic environment for cellular digestion.

Besides those organelles, the other inside the membrane is cytoplasm. It is mainly viscid liquid media, consisting with salts, sugar, fat, vitamins, proteins, amino acid, and RNA. They are all quite important for cellular daily life. A lot of functions of cells are processing in cytoplasm, such as metabolism.

2.2.2 Cell types

There are more than 200 types of cells in human body. Different cells combine together to form different tissues and organs. Here only several normal cells are introduced as following [7]:

1) Epithelial cells have many subgroups like: absorptive cells to increase the area of absorption; mucosal cells to protect cells from inbreak of dirty and microbe; endocrine glands; ciliated cells, and secretary cells.
2) Blood cells have three types of cells: erythrocytes (red blood cells) containing hemoglobin and transporting O_2 and CO_2; leukocytes (white blood cells) including lymphocytes (T cell for cell-mediated immunity and B cell for antibody production) and macrophages/neutrophils (moving to the site of infection to digest bacteria), only 1/1000 of red blood cells; thrombocytes (platelets) for blood coagulation.
3) Muscle cells form muscle tissue and produce mechanical force by contraction.
4) Neurons work for the communication throughout body by nerve network.
5) Stem cells are cells that are not yet differentiated. In theory, they can turn into any type of cell in the specialized stimuli and environment. They have great potential in a lot of fields, especially organ clone, cancer therapy, and fundamental cellular biology.

Tumors and cancer cells are abnormal cells which have differences in growth, morphology, interaction between cells, production of proteins, and expression of

genes with normal cells. In the proliferation of normal cells, the replication of cells needs the participation of some growth-promoting factors. But tumors can grow very fast without those factors. Meanwhile, tumors can not be controlled by the signal of apoptosis, and they are very hard to die. Normal cells can turn to tumors, by the activation of oncogenes in chromosomes stimulated by some unknown factors. This process is called as transformation. Those oncogenes influence the normal processes of cells and the cells are then out of control of proliferation.

Tumors have two types, benign and malignant tumors (cancers). Benign cells are very similar to normal cells with little threatens to body, and can be cut without any influence to normal tissues. But cancer cells can develop very fast, and will not be limited in an area. They can diffuse along the circulation system of the body, and grow in another place. This is called as metastasis.

Cancer cells can produce some special receptors and enzymes, and this has been used to the research of early cancer diagnostic and cancer therapy. Besides, the nuclear plasma of cancer cells is significantly more than normal cells. This enables many imaging methods of cancers, such as x-ray [8], computed tomography [9], and positron emission tomography [10].

2.3 Photo-processes in cells

Cells have sizes ranging from sub-micron to tens of microns, containing a lot of different organelles. Generally speaking, there are two kinds of interactions between cells and photons, scattering and absorption. Considering the size of cells, the cell itself, sub-cellular organelles, and even macro molecules can be the center of Mie or Reighley scattering, as shown in Fig. 2-9. In theory, light at longer wavelength can propagate through cells with less scattering. But water, –CH, and –OH have large absorption at infrared range, and thus the NIR range is usually considered as the window.

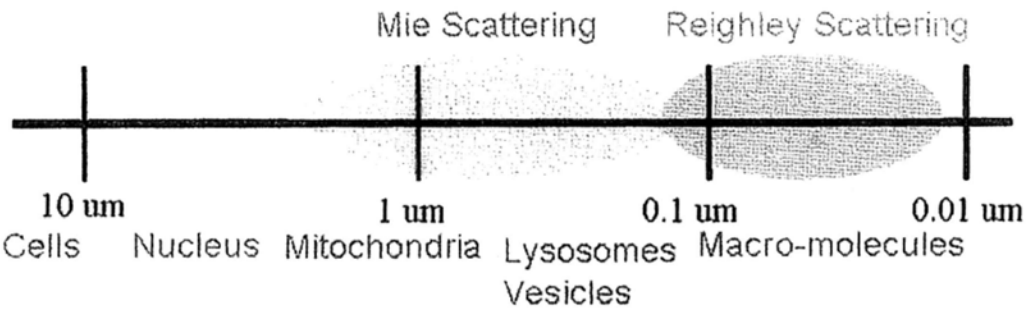

Fig. 2-9. Scattering by cells and subcellular structures.

Absorption by cells is very complicated. From sugars, proteins, DNA and RNA, to water, the absorption band covers from deep UV to infrared range. Such materials absorb photons and can convert the photon energy to thermal and chemical energy, while sometimes some special molecules are even able to emit fluorescence. The chemical processes induced by photons include photo-addition, photo-fragmentation, photo-oxidation, photo-hydration, photo-isomerization, and photo-rearrangement. Photo-oxidation is a very interesting process, which can generate reactive oxygen species related with programmed cell death and

differentiation of stem cells. We have researched this topic using an fs laser and found the fs pulses can be a powerful and precise tool to control the oxidation inside cells. Photo-oxidation is also very widely used in photodynamic therapy. Generally, the shorter the wavelength of the photon is, the more possible such processes occur. For example, photons at UV band can break the double/single strand structure and the combination between molecules of DNA to form DNA fragmentations.

Some macro-molecules inside cells can emit fluorescence after the excitation. At the visible range, NADH, flavins, and elastin are famous natural fluorophores of cells, which are very important for the auto-fluorescence imaging with applications in cancer diagnostics. The excitation and emission spectrum of such molecules are shown as in Fig. 2-10. However, besides these linear absorptions, nonlinear imaging is now more important and attracting more attentions. Raman spectroscopy at NIR range is not very developed in diagnostics to several kinds of cancers.

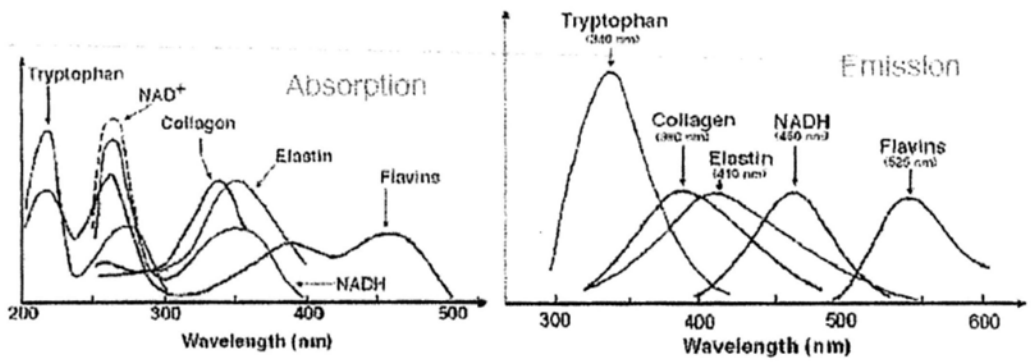

Fig. 2-10. The excitation and emission spectrum of natural fluorophores inside cells [7].

Direct physical effects by photons including thermal effects, optical disruption, plasma formation, and optical breakdown are mainly used in cell surgery. Thermal effect is very common, and most lasers ranging from UV to NIR have thermal effect.

The efficiency depends on the absorption coefficient of different wavelength. Proteins, water, and other molecules in cells have different absorption spectrum. Also, the laser power and pulse duration are two important parameters to calculate the temperature rise. Usually, high thermal effect of lasers is used for small non-invasive surgery on skin by high power long-pulsed and CW lasers. For example, micro-second lasers are widely used to cut tissue by heating the targeted tissue more than 100K in several tens of microseconds. Water in the focal volume can be vaporized and vapor generated in such a short moment can cut the targeted tissue. High power nanosecond pulses can even melt tissues, and this is used for tissue sealing.

Before the invention of fs lasers, optical disruption can be only achieved by excimer lasers at UV range (193 nm -351 nm) with pulse width around 10 ns. The peak power density needs around $10^7 - 10^{10}$ W/cm^2. Actually photo-fragmentation processes are induced by the short UV pulses to form tiny fragmentations of cells, and thus optical disruption effect can cut tissue this way. This effect has a very famous and popular application in refractive corneal surgery, LASIK (laser-assisted in situ keratomileusis) [11, 12].

Fs pulses can generate an even larger power density very easily, and they can generate a very large electrical field. For example, at the optical power 10^{11} W/cm^2 the electrical field is around 10^7 V/cm, whose force on electrons is much larger than the Coulomb force between electrons and atomic nucleus. Thus the electrons can be ionized to form high density of free electrons in the focal volume. And when that

density is more than 10^{18} cm^{-3}, plasma forms.

If the optical power density is even larger, generating plasma with higher density electrons, it will form shock wave and bubbles in cells. Such optical break down effect can cut cells and tissue easily, and much more controllable and precise than the traditional long-pulsed lasers. Surgeries by fs lasers on cells and tissues have been done a lot in labs, and the potential is very promising [13-15].

2.4 Properties of fs pulses in a microscope system

Femtosecond lasers have been used more and more for imaging and operations at cellular and sub-cellular level. Most of such systems are based on a microscope. The laser beam is focused by an objective, which can be used for observation at the same time. To get higher resolution and better focused volume of the laser beam, high N.A. objectives are preferred. By the ultra-high peak power of the fs pulses and the tiny volume of the focal spot (at the level of diffraction limitation), the photon density can reach a high level, at which most nonlinear effects can be introduced. Properties of focused fs pulses are discussed as following.

2.4.1 Plasma formation in media

Low density induced by fs laser is a versatile tool for manipulation of transparent biological samples, with very precise localization and little harm. The plasma formation is a very high order nonlinear effect and in most cases induced by long pulsed lasers it is quite hard to happen. To be simple, only plasma formation in water is analyzed here since the optical breakdown threshold in water is very similar to that in ocular and other biological media [16]. Also, the refractive index of water (1.34) is very similar to most cells (1.45-1.55).

The band gap of electron in H_2O molecule is 6.5 eV. In some breakdown models, it was often assumed that a free electron could be produced as soon as the pump energy exceeded the band gap either by the sum of the simultaneously absorbed photons or by the kinetic energy of an impacting free electron [17-19].

However, pointed by A. Vogel et al. [20], if the electron is ionized by large volume of photons, the band gap energy has to be added by the oscillation energy of the electron due to the electrical laser field. And then the effective band gap is

$$\tilde{\Delta} = \Delta + \frac{e^2 E^2}{4m\omega^2} \qquad (2\text{-}4),$$

where Δ is the original band gap, e and m are the electrical charge and effective mass, E and ω are the electrical field and angular frequency of the light. The second term can be neglected in long pulsed laser cases, but must be considered in fs laser case since the E field of the focused fs pulses is very large.

The ionization of electrons by photons can be explained by the following mechanism. If one electron in the valence band absorbs photons simultaneously the sum of whose energy is larger than the band gap, it can be excited by such a multi-photon absorption and energy transfer. The photon energy is 1.2 eV at 1040 nm, and 0.8 eV at 1550 nm. It means to excite one electron, at least 6 photons at 1040 nm or 9 photons at 1550 nm are needed. The chance that one electron absorb so many photons is very small and thus the efficiency of such high order nonlinearity is ultra low. Only when the photon density is high enough, the nonlinearity can occur. As a macro criterion, one electron in water can be ionized only when the strength of electrical field of the light is larger than 100 MV/cm which means the photon density should be larger than 1.5×10^{13} W/cm^2 at 1040 nm or 2.5×10^{13} W/cm^2 at 1550 nm.

Once a free electron is produced in the medium, it can absorb photons in a

non-resonant process 'inverse Bremsstrahlung' in the course of collisions with heavy charged particles which are necessary. The energy of the photon can be converted to be the kinetic energy of the free electron. After a sequence of several inverse Bremsstrahlung absorption events, the electron gains kinetic energy sufficiently large enough to produce another free electron through impact ionization. Thus, there are two mechanisms in the ionization process by fs pulses in media, direct multiphoton ionization and impact ionization. According to the assumption in [21, 22], the critical energy for impact ionization for water can be estimated as around $1.5\tilde{\Delta}$.

Besides, all free electrons can still gain energy through inverse Bremsstrahlung absorption. The recurring sequence of inverse Bremsstrahlung absorption events and impact ionization leads to an avalanche growth in the number of free electrons if the irradiance is high enough to overcome the losses of free electrons through diffusion out of the focal volume and through recombination. The energy gain through inverse Bremsstrahlung should be more rapid than the energy loss by collisions with heavy particles occurring without simultaneous absorption of a photon. The whole process is called 'avalanche ionization' or 'cascade ionization', as shown in Fig. 2-11.

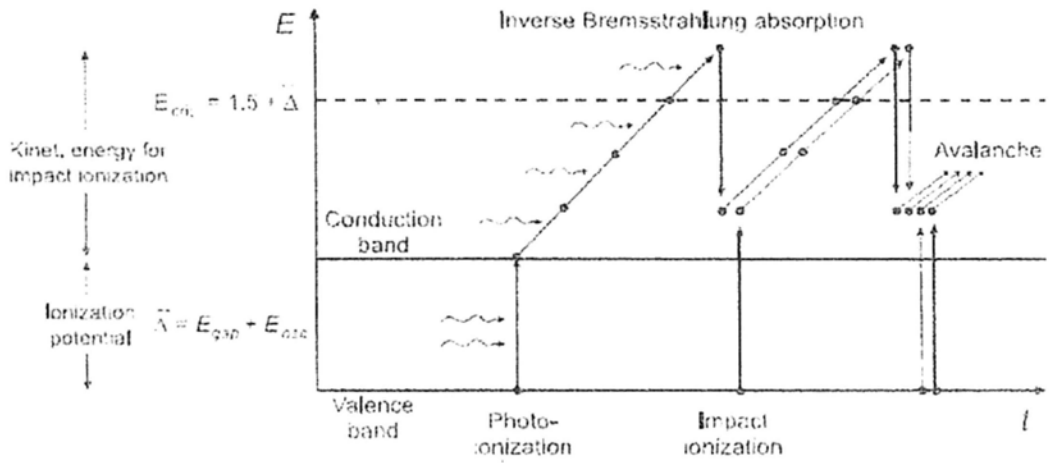

Fig. 2-11. Mechanisms of ionization by fs pulses, multiphoton ionization and impact ionization, leading to an avalanche free electron growth and resulting plasma formation [20].

Assuming the inducing fs pulses at 1040 nm have a pulse duration 100 fs, the effective ionization energy for water $\tilde{\Delta} = 7.3eV$, a little larger than its original band gap 6.5 eV. And thus the energy for impact ionization is even larger, 10.95 eV. To induce multiphoton ionization, one free electron needs seven photons. Suppose the ideal objective can give a focal spot with the diameter around Airy limitation

$$d = 1.22\frac{\lambda}{NA} \qquad (2\text{-}5)$$

where the maximum NA can be as large as 1.45, and thus the focal diameter is around 875 nm. For the Gaussian intensity distribution, we can only consider the main part of the intensity whose diameter is around 500 nm. The requirement of the photon density is 1.5×10^{13} W/cm^2, and thus the peak power of the fs pulse should be 30kW, which means the energy of one fs pulse (100 fs) is around 1 nJ.

At this critical power level of the inducing laser, according to the numerical simulations, [20] presents the result of the average electron density inside the focal volume around $10^{-18} \sim 10^{-19}$ /cm^{-3}. Actually the distribution of the electrons is

exactly depending on the photon distribution, as shown in Fig. 2-12.

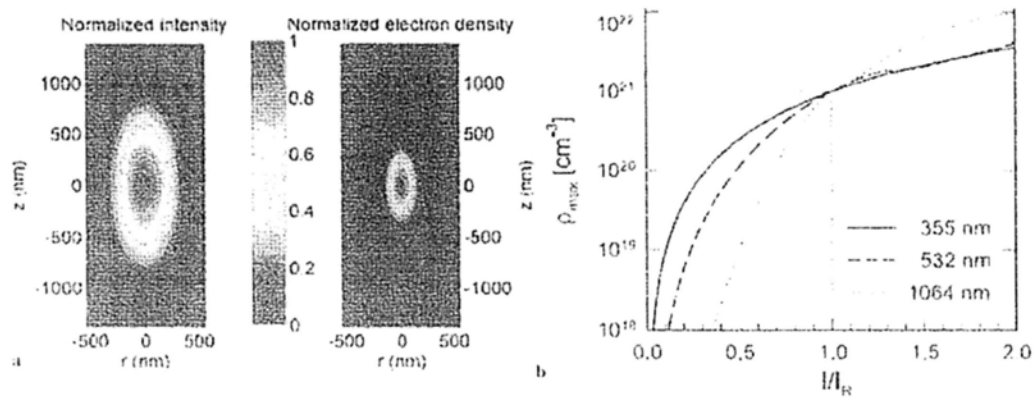

Fig. 2-12. Photon and electron density distribution. (a) Normalized irradiance distribution and electron-density distribution (b) in the focal region for NA = 1.3 and λ = 800 nm, and (b) the electron density vs. the induced laser power at different wavelengths. I_R: the critical laser power density. ρ_{max}, the maximum free electron density [20].

Since the electron density is quite dependent on the peak power in the pulse, the pulse duration is very important to the plasma formation if the average power is the same. To get the threshold, different pulse widths have quite different energy requirements, as shown in Fig. 2-13. It can be found, if the pulse is too long, the energy at the threshold is quite large.

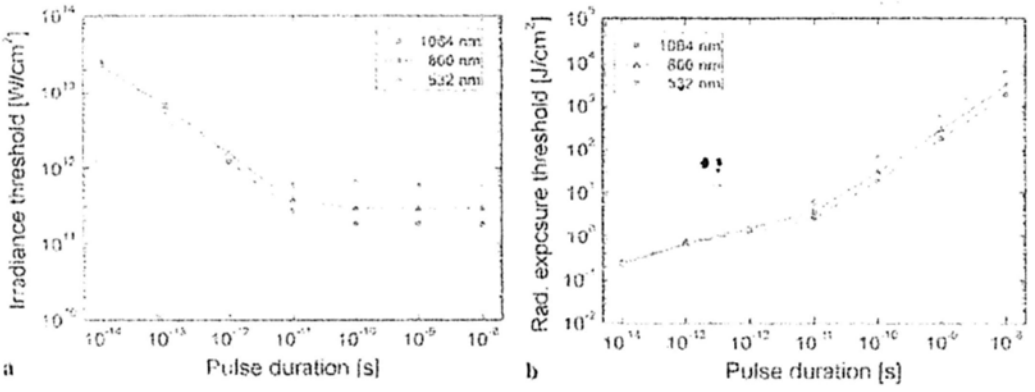

Fig. 2-13. Calculated optical breakdown thresholds (for the electron density $10^{21}/cm^3$) as a

function of laser pulse duration for various laser wavelengths. (a) the threshold of photon density at different pulse widths, (b) the energy density for different pulse widths [20].

2.4.2 Experimental details

In experiments, lasers with pulse width less than 100 fs are usually not considered due to pulse broadening during transmission resulting from optical dispersion in the optical system. The major impact is from the objective, which may consist of a variety of different glass types and thicknesses. Typical optical dispersion values D for glasses in objectives at 800 nm are 251 fs^2 cm^{-1} for CaF_2, 300 fs^2 cm^{-1} for quartz, 389 fs^2 cm^{-1} for FK-3, 445 fs^2 cm^{-1} for BK7 glass, 1030 fs^2 cm^{-1} for SF2, and 1600 fs^2 cm^{-1} for SF10. At shorter wavelengths, these numbers increase [25]. A typical microscopy system can have from 3000 to 20000 fs^2 of dispersion in total.

To complete the microscope system with a fs laser, at first a microscope, such as inverted or confocal microscope is needed, with high N.A. objectives. Leica, Nikon, Olympus, Zeiss, and some other companies have developed a lot of commercial versions for researches. To couple the fs beam into the microscope, an extra port in the microscope is needed, through which the laser beam can transmit into the microscope. Some commercial versions have such special design for additional laser coupling. Inside the microscope, the NIR beam will be reflected into the objective to focus on the target by a dichroic mirror. Commercial mirrors with NIR reflection and visible transmission both more than 90% have been

developed. To improve the coupling efficiency, people can choose objectives with coatings for NIR range. But in that case, the N.A. of such objectives are usually smaller than 1.0 since that type of objectives mostly has no oil-immersion. Even though water immersed objectives with NIR coating have been developed, the N.A. has still such limit since the refractive index of water is not large enough. It should be noted that since the refractive index for visible and NIR light have a difference, and imaging and coupling light path are also different, the focus position of the NIR is usually not the same plane of the imaging plane. Usually, to be convenient, the laser beam can be adjusted to focus at the imaging plane using some lenses, usually a lens pair with tunable distance between them.

2.5 Summary

In this section, we briefly introduced fs lasers and some basis of cells. Fs lasers can be mainly divided into two types, free space and fiber lasers. The mode locking principle of them is quite different. The development of fs lasers is very fast and now more and more advanced ultra-short pulsed lasers can be chosen.

There are many organelles with different functions inside one single cell. The interactions between cells and lasers are quite complex, involving a lot of physical and chemical processes. However, for fs pulses irradiation, nonlinear effect is the main part of the interactions. Due to the ultra short pulse width and ultra high peak power, fs beams show a lot of novel and perfect properties for imaging and manipulation of biological samples. The nonlinear process of how multiphoton pump one electron to high energy level is analyzed here, which is the basis of all nonlinear imaging and manipulation methods. Plasma formation is now considered as the most probable mechanism for changing cellular membrane permeability by fs lasers. The most important side effect, thermal effect, is also analyzed here and some numerical results are given. It can be concluded that fs beams are very powerful for manipulating biological samples, especially at single cellular level, and relatively safe to them.

References

1. D. E Spence, P. N Kean & W. Sibbett, "60-fsec pulse generation from a self-mode-locked Ti:sapphire laser", Opt. Lett., Vol. 16 p.42 (1991)
2. M. Nisoli, S. de Silviestri, O. Svelto, R. Szipocs, K. Ferencz, Ch. Spielmann, S. Sartania & F. Krauz, "Compression of high-energy laser pulses below 5 fs", Opt. Lett., Vol. 22, p.522 (1997)
3. K. Tamura, L. E. Nelson, H. A. Haus, et al., Soliton versus nonsoliton operation of fiber ring lasers, Appl. Phys. Lett. 1994, 64(2): 149-151
4. Bruce Alberts, Alexander Johnson, Julian Lewis, Martin Raff, Keith Roberts, Peter Walter, Molecular Biology of the Cell, 4th edition, Garland. 2002. genomebiology.com/2002/ 3/4/REVIEWS/1008/figure/F1 and "Molecular Expressions (http://micro.magnet.fsu.edu/cells/nucleus/nuclearenvelope.html, http://www.microscopy.fsu.edu/cells/endoplasmicreticulum/endoplasmicreticulum.html)" for the figure of nuclear structure and ER.
5. Wihelma Echevarr, et al., Nature Cell Biology, 5, 440-446, 2003
6. Jacobson MD., "Reactive oxygen species and programmed cell death," Trends Biochem Sci, 21, 83-88 (1996)
7. Thomas Huser, Introduction to Biophotonics, IEEE - LEOS 2004
8. Ji-Xian Wang, John D. Boice, Jr., Ben-Xiao Li, Jing-Yuan Zhang, Joseph F. Fraumeni, Jr., Cancer Among Medical Diagnostic X-Ray Workers in China, Journal of the National Cancer Institute 1988 80(5):344-350
9. David J. Brenner, Eric J. Hall, Computed Tomography — An Increasing Source

of Radiation Exposure, The New England journal of medicine, Volume 357:2277-2284, 2007

10. M E Raichle, Positron Emission Tomography, Annual Review of Neuroscience, Vol. 6: 249-267 1983
11. I. Ratkay-Traub, I.E. Ferincz, T. Juhasz, R.M. Kurtz, R.R. Krueger, J. Refract. Surg. 19, 94 (2003)
12. A. Heisterkamp, T. Mamom, O. Kermani, W. Drommer, H. Welling, W. Ertmer, H. Lubatschowski, Graef. Arch. Clin. Exp. 241, 511 (2003)
13. Le Harzic Ronan; König Karsten; Wüllner Christian; Vogler Klaus; Dnitzky Christof, Ultraviolet femtosecond laser creation of corneal flap. Journal of refractive surgery (Thorofare, N.J. : 1995) 2009;25(4):383-9.
14. Wang Bao-Gui; Riemann Iris; Schubert Harald; Schweitzer Dietrich; König Karsten; Halbhuber Karl-Juergen, Multiphoton microscopy for monitoring intratissue femtosecond laser surgery effects. Lasers in surgery and medicine 2007; 39(6):527-33.
15. Tirlapur Uday K; König Karsten, Femtosecond near-infrared laser pulses as a versatile non-invasive tool for intra-tissue nanoprocessing in plants without compromising viability. The Plant journal : for cell and molecular biology 2002;31(3):365-74.
16. F. Docchio, C.A. Sachhi, J. Marshall, Lasers Ophthalmol. 1, 83 (1986)
17. P.K. Kennedy, IEEE J. Quantum Electron. 31, 2241 (1995)
18. Q. Feng, J.V. Moloney, A.C. Newell, E.M. Wright, K. Cook, P.K. Kennedy,

D.X. Hammer, B.A. Rockwell, C.R. Thompson, IEEE J. Quantum Electron. 33, 127 (1997)

19. A.C. Tien, S. Backus, H. Kapteyn, M. Murnane, G. Mourou, Phys. Rev. Lett. 82, 3883 (1999)
20. A. Vogel, J. Noack, G. Hüttman, G. Paltauf, Applied Physics B: Lasers and Optics, **81**, 1015-1047 (2005)
21. A. Kaiser, B. Rethfeld, M. Vicanek, G. Simon, Phys. Rev. B 61, 11 437 (2000)
22. B. Rethfeld, Phys. Rev. Lett. 92, 187 401 (2004)
23. S. Nolte, C. Momma, H. Jacobs, A. Tünnermann, B.N. Chikov, B. Wellegehausen, H. Welling, J. Opt. Soc. Am. B 14, 2716 (1997)
24. D.N. Nikogosyan, A.A. Oraevsky, V. Rupasov, Chem. Phys. 77, 131 (1983)
25. K. KONIG, Multiphoton microscopy in life sciences. Journal of Microscopy, Vol. 200, 83-104. (2000)

Chapter 3: Transfection by the Femtosecond Laser

3.1 Introduction

The transfer into living cells of macromolecules, named transfection, which monitor or modify molecule-specific intracellular processes, provides an efficient way to study the temporal and spatial regulation of protein systems that underlie basic cellular functions. With recent advances (e.g., worldwide genomic and cDNA sequencing projects) in molecular biology, gene therapy is expected to assume a pivotal role in the treatment of genetic diseases. This innovative therapy involves the introduction of healthy copies of mutated or absent genes into target cells so as to promote the expression of normal protein and to restore correct cellular function. The development of gene therapy vectors with sufficient targeting ability, transfection efficiency, and safety must be achieved before gene therapy can be routinely used in man [1-3]. Thus, transfection of DNA and other molecules has attracted attentions all over the world, even since more than 30 years before [4].

In general terms, gene delivery methods can be sub-divided into two categories: (a) the use of biological vectors and (b) techniques employing either chemical or physical approaches. Biological methods, referred to as infection, however, have many undesired side effects, such as viral toxicity, host immune rejection, as well as being difficult to prepare [5]. Chemical methods are relatively straightforward and easily scaled-up, and do not provoke specific immune responses. But efficiency and

targeting remain extremely poor [2]. Compared with those above, physical or mechanical approaches seem to be simple, safe, and efficient, and thus a lot of techniques have been developed.

3.1.1 Mechanical methods

The most natural idea is to use glass capillary microinjection to introduce DNA or other materials into cytoplasm or nuclei directly, which is developed 30 years ago [6, 7] and now widely used. This technique adopts glass micropipettes with a fine tip of less than 0.5 um (microinjector) and a precise positioning device (a micromanipulator) to control the movement of the micropipette. Therefore, it costs a lot of money and time to buy and be familiar with such a mechanical device system.

As an improvement, gene gun was developed in 1987 [8]. It utilizes heavy, non-toxic, and non-reactive metal particles (e.g. 1–1.5 um golden spheres), onto which naked DNA is precipitated, propelled at a sufficient velocity into the target cell. Acceleration is achieved by a high-voltage electric spark, or a helium discharge [9,10]. It is cheap, fast and convenient, but the efficiency is not high and influenced by many parameters, such as the loading of DNA onto the particles, the particle size, and the timing of delivery. In addition, DNA distribution of coating on the sphere and spheres in the cell influence the final results a lot [11].

3.1.2 Electroporation

To overcome limitations of mechanical devices, electroporation, a no-osculant method, was developed [12]. Microsecond, high-voltage electrical pulses are localized onto membrane of cells, which then becomes highly permeable to exogenous molecules, present in the surrounding medium. But there can be substantial damage associated with the procedure and that this can limit the efficiency of transfection [13]. The method becomes more doubted after finding that transgene expression is not homogeneously distributed in the treated tissue [14].

3.1.3 Femtosecond laser transfection

Compared with electrical field which is not convenient and precise to control and localize, laser is a much better choice to open the door of cells. However, lasers can also harm cells, especially short wavelengths, such as photon-damage outside the focal volume, photo-disruption [15], and what is the worse, it may bring aberrances. But in some infrared range (800-1600nm), continuous wave (CW) lasers have little influence to cells, even very high power density (10^9W/cm^2) [16], which is called as "cell window". Thus, if short wavelengths (usually no more than 700nm) are chosen, enabling each photon with high energy that can disrupt membrane to dill holes in it [17-21], the viability of cells is very low after transfection. To solve this problem, femtosecond infrared laser is the final optimal choice, whose pulses are ultra-short (around 100fs), and thus very high peak power can be got (around 7kW). It has no out-of –focus absorption and no significant transfer of heat or mechanical energy to surrounding structures, thus relatively safe

to cells [22]. Meanwhile, the peak power is high enough to drill holes in the membrane for transfection [22, 23].

In the technique, the laser beam is typically focused through a high numerical aperture objective lens onto the membrane of the targeted cell. The highly localized laser beam serves at least to modify the permeability of the cell membrane if not creating a transient pore, and then it should be shut to protect the cell. Foreign DNA in the surrounding medium can enter before the pore closes, and the cell heals itself. Therefore, if there are several kinds of molecules in the buffer, it can not be ensured that all kinds of molecules have been transferred, and just for one kind, the transferred quantity also can not be controlled. Even though, quite successful transfection for a single kind of DNA experiment was done in 2002 [24], but the efficiency still remains arguments [25]. Besides, the exposing time of cells should be controlled in some milliseconds. Long time exposing will reduce viability of cells significantly, but till now, the optimal time length and laser power have not been work out.

3.1.4 Liposome/Carrier-mediated transfer

Considering properties of cell membrane, indirect transfection methods were also developed. DNA, proteins, or genes can be loaded onto cell-permeable molecules, and then carried into cells. Such molecules are genetic carriers, which can "cheat" membrane to open. The protocols for carrier-mediated transfer are usually simple and allow targeting of thousands or millions of cells at the same time

[26]. But the efficiency is not high, and types and sizes of molecules to be transferred are quite limited by the carrier.

To overcome those limitations, carriers are changed into liposome, and molecules to be transferred are packaged in it. Since no interaction is needed between molecules and carriers, liposome has no harm to cells, and the size of it can be controlled, there is almost no limitation to the molecules. Solutions of liposome and cells are then mixed, and a liposome has a probability to contact with a cell, which can be fused together by some chemical drugs. After the fusion, which is actually a lipid metabolism of the cell (the liposome becomes one part of the cell), the molecules are transferred [27]. The fusion takes a quite long time, usually more than 10 hours, and the transfection efficiency is low, limited by several factors [28]. These methods are shown in Fig. 3-1.

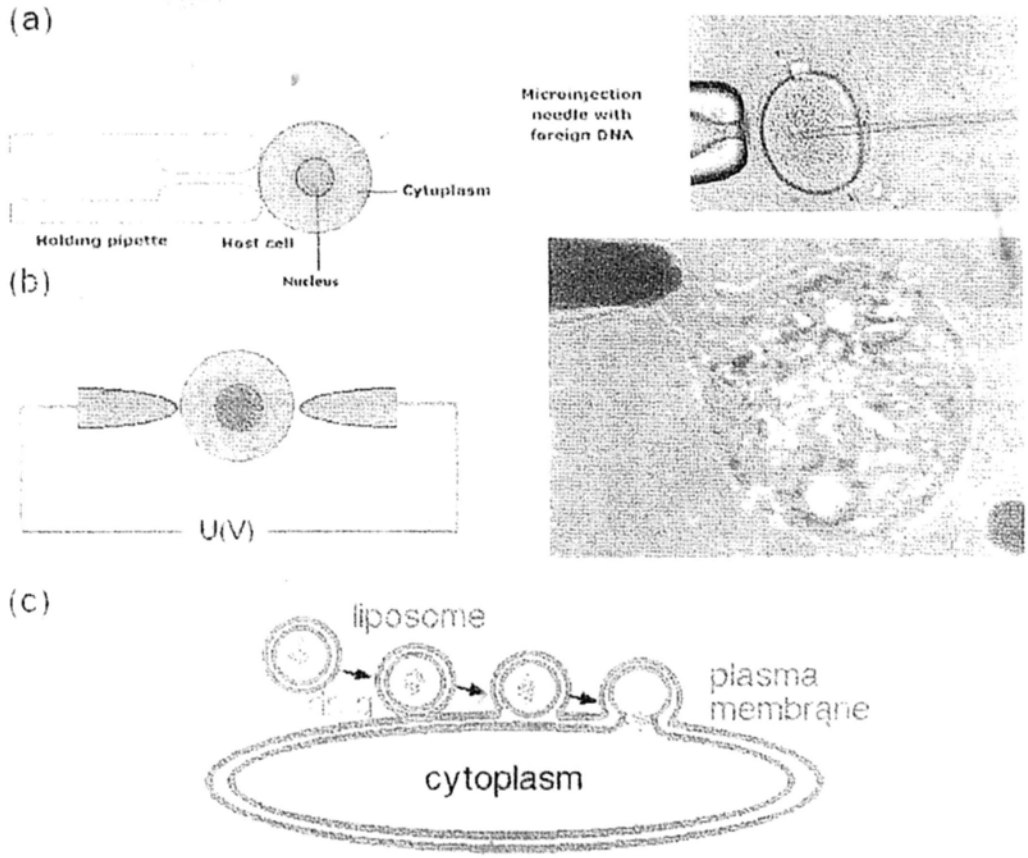

Fig. 3-1. Traditional transfection methods. (a) Micro-injection. (b) Electroporation. (c) Liposome mediated transfection [figure from Nikon website].

3.2 Optical transfection

3.2.1 Introduction

The delivery of foreign molecules such as DNA, proteins, and other macromolecules into cells through the plasma membrane, is a key technique in cell and molecular biology with many important biochemical applications. Traditional methods like electroporation and liposomal transfection normally transfect a large population of cells without selectivity while the efficiency is not very high. On the other hand, microinjection is operated at single cell level but it is an invasive procedure.

Lasers, especially fs lasers working in the near infrared region, have shown a lot of advantages in biological fields. For example, by using laser illumination, there is no mechanical or chemical contact with cells. Also, lasers are clean, and the side effect is quite weak for infrared photons as a result of its lower photon energy and reduced scattering when compared to that of UV beam. In 2002, *Konig et al.* firstly reported the use of Ti:Sapphire fs laser at 800nm with a repetition frequency of 80MHz and a mean power of 50-100mW to transfect Chinese hamster ovarian (CHO) and rat-kangaroo kidney epithelial (PtK2) cells [24]. In their study, they used a very high power laser intensity of $10^{12}Wcm^{-2}$, and such a laser beam produced a single, site-specific, transient perforation in the cell membrane through which DNA could enter. To reduce the damage to cells, they suggested the exposure time should not be longer than 16ms, and the laser beam should be focused on the edge of the membrane of target cells. Subsequently, work from *Stevenson et al.*

(2006) indicated that the efficiency of such a method was around 50% ± 10% [25]. Also, *Stevenson et al.* found that many CHO cells died even when the exposure time was strictly controlled within 100ms. This arises because the fs lasers at a wavelength ≤800nm with a mean power ≥7mW could generate reactive oxygen species, perturb the cell plasma membrane integrity, deform the nuclei, and introduce DNA strand breaks [29]. To solve these problems, it is of interest to try a laser of longer wavelength to reduce the optical damage. In this study, we coupled a fiber fs laser at 1554nm, a setup widely used in optical communication research, into an inverted microscope to examine its effect on transfection and photoporation, whereby exogenous materials were introduced into the human liver cancer HepG2 cells. The energy level of photons at 1554nm is too low to induce any chemical effects directly and the scattering is also smaller than that of 800nm, implying that the use of 1554nm fs laser is relatively safe to biological samples. Our results indicated that the fs laser at 1554nm beam was able to perforate the cell membrane to allow the fluorescent DNA intercalating dye PI to label the nuclear DNA while at the same time no mitochondrial depolarization was detected 1.5 hours after photoporation. Furthernore, the 1554nm fs laser was able to transfect HepG2 cells with a plasmid DNA containing the GFP gene, whose fluorescence was detected 24 hours after phototransfection. The optical design is shown in Fig. 3-2.

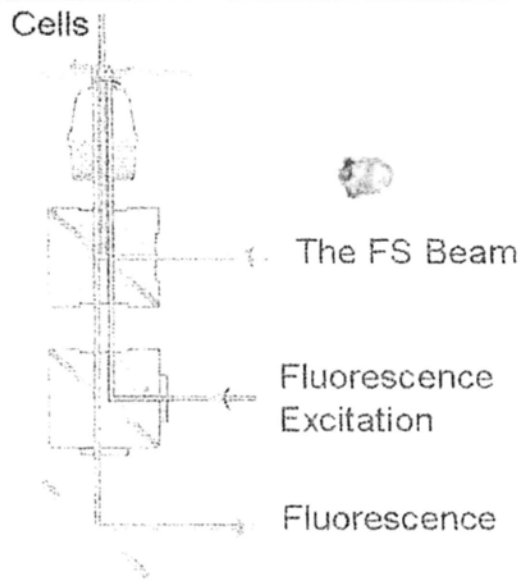

Fig. 3-2 Optical design of the transfection system by the fs laser at 1554 nm.

In our setup, the fs laser was coupled to a Nikon TE2000U inverted microscope with a 40X objective lens (N.A.=1.0). There were 2 lasers in this study. The fs fiber laser had a central wavelength at 1554nm and a repetition frequency of 20MHz with a mean power around 100mW. The pulse width was around 170fs. The diameter of the laser beam focus was around 2um, and thus the peak power was 10^{12} Wcm^{-2} in the focus, which was high enough to perforate the cell membrane[8]. Another laser diode working at 980nm had a power of 400mW, which was used to trap and move cells as an optical tweezer. This laser was continuous wave and had no observable influence on the cells.

Human HepG2 hepatocellular carcinoma cells, obtained from American Type Culture Collection, were cultured in RPMI 1640 medium (Sigma) supplemented with 10% (v/v) fetal calf serum (FCS) (Gibco) or phenol-red free RPMI 1640 medium (Invitrogen) at 37°C and 5% CO_2. For microscopic studies, cells (3×10^5/ml)

were seeded on a 35mm pertri dish with a glass slide (0.17mm thick) at the bottom (MatTek).

3.2.2 Use of PI to show membrane perforation

In our study, PI was used to detect the effect of fs laser on the integrity of the plasma membrane. PI is a DNA fluorescent dye. When it binds to DNA, it emits red fluorescence when excited by UV or 488nm laser. Interestingly, PI can only pass through leaky or damaged plasma membrane to label the DNA in the cell nucleus in the late stage of apoptosis and any red fluorescence observed from live cells under the microscope is an indication of loss of membrane integrity. In our experiments, PI (final concentration 1.5ug/ml) was added into HepG2 cells with phenol-red free RPMI 1640 medium. After 20 minutes of incubation, no red fluorescence could be observed from the healthy cells. The fs laser was then targeted on the healthy cells each with an exposure time of 1 to 10 seconds. Fifty cells were exposed and they were kept on the stage of the microscope at 37°C and 5% CO_2. Red fluorescence was observed from all the cells two hours after the laser exposure (Fig. 3-3), whereas no fluorescence was obtained from cells without the exposure.

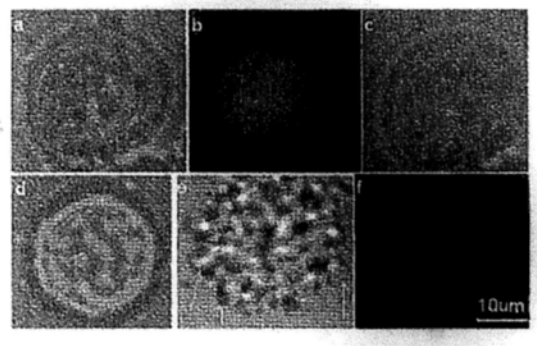

Fig. 3-3. Effect of fs laser on cell membrane. A healthy HepG2 cell at time zero was

exposed to fs laser for 5 seconds; white light (**a**) and red PI fluorescence (**b**) images were observed 2 hours after the fs laser illumination (t=2h). Three hours later, this cell was still viable (**c**) (t=5h). (**d**) is a healthy cell without laser exposure and no PI fluorescence was found at t=4h. As a control, photos of a dying cell judged by membrane blebbing (**e**) without fs laser illumination were taken at t = 2h and no red PI fluorescence was recorded at t=4h (**f**). Scale bar: 10um. White arrow: membrane blebbings on the dying cell.

Fig. 3-3a shows a micrograph of a healthy HepG2 cell under white light while Fig. 3-3b illustrates the red PI fluorescence from the same cell 2 hours after an illumination of 5 seconds with the fs laser at 1554nm. Three hours later, this cell was still in round shape with red fluorescence and no blebbing was found on the cell surface as shown in Fig. 3-3c, suggesting that the cell with fs laser exposure was still alive. As expected, healthy cells in the same dish without fs laser illumination could not be labeled by PI (Fig. 3-3d) indicating that PI could not pass through the plasma membrane of viable cell. For comparison, the photo of an early apoptotic cell judged by the membrane blebbings was also taken before the experiment and no fs laser illumination was performed on this cell (Fig. 3-3e). Again no red fluorescence could be obtained in this apoptotic cell 2 hours after the experiment (Fig. 3-3f). This demonstrates that PI could not diffuse into the early apoptotic cell either. Consequently, the possibility that the red PI fluorescence found in Fig. 3-3(b) was a spontaneous phenomenon during apoptosis can be eliminated. Taken together, our results demonstrate that holes might have been formed on the cell membrane after the exposure to the 1554nm fs laser beam. This process can be

applied to transfer DNA or other molecules into some target cells.

3.2.3 Recovery of the cell membrane

As it is clear that the fs laser pulses could puncture the membrane, it would be of interest to examine whether such holes could be sealed back or not. To study this, cells in a petri dish were divided into 2 groups, A and B, as shown in Fig. 3-4. At first, each of the Group A cells was exposed to the fs laser for 10 seconds, and presumably holes would be formed on their membrane. Immediately after that, PI was added into the buffer. If the membrane holes closed before the PI molecules had sufficient time to diffuse into the cells, the subsequently added PI could not label the DNA in the Group A cells. Then, cells in Group B were exposed to the fs laser for 10 seconds twenty minutes after the addition of PI. After a waiting period of 4 hours, it was no surprise that fluorescence was detected only in the Group B cells but not in the Group A cells. This strongly suggests that the membrane could mend itself during the incubation time with PI.

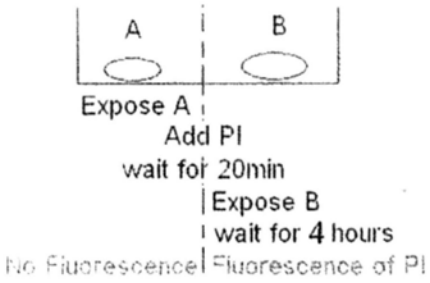

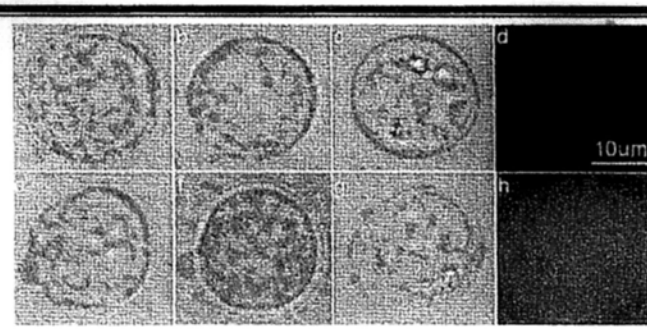

Fig. 3-4. Membrane sealed back after laser illumination. HepG2 cells in petri dish were divided into Group A (a-d) and Group B (e-h) and treated with fs laser at 1554nm for 10 seconds with the procedures as indicated. PI (final concentration 1.5ug/ml) was added after the first laser illumination. (**a**) the cell in Group A before laser exposure (t=0); (**b**) 20 minutes after laser exposure (t=20min); (**c**) the same cell with laser exposure and PI in the medium (t=4h 20 min); (**d**) fluorescence of the same cell; (**e**) the cell in Group B before laser exposure (t=20 min); (**f**) the same cell in Group B after laser exposure (t=20min); (**g**) the same cell under white light (t=4h 20min); (**h**) fluorescence of the cell in (f), (t=4h 20 min).

3.2.4 Cell viability

To determine whether cells underwent apoptosis (a programmed cell death process) after laser illumination, we examined whether the fs laser induced any mitochondrial depolarization, a key step in apoptosis [30], in HepG2 cells by using JC-1. JC-1 is a mitochondrial potential-sensitive fluorescent indicator. It exists in monomeric form in depolarized mitochondria and emits green fluorescence after excitation. In healthy cells with polarized mitochondria, JC-1 aggregates and emits red fluorescence. Therefore, from the JC-1 red/green (R/G) ratio, mitochondrial depolarization during apoptosis can be determined. In our study, JC-1 at a final

concentration of 10ug/ml was added to the culture medium. One hour after labeling, the JC-1signals were acquired and then the cells were exposed to the 1554nm fs laser for different time intervals. Fluorescence photos were taken before and 1.5 hours after the fs laser exposure and shown in Fig. 3-5.

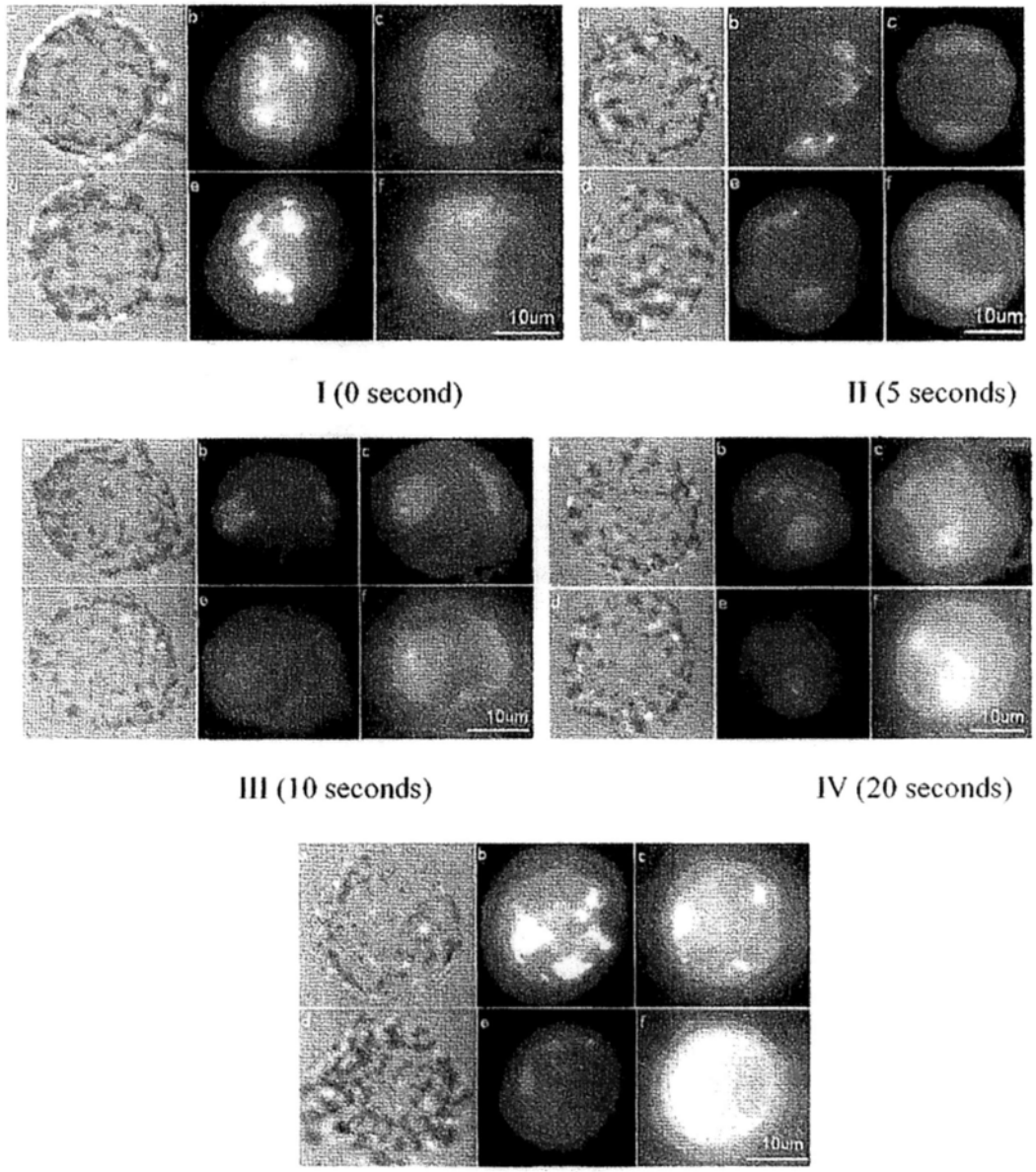

Fig. 3-5. Effect of fs 1554nm laser exposure on the mitochondrial depolarization in HepG2 cells determined by JC-1 fluorescence. HepG2 cells loaded with JC-1 (final concentration

10ug/ml) for 15 minutes. Subsequently, cells were exposed to the fs laser at 1554nm for the time as indicated (I-IV) or treated with valinomycin (1uM) for 5 minutes (V) at 37°C and 5% CO_2. Laser illumination time: I: 0s; II: 5s; III: 10s; IV: 20s. (**a**) and (**d**) are white light micrographs and the JC-1 red (**b**, **e**) and green fluorescence (**c**, **f**) of the cell were acquired before (a-c) and 1.5h after exposure (d-f). Bar: 10um.

Table 3-1. Average R/G Ratio of Cells at Different Exposure Times.

Exposure Time	0s	5s	10s	20s	Valinomycin Treated
R/G Before Exposure (15 cells)	1.31	1.46	1.07	1.18	1.15
R/G 1.5 h After Exposure (15 cells)	1.08	0.99	0.77	0.27	0.39

Fig. 3-5I is a control in which a healthy cell was not exposed to the fs laser, and the JC-1 red and green fluorescence were taken at time zero and 1.5 hours after. It can be seen that no significant change in both JC-1 red and green intensity was observed in the experiment. For comparison, Fig. 3-5V is a positive control treated with valinomycin (1uM), a classical K^+ ionophore that dissipates the mitochondrial membrane potential in cells. After valinomycin treatment, the JC-1 red signal was significantly reduced with a simultaneous increase in green signal, indicating the occurrence of the depolarization of mitochondrial membrane potential. According to the results depicted in Fig. 3-5II-III, the JC-1 red and green signals from the cells before and 1.5 hours after the fs laser exposure (5 and 10 seconds) were nearly the same as those of the control sample with no laser exposure (Fig. 3-5I), thereby

demonstrating that laser exposure times less than or equal to 10 seconds did not trigger mitochondrial membrane potential change, a process known as "the point of no-return" in apoptosis. If the exposure time was prolonged to 20 seconds (Fig. 3-5IV), the change in JC-1 red and green fluorescence was similar to the positive control sample shown in Fig. 3-5V. Obviously a laser exposure time less than 10 seconds is safe to cells.

3.2.5 Targeted transfection with GFP plasmid

Next, we employed the fs 1554 nm laser to introduce foreign DNA plasmids containing GFP gene pEGFP-C1 (4.7kb) into HepG2 cells to test whether the DNA would be expressed after transfection. In this experiment, 50 HepG2 cells adhering on a cover glass in 0.5ml of culture medium containing 20 μg plasmid DNA were individually exposed to the laser beam for 7 seconds. The temperature rise caused by fs beams was calculated to be only around 7K according to the physical model of a previous study, and was confined only in the focal volume. After illumination, the cells were cultured at 37°C and 5% CO_2 for GFP expression for 24 hours. Thirty-eight healthy cells in an elongated form emitted the green fluorescence as shown in Fig. 4, indicating that GFP was expressed. To eliminate the error introduced by cell proliferation (the doubling time of HepG2 is ~48 hours), adjacent cells were intentionally not exposed to achieve a minimum distance between any two exposed cells around 50μm. Consequently, if one single cell with green fluorescence was observed in an area 50μm by 50μm, it should be the mother cell.

In the case of two or more neighboring cells emitting green fluorescence, we only counted them as one transfected cell. This experiment was repeated twice, and 36 and 42 healthy cells with the GFP expressed were observed separately out of 50 exposed cells. Thus, the transfection efficiency was around 77.3% with a p-value of 2.82e-52 according to *Fisher exact test*. A control experiment was also performed in which cells were cultured with the same amount of DNA plasmids for 24 hours but without laser exposure and no fluorescence was found from all those cells, as shown in Fig. 3-6. The perforation of the transfected cells are shown in Fig. 3-7 after 48 hours of the transfection event, which means the transfected cells can not only survive, but also generate next generation.

Fig. 3-6. GFP fluorescence in HepG2 cells with targeted transfection. HepG2 cells were cultured at 37°C and 5% CO_2 for 24 hours. Adherent cells were then exposed to the 1554nm fs beam for 7s in the medium with a plasmid encoding enhanced GFP (final concentration 40ug/ml).

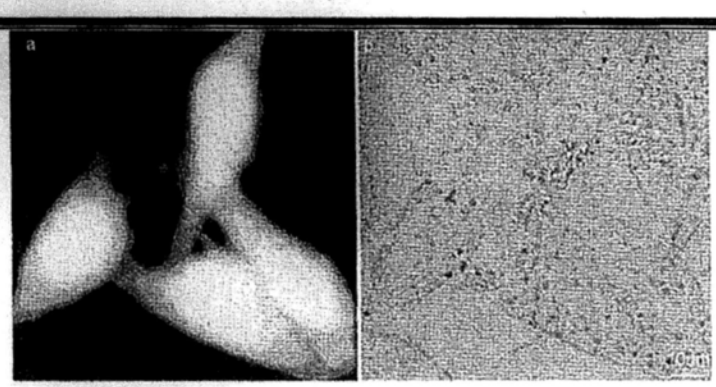

Fig. 3-7. Perforation of transfected cells. (a) Green fluorescence image of several HepG2 cells transfected with GFP plasmid; (b) image of the same cells with GFP expression under white light. Red arrows: cells transfected.

3.2.6 Discussions and conclusion

Finely focused fs pulses above the power threshold for drilling holes on the membrane can be understood as a process of free-electron introduction or plasma formation in the lipid layer [31], which is very similar to the optical breakdown in water [32]. Usually in such processes, water is treated as an amorphous semiconductor for simplification [33]. At a high photon density (10^{12}Wcm^{-2}), efficient multi-photon absorption inside the focus volume can excite electrons originally bound to molecules into the conduction band and set them free. These free electrons can then absorb more photons by some inverse Bremsstrahlung processes and gain a very high kinetic energy (1.5 times of the gap), enough to excite more free electrons. This process will continue to result in an avalanche growth of free electrons. When the density of the free electrons is large enough (10^{17}~10^{21}cm^{-3}), the plasma is formed.

To explain the different results obtained between 800nm and 1554nm illumination, we may invoke the following conjecture. The free electron density depends a great deal on the inverse Bremsstrahlung process, which is much more efficient when the photon energy is higher. Therefore, the avalanche growth of free electrons by the illumination at 800nm (1.56eV) is much more efficient than that at 1554nm (0.79eV) for the same photon density. Thus the plasma formed by 800nm pulses has an enormously higher free-electron density than the one by 1554nm pulses. The high-density-electron plasma resulting from 800nm laser pulses can easily generate a shock wave that can expand, and even produce cavitation bubbles [34]. Not only is the membrane opened this way, but also the cell will be inflicted with severe mechanical harm. Free electrons can also create reactive oxygen species (ROS) in water, forming OH^* and H_2O_2 , both causing cell damage. But for the plasma generated by 1554nm laser pulses, the shock wave is significantly weaker and most free electrons can be captured by the lipid molecules inside the focus volume. The bonds in the lipid molecules will be broken and hence the membrane is opened, by which safe transfection can be performed. Therefore, transfection by 1554 nm fs laser is safe.

Optical perforation for transfection is a clean, precise, and controllable method which can be achieved by fs laser pulses. Compared with 800nm Ti: Sapphire lasers, the 1554nm fiber laser is safe as evidenced by the viability study with JC-1. The high success rate of this cell-compatible method is due to the longer wavelength of the laser at 1554nm. Besides, the exposure time is easily controlled over a wide

window from 1 to 10s. Therefore, the photoporation and transfection by fs laser at 1554nm is an attractive solution for targeted transfection as the fiber laser is very compact and the system is very convenient to use.

3.3 Thermal Effect

Thermal effect of the laser is very important to biological samples since they are very sensitive to temperature and will die if the temperature is not suitable. The temperature rise by fs pulses is quite different from CW laser which is only related with linear absorption. However, in the focal volume of the fs beam, the temperature rise is mainly dependent on the free electron density induced and not very related with the linear absorption.

To estimate the temperature rise, two parameters need to be considered, the characteristic time for electron cooling (the transfer of kinetic electron energy during collisions, around a few picoseconds [35]) and at the time scale for recombination, which in water progresses through hydration of the free electrons, around only 300 fs [36]. Hence these two time constants are both longer than a fs pulse (100 fs). Therefore, the energy density deposited into the interaction volume is simply given by the total number density of the free electrons produced during the pulse multiplied by the mean energy gain of each electron. The mean energy gain of an electron is given by the sum of ionization energy $\tilde{\Delta}$ and average kinetic energy (5/4) $\tilde{\Delta}$ for free electrons produced by cascade ionization. Thus the plasma energy density is given by

$$\varepsilon = \rho^* \frac{9}{4}\tilde{\Delta} \qquad (3\text{-}1)$$

where ρ is the electron density. The temperature rise can be then

$$\Delta T = \varepsilon / \rho_m C_m \qquad (3\text{-}2)$$

where ρ_m is the mass density and C_m is the heat capacity of the medium. It can

be then estimate the temperature rise inside each pulse.

However, it should be noted that this estimation is only for the average thermal effect in the focal volume and inside only one pulse. In fact, in the practical case, the temperature rise is related with the pulse width, repetition rate of the pulse train, and the NA of the objective. It is very obvious that the pulse width and the repetition rate determine the accumulation of the heat. If the heat time is short, the heating duration will be short and then the thermal energy can diffuse away more rapidly. Also, if the space between two pulses is long enough for the heat produced by previous pulse decay away, there will be no accumulation of heat. The critical repetition rate is around 1 MHz, and those lasers with less than 1 MHz repetition rate can increase the temperature only in a single pulse.

The NA of the objective determines the focal volume. If the beam is tightly focused, the focal volume is very small and it is also good for the heat diffusion to the surroundings. Usually if the NA is larger than 1.0, there will be little accumulation of the heat. And if the NA is small, say, 0.6, the heat accumulation will significantly increase the temperature. Fig. 2-14 presents some numerical results of the thermal effect of the fs laser at 800 nm with a repetition rate 80 MHz focused by different objectives. It can be concluded the thermal effect of fs laser can be finely confined inside the focal volume, and is thus safe to biological samples. Besides, at the same inducing power, the thermal effect by fs beam is much less than by CW beam.

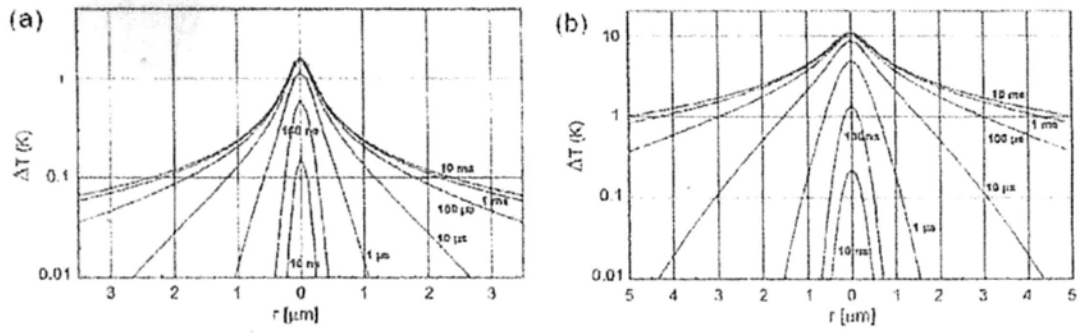

Fig. 3-8. Calculated temperature rise in water induced by fs laser at 800 nm with a repetition rate 80 MHz focused by different objectives. (a) NA=1.3. (b) NA=0.6. r is the distance from the center of the focus.

We would like to state that the ~10K temperature increase in single cell at the focal volume due to fs laser irradiation is commensurate with calculations based on established work and that the cells treated by our fs laser remain alive, as evidenced by the figures attached in below. These figures will not be included in the text because of limitations in the length of the article. The temperature rise caused by the fs laser can be accounted for by the total energy of the free electrons generated by MPI. The energy density deposited into the interaction volume is simply given by the density of free electrons produced during the laser pulse period multiplied by the mean energy gain of each electron. In our case with a photon density of 10^{13} W/cm^2, the free electron density can be estimated as 10^{20} to 10^{21} /cm^{-3} in the nonlinear volume where the laser intensity is high enough to cause MPI (usually FWHM of the peak power), while the mean electron density in the focal volume is around 10^{19}/cm^{-3} [we used the model developed by A. Vogel, J. Noack, G. Hüttman, and G. Paltauf, Applied Physics B: Lasers and Optics, **81**, 1015 (2005)]. The mean

energy gain of an electron is given by the sum of ionization energy and average kinetic energy, which is 9/4 times that of the ionization energy and which amounts to ~14.6 eV. The temperature rise in the focal volume is calculated by dividing the total energy gain by the heat capacity of water, which results in ~10 K. Of course, the temperature in the central part of the focal volume will be much higher than this value, but it will decay very quickly in less than one pulse duration and drop very sharply towards the edge of the focus region (corresponding to the distribution of free electron density). Since the free electrons are considered to be distributed only inside the focal volume, this kind of temperature rise is tightly confined inside a small part of the focus region, which therefore would not result in significant harm to the cells.

3.4 Proposed Mechanism

It is very hard to detect directly what happened when a fs pulse focuses in cell membrane since the process is too fast (less than 1 ps). Thus the mechanism of photoporation remains unclear. Mostly, people believe that the cell membrane can be open because the multiphoton ionization effect, which forms plasma to break the double layer lipid molecules. This point has a good indirect providence that the pulses at around 800 nm can open cell membrane with little thermal effect. However, there is an opinion that the thermal effect in a single pulse is quite different from the thermal effect of CW beam. The "femtosecond thermal effect" just simply changes the permeability of cell membrane without damage the lipid. Inside the pulse or even longer, the membrane seems to be "transparent". For transfection, this "transparence" should be long enough to let DNA molecules diffuse into cells. However, this can not explain why the fs beam can fuse cells (see next chapter) if the membrane keeps the integrality. Besides, the thermal diffusion is also a fast process, and will decay quickly in around some nanoseconds after the fs pulse. This is too short for the DNA molecules outside to diffuse into cells. Only if the fs pulses work as a control, or a "open" of the permeability of the membrane for a longer time, it can explain the photoporation.

To make this clear, we would like to investigate the details of cell membrane. The cell membrane consists primarily of a thin layer of amphipathic phospholipids which spontaneously arrange so that the hydrophobic "tail" regions are shielded from the surrounding polar fluid, causing the more hydrophilic "head" regions to

associate with the cytosolic and extracellular faces of the resulting bilayer. This forms a continuous, spherical lipid bilayer.

The arrangement of hydrophilic heads and hydrophobic tails of the lipid bilayer prevent polar solutes (e.g. amino acids, nucleic acids, carbohydrates, proteins, and ions) from diffusing across the membrane, but generally allows for the passive diffusion of hydrophobic molecules. This affords the cell the ability to control the movement of these substances via transmembrane protein complexes such as pores and gates.

Membranes serve diverse functions in eukaryotic and prokaryotic cells. One important role is to regulate the movement of materials into and out of cells. The phospholipid bilayer structure (fluid mosaic model) with specific membrane proteins accounts for the selective permeability of the membrane and passive and active transport mechanisms. It can be understood that the lipid can "flow" from time to time around the cell for the transportation, kinetic, and kinesis of cells.

A good example is the natural fusion of intracellular vesicles with the membrane (exocytosis). It not only excretes the contents of the vesicle but also incorporates the vesicle membrane's components into the cell membrane. The membrane may form blebs around extracellular material that pinch off to become vesicles (endocytosis). Besides, if a membrane is continuous with a tubular structure made of membrane material, then material from the tube can be drawn into the membrane continuously.

It should be noted that, although the concentration of membrane components in

the aqueous phase is low (stable membrane components have low solubility in water), there is an exchange of molecules between the lipid and aqueous phases.

Thus, the plasma formation mode (see section 2.4.1 in Chapter 2) can explain the photoporation like this. The plasma damages membrane, to form holes through which every thing can pass. But the lipid flow to the hole, and get contacting/connecting again in around less than 1 s, to reseal itself. Then the molecules can not enter the cell again.

However, since the permeability depends mainly on the electric charge of the molecule and to a lesser extent the molar mass of the molecule. Electrically neutral and small molecules pass the membrane easier than charged, large ones. When the fs pulse focused on the membrane, it may depolarize or polarize the membrane or the DNA molecule, which makes the membrane to form a kind of "open" or "transparent" to the DNA molecules, and they can diffuse into cells. After some time, everything recovers the original electrical charge and the membrane seems "resealed".

Till now, there is no experimental evidence of the mechanism of photoporation. It can be expected the fast AFM scanning can detect directly which actually happens when the fs beam "open" cell membrane.

3.5 Summary

With progresses in molecular biology, gene therapy is expected to assume a pivotal role in the treatment of genetic diseases, and thus transfection, which transfers genes, DNA, and other molecules into cells, becomes more and more important in biological and medical researches. Many methods of transfection have been developed in past 30 years, and physical approaches seem to be better than biological and chemical ways. Along with the development of femtosecond lasers, scientists tried to utilize such precise and efficient techniques in this area, and got successes. We firstly use the fs laser at 1554 nm which is quite widely used in optical communication for transfection and the efficiency is relatively high compared with Ti: Sapphire lasers. Besides, this fiber fs laser is much more compact, quite easy to move around, and very cheap. Not like Ti: Sapphire lasers, the commercial fiber lasers do not need any optical adjustments or maintenance for mode locking. People without any optical background can use them easily. This means such an optical transfection approach can be easily used in any other biological research labs.

The exposure time on cells by this laser also do not need strict control. Ranging from 1 s to 10 s, every mechanical or manual shutter can cover it. At the same time, the transfection efficiency is much higher than traditional methods, and even a little higher than Ti: Sapphire lasers. Probably this is due to the longer exposure time which enables larger chance of DNA molecules in the media diffuse into cells and also the lower density of plasma formed by the low-photon-energy of the 1554 nm

laser. Cells after the exposure can still generate daughter cells with GFP showed good viability. The thermal effect of the fs laser is much smaller than the CW one at the same wavelength and cells are well protected this way.

References

1. S. Mehier-Humbert and R.H. Guy, "Physical methods for gene transfer: Improving the kinetics of gene delivery into cells" Advanced Drug Delivery Reviews, vol. **57** pp733–753 (2005)
2. David J. Stephens and Rainer Pepperkok, "The many ways to cross the plasma membrane", PNAS, vol. **98** pp4295–4298 (2001)
3. D.J. Wells, "Gene Therapy Progress and Prospects: Electroporation and other physical methods", Gene Therapy, vol. 11, pp1363–1369 (2004)
4. Graessmann, A., Graessman, M., Hofmann, H., Niebel, J., Brandler, G. & Mueller, N. (1974) FEBS Lett. Vol. **39**, pp249–251
5. M.K. Chuah, D. Collen, T. VandenDriessche, "Biosafety of adenoviral vectors", Curr. Gene Ther. Vol. **3** pp527– 543 (2003)
6. Celis, J. E. Brookhaven Symp. Biol. Vol. **29**, pp178–196 (1978)
7. M.R. Capecchi, "High efficiency transformation by direct microinjection of DNA into cultured mammalian cells", Cell, vol. **22**, pp479–488 (1980)
8. T.M. Klein, E.D. Wolf, R. Wu, J.C. Sanford, "High-velocity microprojectiles for delivering nucleic acids into living cells", Nature, vol. **327**, pp70– 73 (1987)
9. N.S. Yang, J. Burkholder, B. Roberts, B. Martinell, D. McCabe, "In vivo and in vitro gene transfer to mammalian somatic cells by particle bombardment", Proc. Natl. Acad. Sci. U. S. A. vol. **87**, pp9568– 9572 (1990)
10. R.S. Williams, S.A. Johnston, M. Riedy, M.J. DeVit, S.G. McElligott, J.C. Sanford, "Introduction of foreign genes into tissues of living mice by

DNA-coated microprojectiles", Proc. Natl. Acad. Sci. U. S. A. vol. **88**, pp2726–2730 (1991)

11. K.E. Matthews, G.B. Mills, W. Horsfall, N. Hack, K. Skorecki, A. Keating, "Bead transfection: rapid and efficient gene transfer into marrow stromal and other adherent mammalian cells", Exp. Hematol, vol. **21**, pp697–702 (1993)
12. R. Heller, M. Jaroszeski, A. Atkin, D. Moradpour, R. Gilbert, J. Wands, C. Nicolau, "In vivo gene electroinjection and expression in rat liver", FEBS Lett. Vol. **389**, pp225–228 (1996)
13. McMahon JM et al. "Optimisation of electrotransfer of plasmid into skeletal muscle by pretreatment with hyaluronidase – increased expression with reduced muscle damage", Gene Therapy, vol. **8** pp1264–1270 (2001)
14. K. Mikata, H. Uemura, H. Ohuchi, S. Ohta, Y. Nagashima, Y. Kubota, "Inhibition of growth of human prostate cancer xenograft by transfection of p53 gene: gene transfer by electroporation", Mol. Cancer Ther., Vol. **1**, pp247–252 (2002)
15. Paras N. Prasad, *Introduction to biophotonics*, Wiley-Interscience, 2003
16. Karsten König, "Laser tweezers and multiphoton microscopes in life sciences", Histochem. Cell Biol. Vol. **114**, pp79-92 (2000)
17. H. Schneckenburger, A. Hendinger, R. Sailer, W. S. L. Strauss, and M. Schmidtt, "Laser-assisted optoporation of single cells", J. Biomed. Opt. vol. 7, pp410-416 (2002)
18. L. Paterson, B. Agate, M. Comrie, R. Ferguson, T. K. Lake, J. E. Morris, A. E.

Carruthers, C. T. A. Brown, W. Sibbett, P. E. Bryant, F. Gunn-Moore, A. C. Riches, and K. Dholakia, "Photoporation and cell transfection using a violet diode laser", Opt. Express, vol. **13**, pp595-600 (2005)

19. M. Tsukakoshi, S. Kurata, Y. Nomiya, Y. Ikawa, and T. Kasuya, "A novel method of DNA transfection by laser microbeam cell surgery," Appl. Phys. B, vol. **35**, pp135-140 (1984)

20. S. Sagi, T. Knoll, L. Trojan, A. Schaaf, P. Alken, and M. S. Michel, "Gene delivery into prostate cancer cells by holmium laser application," Prostate Cancer Prostatic Dis., vol. **6**, pp127-130 (2003).

21. S. K. Mohanty, M. Sharma, and P. K. Gupta, "Laser-assisted microinjection into targeted animal cells," Biotech. Lett. Vol. **25**, pp895-899 (2003)

22. Wataru Watanabe, Naomi Arakawa, Sachihiro Matsunaga, Tsunehito Higashi, Kiichi Fukui, Keisuke Isobe, and Kazuyoshi Itoh, "Femtosecond laser disruption of subcellular organelles in a living cell", Optics Express, Vol. **12**, pp. 4203-4213 (2004)

23. K. König, P. T. C. So, W. W. Mantulin, B. J. Tromberg, and E. Gratton, "Cellular response to near-infrared femtosecond laser pulses in two-photon microscopes," Opt. Lett., vol. **22**, pp135-136 (1997)

24. U. K. Tirlapur and K. Konig, "Targeted transfection by femtosecond laser," Nature **418**, pp290-291 (2002)

25. D. Stevenson, B. Agate, X. Tsampoula, P. Fischer, C. T. A. Brown, W. Sibbett,A. Riches, F. Gunn-Moore, and K. Dholakia, "Femtosecond optical transfection of

cells:viability and efficiency", Optics Express, Vol. **14**, pp7125-7133 (2006)

26. Schwarze, S. R., Hruska, K. A. & Dowdy, S. F. Trends Cell Biol. **10**, 290–295 (2000)

27. Tilkins, M. L., Hawley-Nelson, P. & Ciccarone, V. in Cell Biology: A Laboratory Handbook, ed. Celis, J. E. (Academic, Dan Diego), Vol. **4**, pp. 145–154 (1998)

28. Yong Liu, Leslie C. Mounkes, H. Denny Liggitt, Carolyn S. Brown, Igor Solodin, Timothy D. Heath & Robert J. Debs, "Factors influencing the efficiency of cationic liposome-mediated intravenous gene delivery", Nature Biotechnology, vol. **15**, pp167 - 173 (1997)

29. Uday K. Tirlapur, Karsten König, Christiane Peuckert, Reimar Krieg and Karl-J. Halbhuber, Femtosecond Near-Infrared Laser Pulses Elicit Generation of Reactive Oxygen Species in Mammalian Cells Leading to Apoptosis-like Death. Experimental Cell Research, 263, 88-97 (2001).

30. Smiley, S. T. et al. Intracellular Heterogeneity in Mitochondrial Membrane Potentials Revealed by a J-Aggregate-Forming Lipophilic Cation JC-1. Proceedings of the National Academy of Sciences of the United States of America, 88, 3671-3675 (1991).

31. F. Docchio, C.A. Sacchi, and J. Marshall, Experimental investigation of optical breakdown thresholds in ocular media under single pulse irradiation with different pulse duration. Lasers Ophthalmol. 1, 83-93 (1986).

32. C.A. Sacchi. Laser-induced electric breakdown in water. J. Opt. Soc. Am. B, 8,

337-345 (1991).

33. A. Vogel, J. Noack, G. Hüttman, G. Paltauf, Mechanisms of femtosecond laser nanosurgery of cells and tissues. Applied Physics B: Lasers and Optics, 81, 1015-1047 (2005).

34. Vasan Venugopalan, Arnold Guerra, Kester Nahen, and Alfred Vogel. Role of Laser-Induced Plasma Formation in Pulsed Cellular Microsurgery and Micromanipulation. Phys. Rev. Lett. 88, 078103 (2002).

35. B. Rethfeld, Phys. Rev. Lett. 92, 187 401 (2004)

36. S. Nolte, C. Momma, H. Jacobs, A. Tünnermann, B.N. Chikov, B. Wellegehausen, H. Welling, J. Opt. Soc. Am. B 14, 2716 (1997)

Chapter 4: Optical Cell-Cell Fusion

4.1 Introduction

At present, couples of cell fusion methods have been developed to introduce genetic molecules into cells or to produce hybrid cells with special properties such as the production of monoclonal antibodies [1]. It is thus a powerful tool for the analysis of gene expression, chromosomal mapping, monoclonal antibody production, and cancer immunotherapy [2]. After some biological techniques invented, for example, mixed cells could fused in the presence of Sendai virus [3, 4], polyethylene glycol (PEG) has become a standard chemical agent for cell-cell fusion [5] and is now quite popular especially in hybridoma technology. It is very easy and cheap to perform, and a very large number of cells can be fused in a short time, around a few minutes to hours. But the fusion efficiency is low, and the fusion pairs are out of control. Many unwanted fusion productions make this method complex on hybrid selection.

To solve such problems, people began to think about physical methods. Electric field was found to be able to break cell membrane and induce cell-cell fusion in 1980 [6, 7], and fusion efficiency was improved. However, new problems came out. Cells could not move to pairs themselves like in the method by PEG, and then it was very hard to find right cell pairs to fuse. Besides, electric field was hard to control. Meanwhile, another method, single ultraviolet (UV) lasers inducing cell fusion was

also found limited with this problem [8], although only it could fuse mammalian cells [8] while electric method could not. Considering moving cells by mechanical ways also causes harm to them, people noticed optical tweezers could manipulate cells [9], which, in fact, was developed to control atoms at first [10].

Optical tweezers were developed quite fast. It was also found laser beam at UV range harm cells very much due to the high photon energy, but at the near infrared (NIR) range, especially 1μm, cells have little absorption and other side effects [11]. Optical tweezers were introduced into the fusion system, and the UV beam was only used to fuse cells [12]. This is the first time people could fuse any targeted cells, and everything was under control except the harm to cells. To protect cells, femtosecond (fs) pulsed lasers at NIR range showed a lot of advantages [13, 14]. *Gong et al.* firstly fused yeast cells using an fs laser and 10% PEG [15], and we firstly fused human hepatocellular carcinoma (HepG2) and HeLa cells all-optically also by an fs beam [16]. Here some traditional methods for cell-cell fusion are introduced as following.

4.1.1 Virus mediated cell fusion

Originally, cell hybridization was an uncontrolled, apparently spontaneous event which occurred rarely when cells were simply mixed [17]. Harris and Watkins firstly fused cells with Sendai virus [18]. Like other paramyxoviruses, it consists of a ribonucleoprotein core and a lipoprotein envelope. Virus particles mature by budding from the cell surface, and the envelope contains virus-determined proteins

and lipids incorporated from the host cell. The bility to fuse cells may also depend on the resence of other components of the viral envelope. Since many cells carry eceptors for Sendai virus, including those of ifferent species, it became possible to fuse a variety f cell types, including differentiated and nondividing cells. But the fusion efficiency was not high, the fusion process was slow, and the system was out of control.

4.1.2 PEG mediated cell fusion

Polyethylene glycol (PEG) of high molecular weight is widely used to mediate cell-cell fusion. PEG causes the redistribution of intramembrane particles (IMPs) of cellular membranes, this ability being attributed to the ordering of water by high concentrations of the polymer. When aqueous solutions of PEG exceed 35%, cell aggregation and fusion are observed, although maximum fusion efficiency occurs at concentrations between 40 and 50%. Since all water is bound to PEG in solutions having concentrations of 35% by weight or greater, dehydration appears to play a role in PEG-mediated fusion. The fusion mechanism is as following: first, adjacent plasma membranes are brought into close apposition. Next, a transient destabilization of the normal bilayer structure of the apposed membranes occurs, leading to a molecular rearrangement which results in the continuity of the two membranes. Finally, the previously separated cytoplasmic compartments of the two cells become one. It permits fusion of large numbers of cells and takes only minutes to hours. The efficiency is still low and very different for different cell species.

Another drawback is it is difficult to select right hybrids, since cells some together very randomly. However, PEG was found very toxic to cells. Organelles were frequently found lost after fusion.

4.1.3 Cell fusion by electric field

Invented in 1980, the electric field-induced fusion technique avoids most of the disadvantages of the chemically and virus-induced fusion procedures, but it is hard to find right cell pairs to fuse, and electric field could also harm cells a lot. People tried to use special electrodes to drive cells come to contact [7]. At low electric field strengths the contact area between two adjacent spherical cells may be rather small. Suitable field strengths are in the range of 100 to 200 V/cm. In order to initiate cell fusion, closer membrane contact has to be established by increasing field strength of the a-c field for a very short time. The optimum conditions for the electric field-induced fusion process are achieved when the membranes of two adjacent cells flatten out on coming into contact with each, thus forming a relatively large zone of contact. Much higher field strengths result in stretching and deformation of the cells, budding and vesicle formation, particularly if the field strength of the a-c field exceeds the breakdown voltage of the membrane.

4.1.4 Cell fusion by UV lasers

Optical fusion system has two very important advantages: it has no mechanical contact with cells and could manipulate cells by optical tweezers. People could fuse

any cell pairs they wanted in a relatively clean environment. A milestone in such field was made by *M.W. Berns et al.* in 1991 [12]. They used a Nd:YAG laser at 1.06 μm and 220mW focused by a 63X objective as an optical tweezer to manipulate cells to anywhere they wanted. A pulsed dye laser at 366 nm was used to fuse cells they selected by a 2 to 8 minutes exposure. But the efficiency was very low. Only 1.3% cells were fused successfully in pure culture medium, and this efficiency could be improved to around 10% if PEG was added.

4.2 All-optical cell-cell fusion by a femtosecond laser at 1554 nm

Cell-cell fusion is a powerful tool for the analysis of gene expression, chromosomal mapping, monoclonal antibody production, and cancer immunotherapy [20]. One of the challenges of in vitro cell fusion is to improve the fusion efficiency without the need of adding extra chemicals while maintaining the cells alive and healthy. Steubing et al. (1991) first described the use of a nanosecond pulsed UV laser to fuse two single cells with an efficiency less than 10% [21]. Not only the high energy UV photons could harm cells a lot, but also the thermal effect by this long pulsed beam could not be confined. To overcome such disadvantages, Gong et al. used polyethylene glycol (PEG) and a Ti: Sapphire femtosecond (fs) laser to fuse yeast cells at a very high efficiency (80%) [15]. However, as PEG is used conventionally as a fusion chemical to generate hybridomas for monoclonal antibody production [22, 23], it is not clear whether the high cell fusion efficiency in the yeast system is due more to the effect of fs laser or of PEG. In fact, PEG is toxic to cells [24]. In this connection, we sought to develop a better method to fuse human cells solely by using an optical technique that does not involve PEG or any other chemical at all. And now here we show for the first time that human cancer cells can be fused by a finely focused femtosecond laser beam at 1550 nm all-optically with high fusion efficiency and the mixing of cytoplasm in the fused cells can be clearly observed.

In our work, we fused human hepatocellular carcinoma (HepG2) and HeLa cells

by using a femtosecond laser under an inverted microscope (Nikon TE2000U). The cells obtained from American Type Culture Collection were cultured in RPMI 1640 medium (Sigma) or phenol-red free RPMI 1640 medium (Invitrogen) supplemented with 10% (v/v) fetal calf serum (FCS) (Gibco) at 37°C and 5% CO_2. For fusion studies, the cells (3×10^5/ml) were seeded on a 35mm culture dish with a 0.17mm thick glass slide at the bottom (MatTek). In our entire experiments, no other chemicals for cell fusion were added while the cells were fused all-optically by an fs laser beam at the wavelength of 1550 nm.

Experimentally, the high intensity fs pulsed laser beam was directed into a 40X oil immersion objective (N.A.=1.0) of the microscope to finely focus at a sub-femtoliter volume of the cell membrane. The beam came from a fiber laser with a repetition frequency of 20MHz, an output mean power of 100mW and a pulse width of 200fs, was then collimated by a fiber collimator, and reflected by a dichroic mirror to couple into the objective. The coupling efficiency at 1550 nm was around 65% and the diameter of the focus of the beam was around 2 μm. Under this condition, the peak optical power density was larger than $10^{12}Wcm^{-2}$. This power level could photoionize the lipid and water at the interface of two contacting cells. The free electrons generated would puncture the membrane in the focal volume of the beam, providing a channel for contact and exchange of cytoplasm molecules from the two cells. The broken lipid membrane of the two cells could connect and join together because of the flowing property, forming a stable exchange channel, and this channel would be broaden by the increasing exchange of

the cytoplasm. Finally a hybrid cell was formed by the mixing of the cytoplasm [25, 26]. Photons at 1550 nm had a very low energy (0.79 eV), and thus it needed a nine-photon absorption to ionize one H_2O molecule (band gap 6.5eV). Compared with photons at 800 nm (1.56eV), which was needed only five to excite an H_2O molecule, the efficiency of the multi-photon ionization by 1550 nm photons would be much lower. And thus the illumination time for fusion by 1550 nm beam would be much longer than the previous work [15], around 5s to 10s.

To move a targeted pair of cells to contact with each other, a laser diode at 980 nm was also coupled into the same light path working as an optical tweezer. The output power of the 980 nm laser was 150 mW with a coupling efficiency of 60%, and it took usually no more than 20s to move the cell to the target. The influence of this optical tweezer to cells was very little according to the previous works [27]. As shown in Fig. 4-1(a), a HepG2 cell was moved to contact with another, and this cell pair was then illuminated by the fs beam at 1550 nm at for 10s at the contacting interface. Each pulse had a power at 1.6×10^{4}W. Afterwards, the two HepG2 cells were then incubated at 37°C and 5% CO_2. Ninety minutes later, the fusion process could be observed as shown in Fig. 1(b). The hybrid cell eventually became round and round as shown in Fig. 4-1(c) to (d).

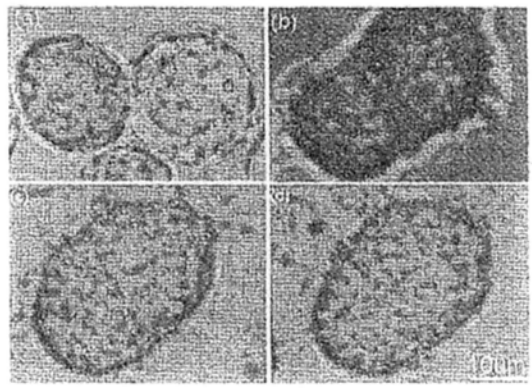

Fig. 4-1. A pair of HepG2 cells fused by a 1550 nm fs laser. (a) The targeted pair of HepG2 cells to be fused at laser power of 100mW for 10s. Red arrow: the laser spot at the interface of the two cells. (b) At 1.5 hours after laser exposure, the membranes fused together. (c) At 3 hours after exposure, the hybrid cell became rounded. (d) At 4 hours after exposure, the two contacting cells became one single hybrid cell. Bar: 10 μm. This is a typical example of 21 similar cases.

In this study, we had irradiated 56 HepG2 cell pairs by the fs laser, and 21 pairs were successfully fused. The efficiency was therefore around 37.5%. The unsuccessful cases might be due to the fact that cells were in loose contact and could not stick together tightly initially for fusion to take place. Also, since lipid could flow along the membrane, the cells might repair the holes in the membrane opened by the laser beam and thus close the exchange channel.

Next, we examined whether this method is cell type specific. In this regard, two contacting HeLa cells, one of which had been loaded with a non-toxic fluorescent dye calcein/AM (Molecular Probes) as a label, and was then moved by the optical tweezer to contact with the other without the dye, were irradiated by the same fs

laser for 10s and then cultured at 37°C and 5% CO_2. Subsequently, any mixing of cytoplasm between the two cells could be observed by the fluorescence under a UV microscope. Figure 4-2(a) shows the fused HeLa cell pair immediately after laser exposure. Here the fluorescence was observed to come from only the lower cell in the adjoining fluorescence micrograph. Two hours after laser fusion, the cell membranes were already connected together and calcein diffusion into the "upper" cell was seen, indicating that cytoplasm mixing had occurred, as displayed in Fig. 4-2(b). Fig. 4-2(c) reveals that the hybrid cell became rounded up four hours after fusion while Fig. 4-2(d) indicates that cytoplasm mixing was still continuing eight hours after fusion had taken place. In our experiment, 7 pairs were successfully fused among 20 exposed pairs. This efficiency of 35% was similar to that of the HepG2 cell-cell fusion.

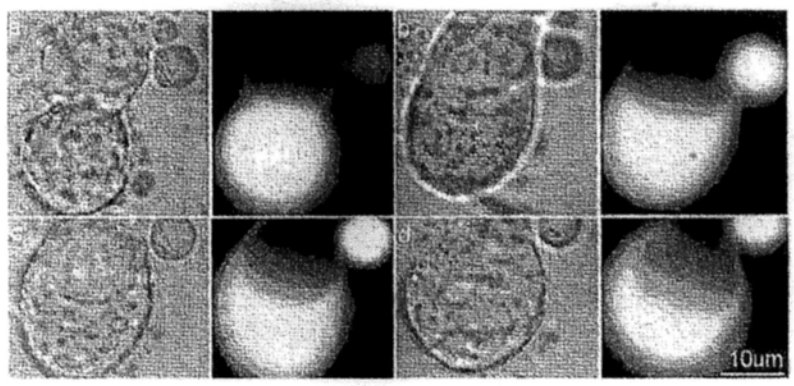

Fig. 4-2. Mixing of cytoplasm of fused cells. (a) Two HeLa cells were fused together in which one was loaded with calcein and the other was not. The two cells were exposed to the fs laser for 10s and cultured at 37°C and 5% CO_2. (b) Two hours later, the two membranes fused into one and calcein diffusion into the upper cell was observed. (c) Four hours later, more

calcein diffusion was observed and (d) The mixing of cytoplasm was still continuing at 8 hours after fusion. The bubble in the right was a fragment from other cells. Bar: 10 μm.

In order to test whether the artificial hybrid cell synthesized by fs laser fusion is viable, we added propidium iodide (PI) into the culture medium containing fused HeLa-HeLa cells. In principle, the plasma membrane of viable cells is impermeable to PI while that of apoptotic or necrotic cells allows PI to pass through, which subsequently labels the nuclear DNA by emitting a red fluorescence. Figure 4-3 compares the white light and UV images of a live HeLa-HeLa fused pair with those of a control dead cell. No red fluorescence was emitted by the fused cell 40 minutes after PI had been added to the culture medium at 4 hours after fusion. This strongly suggests that the hybrid cell was viable and alive.

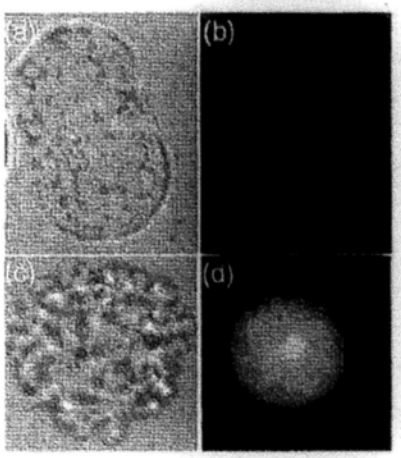

Fig. 4-3. PI test of the fused cells. (a) Image of the fused HeLa-HeLa cell at 4 hours after fusion; (b) absence of fluorescence signal from the fused cell; (c) Image of a control dead cell and (d) its associated red PI fluorescence. All images were recorded at 40 minutes after adding the PI.Paper size should be U.S. Letter, 21.505 cm x 27.83 cm (8.5 in. x 11 in.). The printing

area should be set to 13.28 cm x 21.54 cm (5.25 in. x 8.5 in.); margins should be set for a 2.54-cm (1 in.) top and 4.11-cm (1.625 in.) left, right, and bottom.

As a step further, we also investigated whether this fusion technique could be applied between two different cell types, such as HepG2 and HeLa. The HeLa cells were also loaded with calcein, and then mixed with HepG2 cells at 1:1. Thirty HepG2-HeLa cell pairs were irradiated by the fs laser for 10s and then cultured at 37°C and 5% CO_2. Fig. 4-4 shows that three hours after fusion, the two cells were already fused together. In our attempts, the fusion efficiency between HepG2 and HeLa was only 10%, much lower than in the case of HepG2-HepG2 or HeLa-HeLa. The cells not fused together might be due to the process of incubation. Because HepG2 and HeLa cells were both adherent and would flat on the bottom at 37°C and 5% CO_2, the deformation process of these two different cell types would be very different. And thus, after the exposure under the fs beam, the contacting cytoplasm of the two contacting cells might depart from each other during the incubation because of the different deformation ways, and thus they could not be fused together.

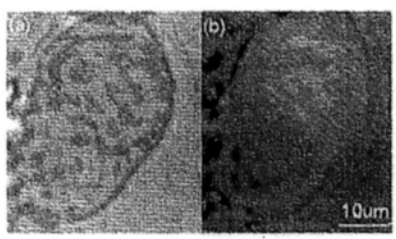

Fig. 4-4. A labeled HeLa cell was fused with a HepG2 cell without calcein. (a) A white light image of the hybrid cell taken at 3 hours after laser illumination. (b) Corresponding

fluorescence image of the hybrid cell. The cytoplasm of HeLa cell with calcein was shown in green. Fusion condition: exposure for 20s with 100mW laser power. Bar: 10 μm.

Just like HeLa-HeLa, the mixing of cytoplasm between HepG2-HeLa cells was also slow, taking longer than 8 hours. In the human lymphoid cell line TF228.1.16, the rate of cytoplasm fusion was slow as well (>6 hours after membrane fusion) [28]. In extreme cases, the cytoplasm did not exchange [29] at all. On the other hand, in human embryonic kidney 293T cells, the exchange of cytoplasm was as fast as within seconds [30]. The reason for this extremely different cytoplasmic mixing behavior is unclear at the moment.

In conclusion, we have developed an all-optical technique of using fs fiber laser at 1550nm to fuse together cells of either the same (HepG2-HepG2 and HeLa-HeLa) or different types (HepG2-HeLa) that exhibits a high efficiency and easy targeting without any detrimental effects. This method of synthesizing viable fused cells free of any chemical addition may become an important tool for cell-cell fusion in biotechnology and bioengineering.

4.3 Summary

Cell fusion happens naturally, but the ability to do it artificially provides cell biologists with a better understanding of the process. This in turn could lead to developments in genetic techniques and cancer treatments. Previous optics-based fusion techniques, such as the use of nanosecond-long pulses of UV light, have suffered from poor fusion success rates, about 10%, and surrounding cells were damaged by scattered light. Polyethylene glycol was found to improve the efficiency for fusing yeast cells, but it is toxic. Besides, the effect of solving lipids of PEG produces the argument of where the high efficiency comes from and the confusing mechanism of cell-cell fusion by lasers. Thus, the challenge of cell-cell fusion by lasers is to improve the efficiency, but at the same time keep the cells alive.

In this work, we take an all-optical approach that does not require any chemicals. Optical tweezers moved two human heptocellular carcinoma cells (HepG2) into contact. Pulses of light 200 fs long, at a wavelength of 1,550 nm were focused onto the contact area for about 10 s. The cells were then incubated for 90 minutes at 37 °C. The fusion was successful in 37.5% of the tests. Thermal effects were limited to the focal volume, reducing disruption to surrounding cells. The technique was also used to join two different types of cell, HepG2 and human cervical cancer cells, although this was achieved at a much lower efficiency of 10%.

The exposure time on cells by this laser, around 5 s to 10 s, very similar to the optical transfection, also do not need strict control. Mechanical or manual shutter

can cover this. The fs pulses generate plasma at the contacting interface of the cell pairs, which will open the membrane resulting in a free exchange for any molecules diffusing. The two cells can then exchange materials through this channel if it remains stable. After some hours, the broken membrane will connect again, but with the lipid from the other cell. In this way, the cells can be fused together. However, during the incubation period, if the exchange channel is unstable, for example, the two cells are not contacting very tightly, or the cytoplasm inside them have very strong kinetics, the fusion can not be finished. The membrane of the two cells will reveal them selves and be still independent. Unlike PEG solving effect, the exchange channel by the laser is very unstable. This factor is the reason of the low efficiency.

References

1. MATHEW M. S. LO, TIAN YOW TSONG, MARY K. CONRAD, STEPHEN M. STRITTMATTER, LYNDA D. HESTER & SOLOMON H. SNYDER, Monoclonal antibody production by receptor-mediated electrically induced cell fusion, Nature 310, 792 - 794 (1984)
2. U Trefzer, G Herberth, K Wohlan, A Milling, M Thiemann, T Sherev, K Sparbier, W Sterry, and P Walden, Int. J. Cancer **110**, 730 (2004).
3. PW Choppin, HD Klenk, RW Compans, LA Caliguiri, The parainfluenza virus SV_5 and its relationship to the cell membrane, Perspectives in Virology, 7, 127-158 (1971)
4. Scheid A, Choppin PW, Identification of biological activities of paramyxovirus glycoproteins. Activation of cell fusion, hemolysis, and infectivity of proteolytic cleavage of an inactive precursor protein of Sendai virus. Virology, 57, 475-90. (1974)
5. de StGroth SF, Scheidegger D, Production of monoclonal antibodies: strategy and tactics, J Immunol Methods.35, 1-21.(1980)
6. Neumann, E.; Gerisch, G.; Opatz, K., Cell fusion induced by high electric impulses applied to Dictyostelium, Naturwissenschaften, 67, 414-415 (1980)
7. U. Zimmermann, Electric field-mediated fusion and related electrical phenomena, Biochimica et Biophysica Acta (BBA) - Reviews on Biomembranes, Volume 694, 227-277 (1982)
8. Schierenberg E: Laser-induced cell fusion. Cell Fusion, Sowers AE (ed).

Plenum Press, New York, 1987, pp 409-418.

9. Ashkin A, Dziedzic JM, Bjorkholm J, Chu S: Observation of a single-beam gradient force optical trap for dielectric particles. Opt Lett 11:288-290, 1986.
10. Ashkin A: Trapping of atoms by resonance radiation pressure. Phys Rev Lett 40:729, 1978.
11. Paras N: Prasad, *Introduction to biophotonics*, Wiley-Interscience, 2003
12. R. W. Steubing, S Cheng, W. H. Wright, Y. Numajiri, and M. W. Berns, Cytometry **12**, 505 (1991)
13. R. M. Kuetz, X. Liu, and V. M. Elner, J. Refract. Surg. 13, 653 (1997)
14. A. Vogel, J. Noack, G. Hüttmann, G. Paltauf, Appl. Phys. B: Lasers Opt. 81, 1015 (2005)
15. Jixian Gong, Xueming Zhao, Qirong Xing, Fang Li, Huanyu Li, Yanfeng Li, Lu Chai, and Qingyue Wang, Appl. Phys. Lett. **92**, 093901 (2008)
16. Hao He, Kam Tai Chan, Siu Kai Kong, and Rebecca Kit Ying Lee, APPLIED PHYSICS LETTERS 93, 1 (2008)
17. B Ephrussi and M C Weiss, Interspecific hybridization of somatic cells, Proceedings of the National Academy of Sciences (1965)
18. HENRY HARRIS & J. F. WATKINS, Hybrid Cells Derived from Mouse and Man : Artificial Heterokaryons of Mammalian Cells from Different Species, Nature 205, 640 - 646 (1965)
19. Gereon Hüttmanna, Benno Radta, Jesper Serbina, Björn Ingo Langea and Reginald Birngruberа, High Precision Cell Surgery with Nanoparticles?

Medical Laser Application. Volume 17, 9-14 (2002)

20. Trefzer U, Herberth G, Wohlan K, Milling A, Thiemann M, Sherev T, Sparbier K, Sterry W, and Walden P., Vaccination with hybrids of tumor and dendritic cells induces tumor-specific T-cell and clinical responses in melanoma stage III and IV patients. Int. J. Cancer, **110**, 730-740 (2004)
21. R. W. Steubing, S. Cheng, W. H. Wright, Y. Numajiri, and M. W. Berns. Laser induced cell fusion in combination with optical tweezers: The laser cell fusion trap. Cytometry, **12**, 505- 510 (1991)
22. Richard L. Davidson and Park S. Gerald. Improved techniques for the induction of mammalian cell hybridization by polyethylene glycol. Somatic Cell and Molecular Genetics, **2**, 165-176 (1976).
23. Lane RD. A short-duration polyethylene glycol fusion technique for increasing production of monoclonal antibody-secreting hybridomas. J. Immunol Methods. **81**, 223-8 (1985).
24. T. H. Norwood, C. J. Zeigler and G. M. Martin. Dimethyl sulfoxide enhances polyethylene glycol-mediated somatic cell fusion Somatic Cell and Molecular Genetics. **2**, 263-270 (1976)
25. Vogel A, Noack J, Hüttmann G, Paltauf G. Mechanisms of femtosecond laser nanosurgery of cells and tissues. Appl. Phys. B, **81**, 1015-1047 (2005).
26. A.E. Wurmser and F.H. Gage, Cell fusion causes confusion, Nature, **416**, 485-486 (2002)

27. Mohanty S.K., Sharma M., Gupta P.K., "Generation of ROS in cells on exposure to CW and pulsed near-infrared laser tweezers," Photochem Photobiol Sci., **5**, 134-139 (2006)

28. Isabel Muñoz-Barroso, Stewart Durell, Kazuyasu Sakaguchi, Ettore Appella, and Robert Blumenthal. Dilation of the Human Immunodeficiency Virus-1 Envelope Glycoprotein Fusion Pore Revealed by the Inhibitory Action of a Synthetic Peptide from gp41. J. Cell Biol., **140**, 315-323 (1998).

29. Amir Sapir, Clari Valansi, Meital Suissa,Gidi Shemer, and Leonid V. Chernomordik. The C. elegans Developmental Fusogen EFF-1 Mediates Homotypic Fusion in Heterologous Cells and In Vivo. Benjamin Podbilewicz, Evgenia Leikina, Developmental Cell, **11**, 471-481 (2006).

30. Rika A. Furuta, Masao Nishikawa and Jun-ichi Fujisawa. Real-time analysis of human immunodeficiency virus type 1 Env-mediated membrane fusion by fluorescence resonance energy transfer. Microbes and Infection, **8**, 520-532 (2006).

Chapter 5: Analysis of Apoptosis Induced by Femtosecond Laser

5.1 Introduction

Failure of apoptosis may be one of the most important reasons of causing cancers and the anti-apoptosis protein, BCL-2 family, is found in the endoplasmic reticulum (ER) structures in cancer cells [1]. Naturally, apoptosis can be induced by the legation of death receptors in cell membrane stimulating the extrinsic pathway, or by the perturbation of intracellular homeostasis, the intrinsic pathway. The apoptosis is very complex, and a lot of probable mechanisms have been proposed to explain and describe such a process. Organelles inside cells will be all involved, but the most important participants are mitochondria [2], which are the main source of cellular adenosine triphosphate, also modulate and synchronize Ca^{2+} signaling. Ca^{2+} can be released from cellular calcium store under some other kinds of triggering or stimuli, and can be also taken up by mitochondria. It has long been recognized Ca^{2+} is also a participant in apoptotic pathways, and a prominent modulator of mitochondrial permeability transition controlled by the permeability transition pore. The permeability transition has been implicated as a mechanism of both apoptotic and necrotic cell death after selected stimuli. It has been found the overexpression of BCL-2 protects cells from death responsible for uptake of Ca^{2+} from the cytosol into the ER lumen [3]. Cells overexpressing BCL-2 display reduced ER Ca^{2+} concentration and decreased capacitative Ca^{2+} entry [4, 5].

Numerous pro-apoptotic signal transduction and damage pathways converge on mitochondrial membranes to induce their permeabilization (mitochondrial membrane permeabilization (MMP)). MMP differentially affects the outer membrane, which becomes protein-permeable, and the inner membrane, which continues to retain matrix proteins yet can dissipate the mitochondrial transmembrane potential ($\Delta\Psi m$). The temporary order of outer and inner membrane permeabilization, as well as their relative contributions to cell death, are a matter of debate and probably depend on the MMP-initiating stimulus. MMP triggers the activation of catabolic hydrolases, mainly caspases and nucleases. Such hydrolases are activated secondarily to the release of proteins that are normally strictly confined to the mitochondrial intermembrane space, in particular cytochrome c and apoptosis-inducing factor (AIF, which activates a DNase located in the nucleus).

Numerous proteins translocate to, reside in, act on or are released from mitochondria in different models of cell death induction, and the most important one is BCL-2, with members like Bax and Bak. It is a continuing conundrum whether Bax-like proteins form pores and induce MMP autonomously or whether they induce MMP upon interaction with a multi-protein complex built up at the contact sites between the outer and inner membranes, the permeability transition pore complex [6, 7]. Besides, reactive oxygen species (ROS) and ions like Ca^{2+} also take their own roles in forming MMP. This is very direct and significant if the cells are stimulated by some physical tools, after which a lot of ROS and Ca^{2+} will be generated. It should be noted MMP depends on the membrane potential, which can

be depolarized by ROS and uptake of too much ions. ROS and Ca^{2+} released from mitochondria or other resources can then induce more mitochondria depolarized. In such a loop, if the volume of ROS and Ca^{2+} is too much, ROS and Ca^{2+} will be accumulated in cells and MMP will be caused in more and more mitochondria. However, since this mechanism is too complicated, a lot of unclear processes remain still arguments, and the probable mechanism can be shown in Fig. 5-1 [2].

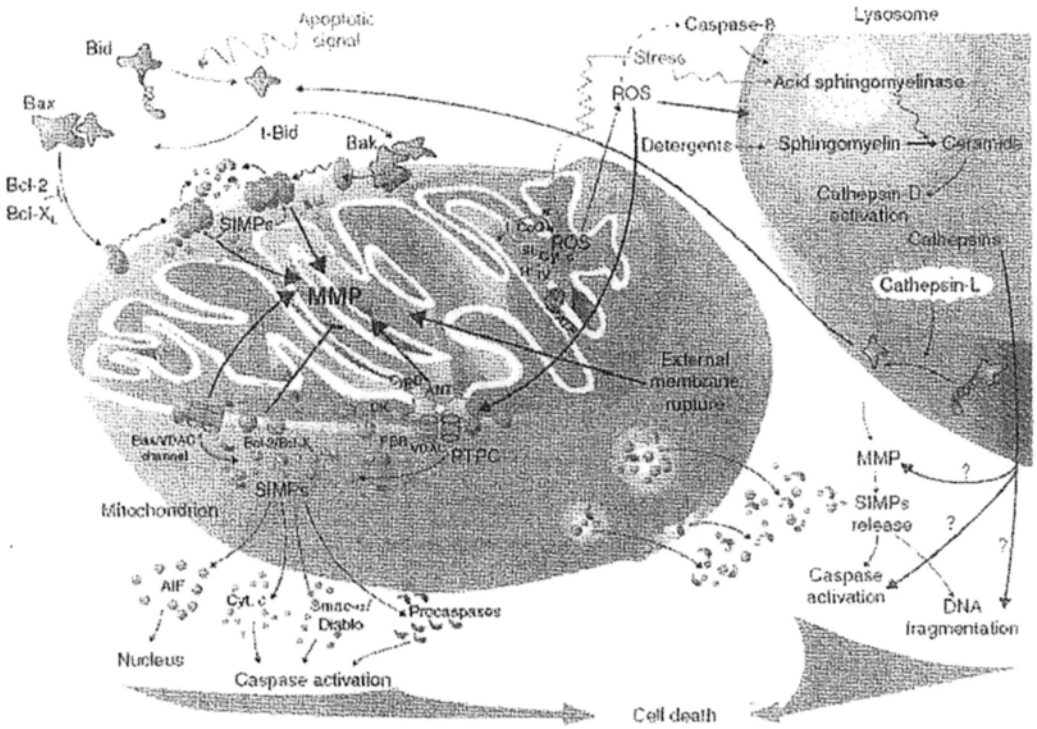

Fig. 5-1. Proposed organelle-specific permeabilization reactions in apoptosis [2].

Nuclear DNA damage is also an important process during cell death and finally forms DNA fragmentations. It seems that the apoptotic DNA damage response is mediated mainly by MMP induction. However, the interactions between those organelles are very complex and it is very difficult to get a clear regulation by which the cell dies step by step. But signals passing apoptosis messages between

organelles and inner and outer of nucleus have been well studied. These signaling are related with the ER and nuclear membrane, which can pass those signals into nucleus. The mechanism of how such signals diffuse into nucleus also remains unclear. Fig. 5-2 shows the summary and a plausible mechanism of the programmed cell death.

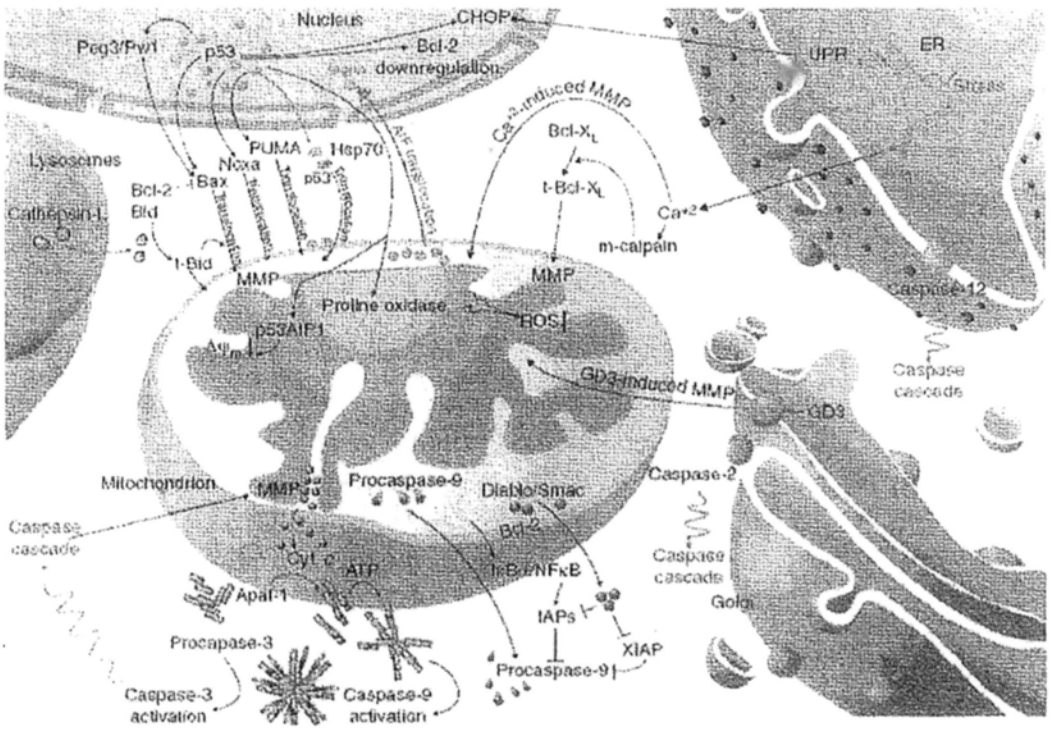

Fig. 5-2. Proposed interactions between organelles during apoptosis [2]. The most important player is the mitochondria. The resources of those molecules and how they diffuse in cells are the problems we are trying to solve.

5.2 Mechanism of oxidative stress generation in cells by localized near-infrared femtosecond laser excitation

Using lasers to manipulate cells is a very useful and fast developing technology [8]. In particular, pulsed lasers, especially femtosecond (fs) lasers, have been applied to precise microsurgery on cells [9], cell transfection [10], cell fusion [11] and multiphoton imaging [12]. All of these applications need to focus the beam to a tiny focal volume to create a high density of localized photons. However, this may induce undesirable side effects such as DNA fragmentation [13], mitochondrial transmembrane ($\Delta\psi m$) depolarization, or generation of ROS [14], which can trigger stem cell differentiation [15] and programmed cell death [16]. Hence, the effects of laser irradiation on cells should be investigated more thoroughly in order limit their potential damage. In this study, we compared the effects of continuous-wave (CW) lasers at both 1550 nm and 980 nm with an fs fiber laser at 1554 nm on the production of ROS, $\Delta\psi m$ depolarization and DNA fragmentation in a human hepatocellular carcinoma cell line, HepG2, under different excitation conditions. Based on our experiment results, we propose that the ROS are generated mainly by the induced thermal effect due to laser excitation and partly by the free electron liberation in the case of fs laser excitation.

In our setup, the laser light was coupled to a Nikon TE2000U inverted microscope with a 40X objective lens (N.A.=1.0). There were three lasers in this study and the diameter of the laser beam focus was around 2 μm (~ λ/N.A.), corresponding to an area of 3×10^{-8} cm^2. The fs fiber laser had a central wavelength

at 1554 nm and a repetition frequency of 20 MHz with a maximum mean power around 100 mW and a pulse width around 170 fs (the peak power was thus ~10^5 W, and the peak photon density in the focus region was ~10^{13} Wcm^{-2}). The other two were CW lasers at 1550 nm with a variable power up to 120 mW and at 980 nm with a maximum power up to 350 mW. These lasers were fiber-coupled into the microscope to excite target cells with an efficiency of around 70 %.

Human HepG2 cells, obtained from American Type Culture Collection, were cultured in RPMI 1640 medium (Sigma) supplemented with 10% (v/v) fetal calf serum (FCS) (Gibco) or phenol-red free RPMI 1640 medium (Invitrogen) at 37℃ and 5% CO_2. For microscopic studies, cells (3×10^5/ml) were seeded on a 35 mm culture dish with a glass slide (0.17 mm thick) at the bottom (MatTek).

The ROS inside the HepG2 cells were measured by loading the cells with dihydroethidium bromide (DHE, Invitrogen, final concentration: 5 μM) and detecting the red fluorescence emitted by the ROS thus labeled. The cells had been randomly selected and assigned to one of four groups, where they were individually and separately irradiated by the CW laser at 1550 nm and 80 mW, CW laser at 980 nm and 120 mW, the fs laser at 1554 nm and 80 mW, and no laser at all. The laser power at 980 nm was higher in order to compensate for its higher loss since the optical components in this system were designed for 1550 nm. The laser exposure time was 10 s in all the cases and the laser powers were commonly used levels for optical transfection (fs laser). After laser exposure, the fluorescence intensity (FI) of DHE from each cell was recorded by a CCD camera at different times with the

shutter open for 1 second at the excitation wavelength of 510 nm as shown in Fig. 5-3. The temporal FI signals averaged over 50 samples each and normalized by the signal at time=0 were then plotted and shown in Fig. 5-4. As can be seen in Fig. 5-3, the control Cell IV receiving no laser illumination showed the least FI, while Cell I illuminated by CW 1550 nm laser gave the strongest FI, followed by Cell II (fs 1554 nm laser) and then Cell III (CW 980 nm laser). The FI measured represents the amount of ROS produced. Besides, we also tested different exposure durations ranging from 5 seconds to 30 seconds, and found they did not significantly affect the rate of increase of the FI (data not shown). From these results, we hypothesize that ROS are mainly generated by the thermal effect of lasers, which can heat the cell up to a maximum stable temperature within a short interval of 10 ms [17]. It is this fast response time that explains why the FI obtained from longer exposures are not much different from those obtained at shorter exposures.

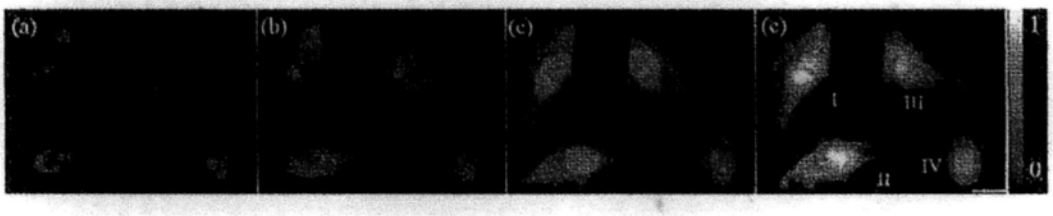

Fig. 5-3. The ROS response from cells exposed to different lasers. I: CW 1550 nm laser; II: fs 1554 nm laser; III: CW 980 nm laser; IV: no laser illumination. Panels A to D are typical results recorded respectively at 1, 5, 10, and 15 minutes after laser exposure. Bar: 10 μm. Color palette: the relative DHE fluorescence. Green cross: laser focus.

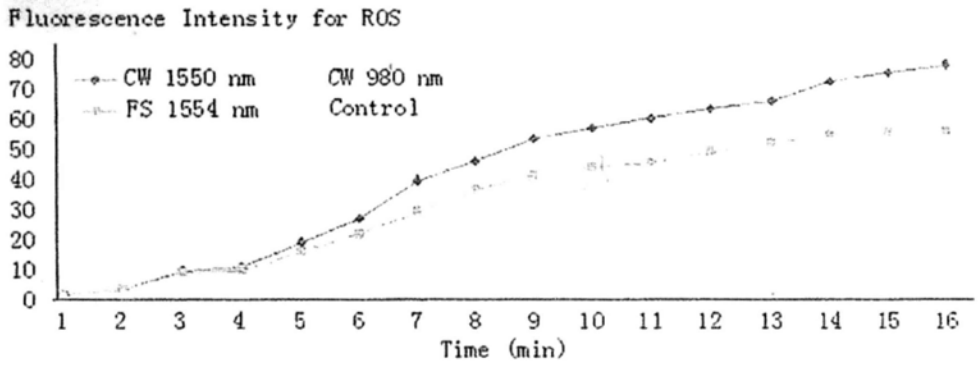

Fig. 5-4. The temporal ROS response from cells after different laser exposures. The plots show the normalized signals [FI(t)/FI(0)] versus time.

To study the mechanism of ROS generation by laser irradiation and where the source of ROS is, we added sodium azide into the culture medium to inhibit the mitochondrial electron transport chain (ETC) in cells so that ROS from the mitochondria would have been liberated completely after this treatment. We reason that if laser light acts on the same path as sodium azide does, there will be no more ROS generation by irradiating the treated cells with laser. In this set of experiments, cells were treated with sodium azide at a final concentration of 50 μM for one hour and then DHE was added. Fluorescence measurements were made after staining the cells with DHE. Five minutes later, three cells in one group were given different laser treatments. The first was exposed to the CW 1550 nm laser, the second to the fs 1554 nm laser, both for 10 seconds, while the last received no laser treatment as control. Fluorescence was recorded again afterwards and results from averaging 39 groups are shown in Fig. 5-5. It is worth to note that the control cell (only sodium azide treated) and the cell exposed to both sodium azide and subsequent CW laser excitation showed a similar response as shown in Fig. 5-5(a). Coupled with the

previous hypothesis regarding the generation of ROS from thermal effect, one can further infer here that the thermal effect can generate ROS only when the mitochondria are intact. Once the mitochondria ETC is disrupted by the sodium azide, the laser induced thermal effect cannot generate any more ROS than that caused by sodium azide alone as observed. On the other hand, the fs laser could somehow elicit an additional FI signal. This can be seen more clearly in Fig.3(b), which shows the relative change of the FI shown in Fig. 5-5(a) for each successive minute that is calculated by [FI(t+1)- FI(t)]/<FI>, with <FI> being the average intensity over 39 samples. The peak at the sixth minute observed only from the fs laser excited cell is a direct and obvious result of the fs laser excitation. It is therefore quite possible that fs laser excitation can also generate ROS from some other avenue as will be discussed in below.

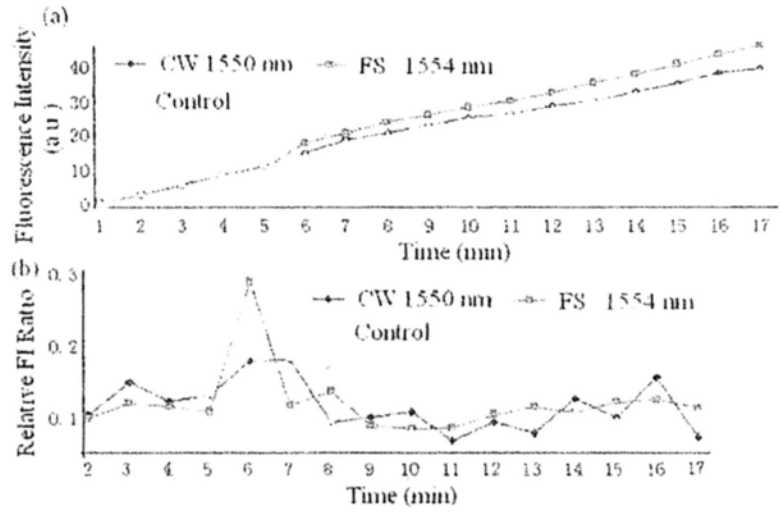

Fig. 5-5. The temporal ROS response from cells exposed to different lasers in the presence of sodium azide. (a) The normalized intensity [FI(t)/FI(0)]. (b) The ratio of relative change in the FI calculated by [FI(t+1)- FI(t)]/<FI>

Subsequently, we studied the depolarization of mitochondria $\Delta\psi m$ by ROS after laser exposure, which could induce cells to undergo apoptosis [18]. In this investigation, the cells were loaded with JC-1, whose fluorescence would turn from red to green when mitochondria were depolarized, and the Red/Green fluorescence ratio was calculated from the fluorescence signals collected by the CCD camera and treated as an indicator of the degree of depolarization. Three cells chosen randomly as a group were irradiated by the three lasers under conditions identical to those used in the ROS study described above. Both the red and green JC-1 fluorescence were recorded before and after the laser exposure, as shown in Fig. 5-6. The average R/G ratios from the 50 groups were calculated and shown in Table 5-1. The extent of increase in $\Delta\psi m$ depolarization due to laser irradiation is observed to be consistent with the ROS response behavior: Set I (CW laser at 1550 nm) > Set II (fs laser at 1554 nm) > Set III (CW laser at 980 nm). Set IV is the control receiving no laser treatment. For the positive control shown in Set V, it had been treated with valinomycin (1 μM), a classical K^+ ionophore that dissipates the $\Delta\psi m$, for 30 minutes [19], which caused a significant reduction of the JC-1 R/G ratio, thereby verifying the occurrence of the depolarization of $\Delta\psi m$. Since this depolarization behavior of mitochondria correlates well with the extent of ROS generation when the cells were subjected to the same laser excitation, the ROS must originate from the mitochondria.

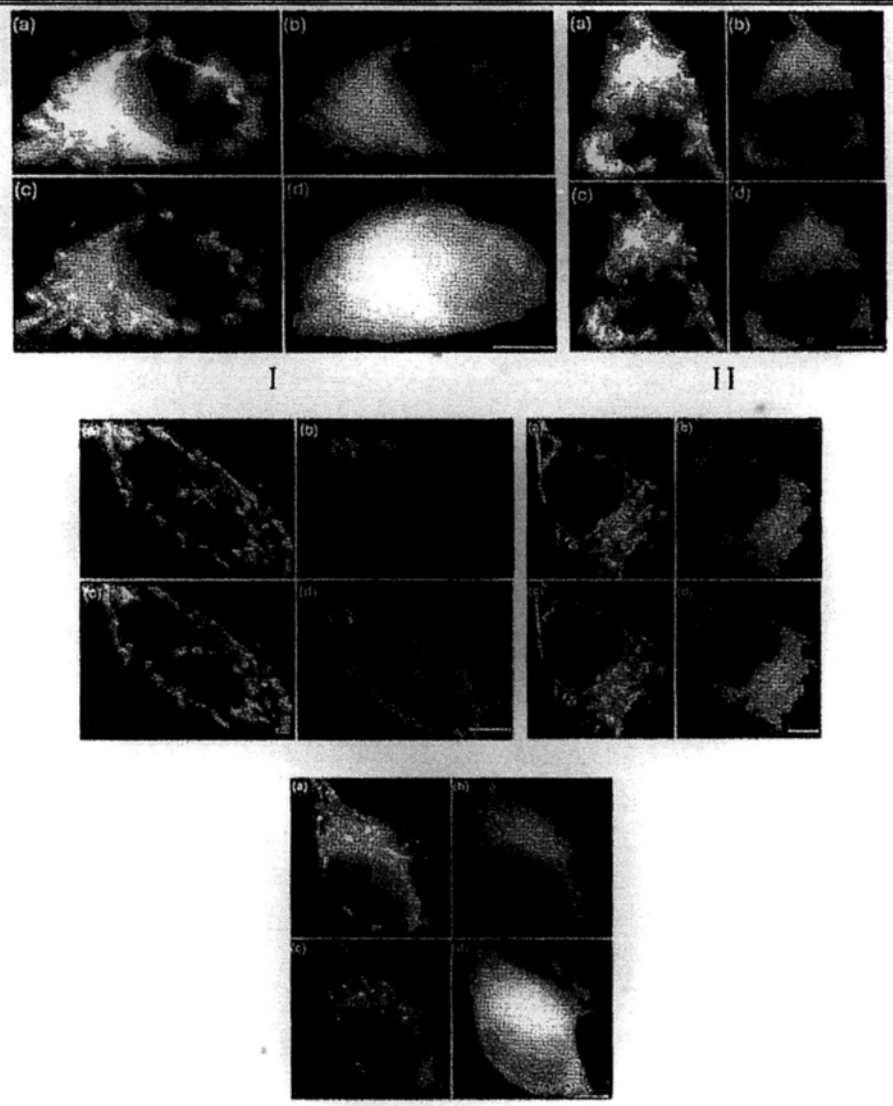

Fig. 5-6. Effect of different lasers on the mitochondrial depolarization in HepG2 cells loaded with JC-1. The changes in $\Delta\psi m$ from cells exposed to different lasers were determined by using JC-1 and fluorescence microscopy. HepG2 cells after loading with JC-1 (final concentration of 10 μg/ml) as described in the 'Materials and Methods' were exposed to different lasers for 10 seconds at room temperature. Five minutes after laser exposure, both the JC-1 red and green fluorescence were captured with appropriate band pass filter. Laser illumination: (I) CW laser at 1550 nm; (II) CW laser at 980 nm; (III) fs laser at 1554 nm. (IV)

cells without any laser exposure. (V) cells treated with valinomycin (1 μM) for 30 minutes without laser illumination. Panels (a, c) and (b, d) were the JC-1 red and green images, respectively, acquired before (a, b) and 5 minutes after laser exposure (c, d). Bar: 10 μm. Green cross: laser focus.

Treatment	I: CW 1550 nm laser	II: fs 1554 nm laser	III: CW 980 nm laser	IV: No laser Exposure	V: Valinomycin
R/G Before Exposure	2.98 ± 0.34	3.17 ± 0.26	3.04 ± 0.41	3.06 ± 0.35	2.81 ± 0.32
R/G After Exposure	0.61 ± 0.57	1.93 ± 0.47	2.10 ± 0.46	2.76 ± 0.39	0.28 ± 0.19
Net Change	2.37	1.24	0.94	0.30	2.53

Table 5-1. Changes in the mitochondrial potential of HepG2 cells after exposure to different lasers. The changes were determined by the JC-1 Red/Green fluorescence ratio. (I) CW laser at 1550 nm; (II) CW laser at 980 nm; (III) fs laser at 1554 nm; (IV) cells without any laser exposure; (V) cells treated with valinomycin (1 μM) for 30 minutes without laser illumination.

To explore the degree of apoptosis induced by laser excitations, DNA fragmentations in cells receiving different laser treatments were examined by the TUNEL assay [20]. As shown in Fig. 5-7, the severity of DNA damage caused by these lasers as measured by the fluorescence intensity was (in descending order): CW laser (1550 nm) > fs laser (1554 nm) > CW laser (980 nm).

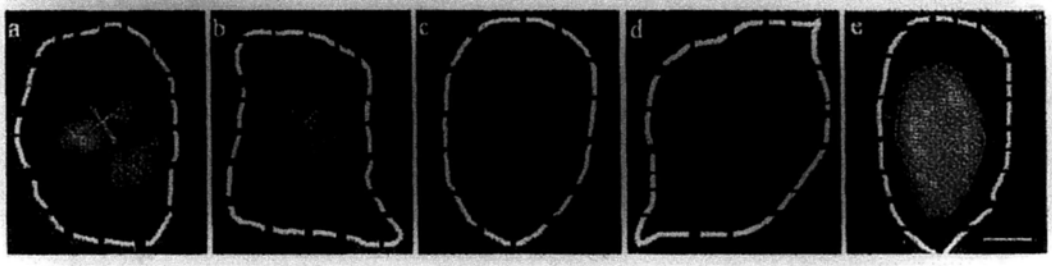

Fig. 5-7. DNA fragmentations induced by lasers focused at site X as indicated in HepG2 cells. Cells have been exposed to:'(a) CW laser at 1550 nm; (b) fs laser at 1554 nm; (c) CW laser at 980 nm; (d) medium alone; and (e) staurosporine (0.7 μM). Dotted line: cell shape. Bar: 10 μm.

The above findings can be discussed as follows. The absorption coefficient of water at 980 nm is 0.5 cm^{-1} and the temperature rise in the focal volume was estimated to be about 2.7 K, which was too small to produce any significant ROS. By contrast, the absorption coefficient at 1550 nm was around 9.6 cm^{-1} so that the local temperature rise due to the CW 1550nm laser at the same power level was estimated to be 30 K. It is therefore quite reasonable to assert that it was this large thermal effect that caused such a significant ROS production in samples treated with CW 1550 nm laser. The similar behavior between the CW 1550 nm laser treated sample and the control sample in terms of DHE FI as shown in Fig. 5-5 strongly suggests that the ROS generated in the former sample should occur preferentially in the mitochondria, and only by means of thermal effect. In the case of fs laser excitation at 1554nm, the final temperature rise can be evaluated from the total energy of the free electrons generated. In our case, the free electron density in the nonlinear volume can be estimated as 10^{20} to 10^{21} cm^{-3} (nonlinear volume refers

to the region where the photon density is high enough to cause nonlinear effect, such as MPI; here the photon density is ~10^{13} W/cm^2, corresponding to the field strength around 100 MVcm^{-1}, which according to the model of Keldysh [21] can ionize one H_2O molecule to free one electron from 9 photons at 1554 nm and cause further impact ionization to create MPI) while the mean free electron density in the focal volume is around 10^{19} cm^{-3}. The average energy gain of an electron is given by the sum of the ionization energy and the average kinetic energy, which is 9/4 times that of the ionization energy and which amounts to ~14.6 eV. The temperature rise is then calculated by dividing the total energy gain of the free electrons in the focal volume by its heat capability, which results in ~10 K. Since the free electrons are distributed only inside the focal volume, this kind of temperature rise is tightly confined within a small part of the focal volume, which therefore would not create significant harm to the cells. As this temperature increase will not produce much ROS, there must an additional avenue for ROS generation. This other avenue naturally comes from the free electrons described in above, which can generate ROS in an aqueous environment by the following dissociative attachment (DA) process:

$e + O_2 \rightarrow O_2$-;

$2O_2$- + $2H_2O \rightarrow O_2 + H_2O_2 + 2$ OH(*)

The spike signal from the fs laser treated sample shown in Fig. 5-5(b) tends to confirm this hypothesis because even the CW 1550 nm laser treated sample did not show any extra signal above that of the control sample as the CW beam has little

nonlinear effect. This hypothesis is further supported by the behavior of $\Delta\psi m$ depolarization induced by ROS shown in Table 5-1. From the data shown, the net change of mitochondria polarization due to fs beam (1.24-0.3=0.94) is slightly less than 50% of that due to the CW 1550 nm laser (2.37-0.3=2.07), where 0.3 is subtracted from the tabulated net change to account for photo-bleaching. If the net change of $\Delta\psi m$ depolarization can be considered to represent the degree of ROS generation caused by local heating of mitochondria, then one may argue that the amount of ROS due to the fs laser is slightly less than 50% of that due to the CW 1550 nm laser. However, the ROS generated by the fs laser is more than 70% of that by the CW laser from data shown in Fig. 5-4. These two results can reconcile with each other only if the fs laser has another mechanism to generate extra ROS apart from the thermal effect acting on mitochondria. This additional mechanism is nothing other than the DA process enabled by the free electrons liberated by the fs laser beam.

In conclusion, our study has clarified the mechanism of ROS generation in animal cells by the fs laser, which is through both thermal effect and free electron generation. It can be inferred that a fs laser at around 1000 nm will have little thermal effect while possessing the ability to liberate appreciable quantities of free electrons in the cells. Since ROS are critical in many biological processes, our study may help the selection of an optimal laser for specific biological or medical applications.

5.3 Role of nuclear tubule on the apoptosis of HeLa cells induced by femtosecond laser

Failure in the induction of apoptosis or programmed cell death is one of the major contributions to the development of cancer and autoimmune diseases [22]. With the intense research effort in the past 15 years, specific apoptogenic molecules such as cytochrome *c*, caspases, anti- and pro-death BCL-2 family proteins have been identified [23]. During apoptosis, apoptogenic proteins will be released from mitochondria, and double-stranded DNA will be broken down into small fragments, a hallmark of apoptosis. Although signals for DNA fragmentation during apoptosis have well been studied [24], however, the mechanism of how the signals diffuse into nucleus remains unclear. It has been reported that the nuclear envelope (NE) forms tubular or tunnel-like structures inside the nucleus to facilitate apoptosis after stimulation with apoptotic chemicals [25-27]. These nuclear tubule (NT) structures are double-membrane invaginations of NE and usually orient to the center of nucleus horizontally or vertically. However, to induce apoptosis, staurosporine A, a common apoptogenic agent, has to be added and incubated for 24 hours. And then there will be some percentages of cells undergoing the apoptosis program, and it is hard to select them out. Besides, the time slot of when the cells going to the programmed death is unknown and totally out of control. Thus there are few progresses on the research of NTs due to these limitations of traditional chemical methods.

In this study, we exposed target cells to a femtosecond laser at 1554 nm under

microscope, which can trigger apoptosis in seconds but keep cells in shape for observation [28]. We found that all the cells exposed for 40 s significantly exhibited more NT development inside their nuclei 6 hours after illumination. In one such experiment, the development of a NT was observed since its start after laser illmination, and it was found that the NT was eventually merged with another one to form a larger NT. Meanwhile, mitochondria and tubulin (a track for mitochondrial motility) were found inside the NT. In the TUNEL (Terminal deoxynucleotidyl transferase dUTP nick end labeling) assay [29], more signals for DNA fragmentation were found in the region around the NTs. Our results therefore strongly suggest that NTs are developed during apoptosis and mitochondria migrate into the nucleus through the NTs to release death signals to trigger DNA fragmentation. Obviously, our method provides a precise direct trigger at the subcellular level to observe dynamic changes in the cell nucleus during apoptosis when compared to other invasive interventions.

To induce apoptosis, cells were selected randomly and exposed under the fs laser for 40 s. This exposure time was used according to our previous test [30]. Six hours after fs laser illumination, formation of NTs was studied by using confocal microscopy and DiOC6(3), a fluorescent dye for staining internal membrane. In our experiment, 80 cells were treated with the laser for 40 s. The interaction between the laser and cells is mainly multiphoton absorption and thermal effect [31], causing ionization and temperature rise. NTs were found in all the treated cells (Fig. 5-8). Usually, if structures in the nucleus have a horizontal tubular shape with a length

more than 1 μm, they will be counted as NTs. The number of NTs per cell on average was 4.7 and 2.2 respectively in the laser-treated and control cells (n=80, $p=1.2\times10^{-25}$). The number of NTs here is underestimated because in our study only horizontal NTs were counted (vertical NTs are easily missed during examination since they only appear as a small spot in the x-y cofocal plane). Furthermore, focusing the fs laser beam onto the nucleus or to the cytoplasm near the cell nucleus made no difference in the numbers of NTs suggesting that the trigger was mediated by diffusible molecules across the nucleocytoplasmic interface. The size and length of the NT in the laser treated cells were invariably much larger and longer (7-10 μm in length) when compared with those of the control (<5 μm). Besides, if the exposure time was reduced to a harmless duration of 10 s, in terms of change in the mitochondrial transmembrane potential, the average number of NT per cell was only 2.3 (n=80), a number similar, if not identical, to the control. These observations therefore strongly suggest that NTs are generated and gradually develop during apoptosis after laser illumination for 40 s.

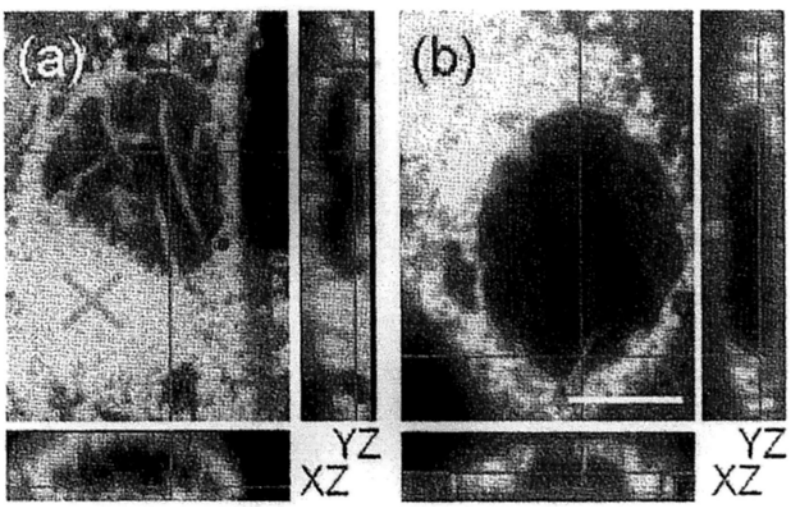

Fig. 5-8. NTs were formed inside the nucleus of HeLa cells 6 hours after laser exposure. HeLa cells with (**a**) or without (**b**) fs laser illumination) at the site X for 40 s were labeled with DiOC6(3) (final concentration: 100 nM) 6 h after illumination and optical sections were obtained by confocal microscopy. Bar: 10 μm. X: laser focal point.

By controlling the laser exposure duration, cells could be induced to undergo apoptosis in an efficient and rapid manner. As shown in Fig. 5-9, a cell was selectively illuminated with the fs laser for 80 s and the development of NTs was recorded by confocal microscopy for 80 min. As can be seen, the target NT was small originally and it grew larger and wider in a time-dependent manner. Interestingly, two neighboring NTs merged together to form a large NT. The connection between the second NT and the NE did not show in the photos since it is out of the plane. These results indicate that NTs could be formed within one hour after long fs laser illumination. A second finding worth to note is that the NT might be large enough to allow cytoplasm and organelles to migrate into the core region of cell nucleus.

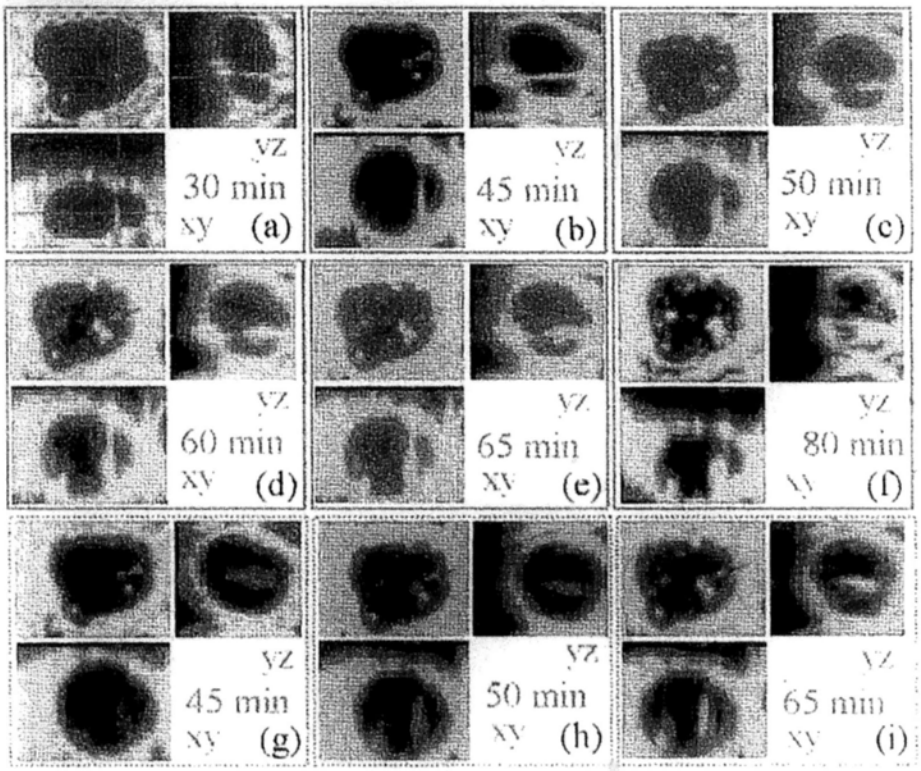

Fig. 5-9. Spatial and temporal development of NT after fs laser illumination. Cells were treated as mentioned in Fig.1 except that the illumination time was 80 s. **(a)** The original NT was small (30 min after laser illumination). **(b)** The original NT became larger and a neighboring NT appeared (red arrow) (time: 45 min). **(c-d)** The original and the neighboring tubule developed into larger NTs (time: 50 and 60 min). **(e-f)** These two NTs merged together to form a large new NT (time: 65 and 80 min). **(g-i)** The neighboring NT (the second NT) developed very quickly (time: 45, 50, and 65 min). Bar: 10 μm. X: laser focal point. Red arrow: the neighboring NT.

To explore this possibility, we labeled cells first with JC-1 for mitochondria [32] and then with DiOC6(3) for internal membrane labelling after laser treatment. By comparing the corresponding JC-1 and DiOC6(3) confocal sections, we noticed that mitochondria not only appeared in the nucleus but were also found inside the NT

(Fig. 5-10 (a) and (b)). To prove this notion, we further examined whether cytoskeleton tubulin was located in the NTs since tubulin is a running track for mitochondria to move around in the cytoplasm [33]. As shown in Fig. 5-10 (c) and (d), fluorescence of tubulin tracker green (Invitrogen) was found inside the NT of a fs laser-illuminated cell, indicating that tubulin also went into NTs. On the contrary, we could not find such phenomenon in the control cells (data not shown). Hence these results provide evidence that mitochondria had access to move into the NTs during apoptosis. The existence of tubulin inside NTs is also an evidence that the NT was formed by the double-membrane invagination of the NE.

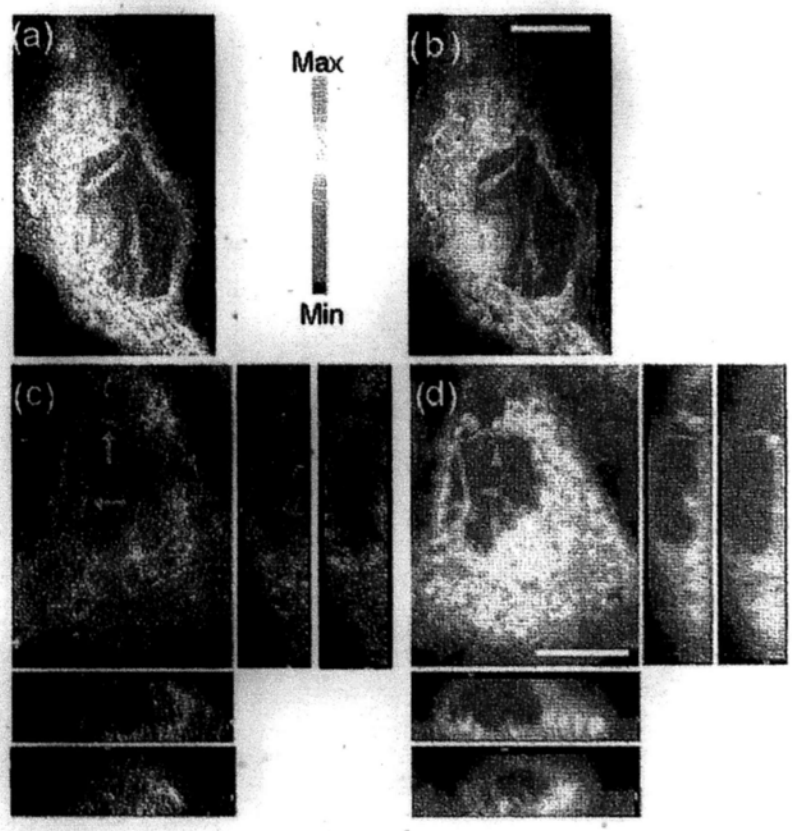

Fig. 5-10. Mitochondria were found inside the NTs after laser treatment. (a) HeLa cells treated with laser for 40 s were labeled with JC-1 (final concentration: 1 μg/ml) for 30 min. (b) DiOC6(3) (final concentration 100 nM) signals of the corresponding NT at the same position.

Arrow: a mitochondrion inside a NT. Bar: 10 μm. X: laser focal point. (c) Tubulin was found inside the NTs after laser treatment. HeLa cells treated with laser for 40 s were labeled by tubulin tracker green (final concentration: 200 nM) for 30 min. Arrow: tubulin inside the NTs. (d) DiOC6(3) (final concentration 100 nM) signals of the corresponding NT at the same position (Arrowhead). Bar: 10 μm. X: laser focal point. Color palette represents the tubulin tracker green fluorescence intensity.

Mechanism of the development of NTs remains unclear. Results from our previous study indicate that NT formation always occurs after an upsurge of cellular Ca^{2+} concentration, which has also long been recognized as a stimulus in apoptotic pathways [34]. The fs pulses can interact with cells by introducing photoporation and free electron inducing through the nonlinear effect, in which multi photons pump an electron from the valence band to be free, a kind of multiphoton ionization. Aided with the fs beam, it can be hypothesized that there are several possible processes inside the cells exposed to the fs laser: i) the fs beam discharges the Ca^{2+} from intracellular Ca^{2+} stores by multiphoton ionization [35]; ii) Ca^{2+} released from the stores and triggers more Ca^{2+} release [36]; iii) Cell membrane was opened by the fs laser photoporation effect causing extra Ca^{2+} in the buffer influx into cells [37]; iv) mitochondria uptake Ca^{2+} [38]; v) the fs beam depolarizes the mitochondria membrane by multiphoton ionization or induces mitochondria directly by heat; vi) too much Ca^{2+} uptaking causes mitochondrial permeability transition dysfunction; vii) molecules inside mitochondria, including ROS, Ca^{2+}, and AIF, thus diffuse out freely, and the ROS and Ca^{2+} then induce dysfunction of more

mitochondria; viii) NE form NTs under the stimulus of Ca^{2+} and other molecules such as ROS; ix) mitochondria migrate into nucleus along NTs to release AIF to form DNA fragmentations; and Ca^{2+} to stop the gene transcription, development, and cell growth [39]. Those processes work simultaneously or subsequently to trigger the programmed death. And it could be explained why in the short exposure (10 s) treatment case, the average number of NTs was only 2.3 per cell. Since in this exposure, mitochondria were not influenced a lot, even though there was a rise of Ca^{2+}, those free Ca^{2+} would be uptaken by mitochondria very quickly and the cells would not probably go to the programmed death, and NTs would not develop.

It has been proposed NTs are complex reticular network that works as a Ca^{2+} storage organelle inside nucleus [40], but here according to our results, Ca^{2+} diffuse into the nucleus along the NTs, and NTs should not be the storage of Ca^{2+} since mitochondria could migrate inside NTs to uptake Ca^{2+}. as shown in Fig. 5-11 and 5-12. We first exposed cells to the laser for 40 s to induce NT formation (there would be a rise of Ca^{2+} at the same time, as shown in Fig. 5-11(a)). Six hours later, the cells were loaded with Fluo-4/AM (10 μM) to measure the changes in the intracellular Ca^{2+} level under the second time laser exposure (10 s) to trigger the Ca^{2+} rise. A high concentration of Ca^{2+} was found inside the NTs and the free Ca^{2+} ions diffused rapidly into the nucleus along the NT (Fig. 5-11(b) and (c)). Also, it can be explained why focusing the fs laser beam onto the nucleus or cytoplasm made no difference in the numbers of NTs formation as Ca^{2+} ions are diffusible entities across the NE.

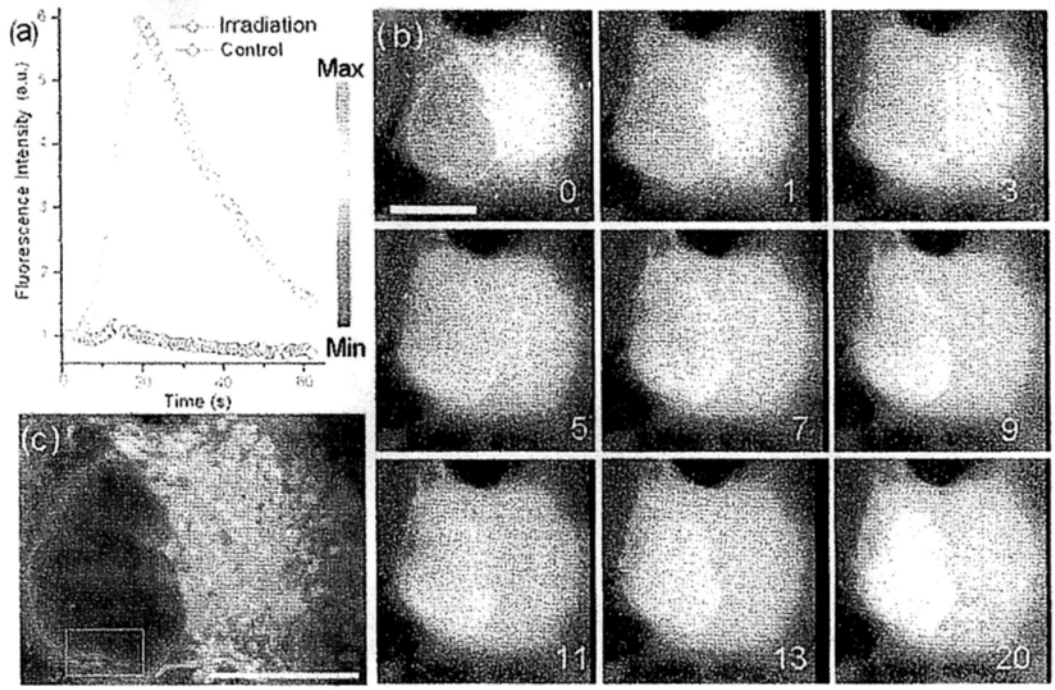

Fig. 5-11. Intracellular Ca^{2+} level increased inside the cell after laser illumination. (a) Ca^{2+} was determined by Fluo-4/AM and the cell was exposed for 10 s. There is an increase of Ca^{2+} in the cell. (b) Fast confocal scanning of the cell plane along time (time unit: s). Red box: strong Fluo-4 fluorescence was found along the NT after the laser treatment, and diffused to surroundings. (c) The corresponding NT labeled by DiOC(6) at the same position (Red box). Bar: 10 μm.

Meanwhile, we found during the diffusion of Ca^{2+} triggered by laser, the fluorescence of Fluo-4 along the NT, corresponding to concentration of Ca^{2+}, was weaker than surroundings. It is very possible that there were mitochondria uptaking Ca^{2+} in NTs. To make the contrast higher, we firstly labeled mitochondria by JC-1 and Ca^{2+} by Fluo-4/AM in the treated cells with NTs, and then added ionomycin to the solution to let huge extracellular Ca^{2+} from outside into cells. By confocal scanning, mitochondria labeled by JC-1 were found inside NTs in the scanning

period, as shown in Fig. 5-12. It is clear the Ca^{2+} concentration along the NT is lower than the surroundings after the trigger. In our experiments, this phenomenon occurs only when there are mitochondria inside NTs. However, since the Ca^{2+} influx stimulated by ionomycin was very large and fast, the diffusion path of Ca^{2+} could not be seen clearly but like a sudden increase.

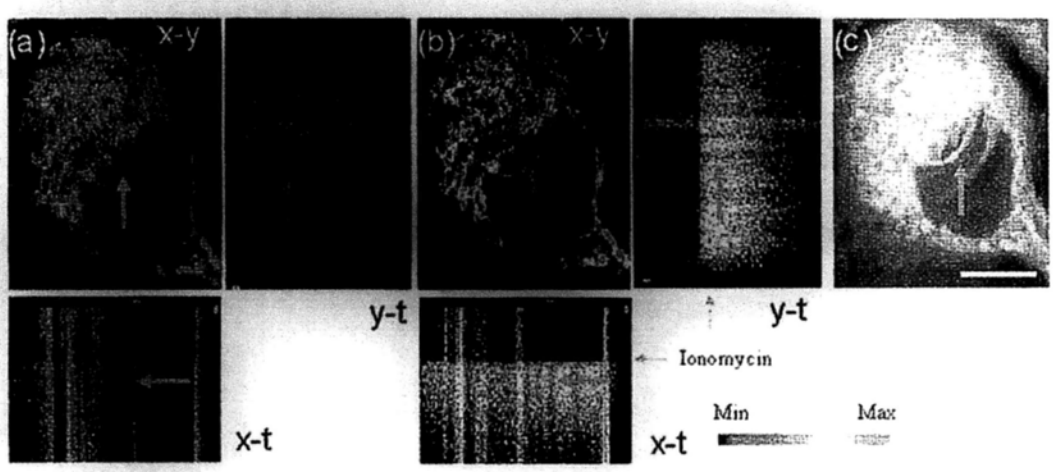

Fig. 5-12. Ca^{2+} change if mitochondria migrated into NT. (a) Mitochondria labeled by JC-1 inside the NT along time (100 s). (b) Ca^{2+} inside the cell, triggered by ionomycin along time (100 s). It can be found after the trigger, Ca^{2+} rise quickly and dramatically, and the area along the NT has a lower Ca^{2+} concentration than its surroundings. (c) The corresponding NT labeled by DiOC(6). Bar: 10 μm.

Confocal microscopic scanning was performed with a 510 nm long pass filter when observing JC-1, Tubulin Tracker Green, Fluo-4/AM, and TUNEL assay. JC-1 (final concentration: 1 μg/ml), Tubulin Tracker Green (final concentration: 200 nM), and Fluo-4/AM (final concentration: 10 μM) were incubated with cells for one hour at 37℃ and 5% CO_2. Before observation, cells were washed two times by PBS. After scanning, the voltage of the PMT was turned down until no fluorescence signal was

obtained. Then DiOC6(3) (final concentration 100 nM) was added and 5 minutes later confocal scanning was performed again to get the imaging of NTs.

Ionomycin stimuli: ionomycin was added into cell solution directly to reach a final concentration of 2 μM in the presence of extracellular Ca^{2+}, and the ionophore caused an increase inside cells due to Ca^{2+} influx. Free Ca^{2+} in the media (concentration: 1-2 mM) diffuse into cells (Ca^{2+} concentration: 1-100 nM) very fast.

Mitochondria have long been reported to play a key role in cell death by releasing apoptosis-inducing factor (AIF) for caspase-independent DNA fragmentation. In fact, results from previous studies indicate that the fs laser exposure can induce some other important apoptotic events related to mitochondrial membrane permeabilization, such as mitochondrial depolarization and reactive oxygen species (ROS) production. The subsequent outcome is that mitochondrial proteins such as AIF can diffuse out of mitochondria. If mitochondria are found in NTs, it is very likely that the NTs are tunnels to transport death executors into the nucleus. Further evidence to support this notion was obtained by TUNEL assay, a common method to detect apoptotic DNA fragmentation by labeling the 3'-hydroxyl DNA ends generated during apoptosis with fluorescein-labeled nucleotides and terminal deoxyribonucleotidyl transferase. As shown in Fig. 5-13, strong TUNEL signals appeared along the NT, suggesting that more DNA fragmentation occurred around the NT six hours after exposure to the fs laser for 40 s. Again, no such phenomenon was found in the control cells. This observation suggests that mitochondria migrate into the NTs to speed up DNA fragmentation.

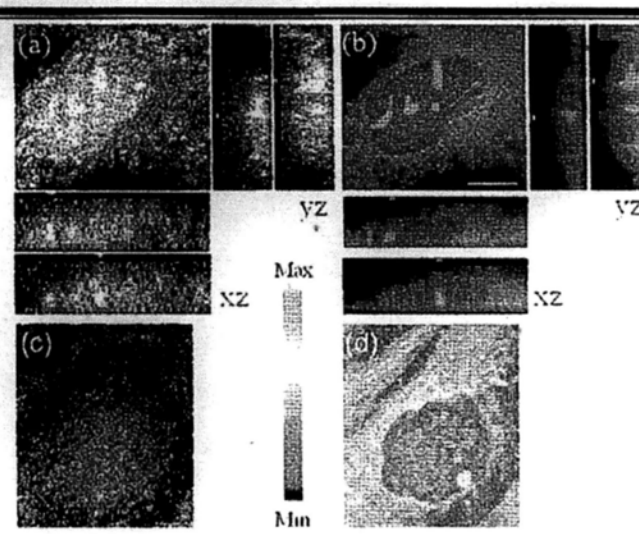

Fig. 5-13. DNA fragmentations appeared around the NTs of the laser-treated HeLa cells. (a) HeLa cells were treated for 40s and confocal microscopy was done 6 hours later. TUNEL signals were very strong along NTs of the treated cell. (b) DiOC6(3) signals of the NT. (c and d) The TUNEL assay and DIOC(6) signals of the control cell. Bar: 10 μm. X: laser focal point. Color palette represents the TUNEL signal intensity.

In conclusion, we report here for the first time that NTs were developed in HeLa cells after an exposure to a fs laser at 1554 nm for 40 s. The spatial and temporal development of NTs was successfully recorded, and fusion of two NTs was observed in one sample. Mitochondria and tubulin were found inside the NT. Besides, more DNA fragmentation was produced along the NTs. Also, it is highly possible that the laser effect on the NT formation is mediated by the change in Ca^{2+} level, and the NT works for the mitochondria migration and Ca^{2+} diffusion. Collectively, our findings provide new information to the research field of apoptosis in terms of the change in cell structure and a new precise tool to trigger cell death at subcellular level with a direct and precise optical system.

5.4 The source of Ca^{2+} released by the fs laser

Calcium (Ca^{2+}) is a very important messenger in all cells and tissues, relaying information within cells to regulate their activity [41], especially related with apoptosis signaling [42]. In cytosol and nucleus, and different organelles, calcium plays very different roles [43]. For example, the endoplasmic reticulum (ER) has been well known as the principal intracellular calcium store [44], and mitochondria can work as a modulator of calcium, which can both release and uptake free calcium [45]. Free calcium in the nucleus has very important effects on gene transcription and cell growth. It has been reported that calcium can be released from the nuclear envelope directly into the nucleoplasm [46], and calcium can diffuses into the nucleus from the cytosol through nuclear pores [47] or nuclear tubular structure. However, in any of such mechanisms, the stores of calcium are still unknown. Several possible Ca^{2+} stores have been proposed [48], but in traditional methods, Ca^{2+} stimuli mostly by chemicals such as InsP3 , is a kind of global effect and thus can not identify Ca^{2+} store in a subcellular level and get the pathway of how Ca^{2+} diffuse into nucleus. With the progresses of lasers, femtosecond (fs) laser pulses have been proved to be a powerful and precise tool on biological problems, and previous works have been performed successfully as a non-invasive and controllable Ca^{2+} stimulation in both space and time [49]. Based on these, we used a fiber fs laser to trigger Ca^{2+} release precisely in a subcellular region, localized the Ca^{2+} stores, and presented Ca^{2+} diffusion pathways in HeLa cells. Our results suggested that intracellular Ca^{2+} was stored mostly in cytoplasm, which could later

diffuse into the nucleus after being triggered by the fs laser pulses.

Femtosecond (fs) laser has been firstly used as a Ca^{2+} trigger in 2001 [50]. It was found that if the fs beam was finely focused inside cells, it could induce Ca^{2+} wave in a cell by directly activating both the intracellular store and the stretch-activated channel or other channels by light-induced pressure on the membrane or by shock waves generated from the focal spot to induce extracellualr Ca^{2+} influx [51]. These mechanisms were further verified by the subsequent work in 2009 [49]. However, these works only simply triggered the Ca2+ rise, with the loss of further analysis on Ca^{2+} regulation mechanisms.

In this study, HeLa cells obtained from American Type Culture Collection were cultured in RPMI 1640 medium (Sigma) supplemented with 10% (v/v) fetal calf serum (FCS) (Gibco) at 37℃ and 5% CO_2. For microscopic studies, cells (3×10^5/ml) were seeded on a 35 mm petri dish with a glass slide (0.17 mm thick). For Ca^{2+} study, cells were stained with Fluo-4/AM (Invitrogen, final concentration: 10 μM) for 40 minutes, and washed two times by PBS. The fluorescence was excited by a laser at 488 nm. The central wavelength of the fs laser was 1554 nm, and the average power was about 100 mW, with a pulse width of 170 fs and a repetition rate of 20 MHz. The fs laser was coupled into the microscope by a fiber collimator and a dichroic mirror, and then focused by a 40X objective (N.A.=1.0). The diameter of the focus was around 2 μm, and the focal plane was controlled by the confocal scanning. Total optical design is shown as in Fig. 5-14 (a).

Cells were firstly exposed at cytoplasm and nucleus respectively for 1 s to observe the diffusion of Ca^{2+} into the nucleus, as shown in Fig. 5-14 (b) and (c). The fs laser illumination in cytosol elicited a slow release of Ca^{2+} in the cytosol, and then spread into the cell nucleus. The initial Ca^{2+} release can trigger more Ca^{2+} release from the store, forming loop amplification [52] or Ca^{2+} induced Ca^{2+} release (CICR) [53], and our observed results consist with this. Since the spreading of Ca^{2+} is a result of diffusion along a concentration gradient, the Ca^{2+} concentration inside the nucleus should be less than that of the cytosol. In the experiment the fluo-4 fluorescence in the nuclear region was stronger, and this is because Fluo-4 excited at 488 nm laser gives a stronger fluorescence in cell nucleus [54]. Subsequently, the fs laser beam was applied to the cell nucleus. Similar to Fig. 5-14(a), the fs laser triggered a slow release of Ca^{2+} in the nucleus and the Ca^{2+} diffused out into the cytosol. And when nucleus and nuclear membrane was exposed, the Ca^{2+} would expand from the focus spot. At last, Ca^{2+} store in cytoplasm could be also influenced and released. Thus Ca^{2+} is stored in both cytosol and nucleus, and can influence each other.

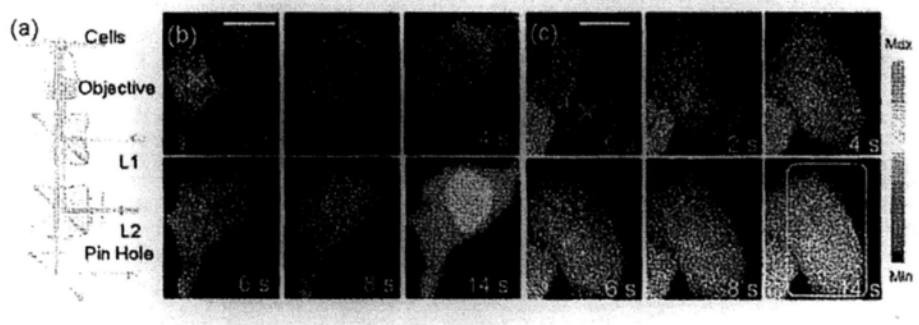

Fig. 5-14. Ca^{2+} diffusion induced by fs pulses at different sites of cells. (a) Optical path of

the experiment. L1: the fs laser at 1554 nm. L2: the laser at 488 nm for fluorescence excitation. Ca^{2+} was released after the 1 s exposure (b) on cytoplasm and (c) on nucleus. In (c), another cell in the left-down part of the figure was neighboring with the targeted cell. Red cross: exposure spot. Bar: 10 μm.

Cells were then incubated in Ca^{2+}-free HEPES buffer (concentration in mM: 1 EGTA, 140 NaCl, 5 KCl, 1 $MgCl_2$, 10 glucose, 10 Na^+-N-2-hydroxyethylpiperazine-N'-2-ethanesulphonic acid (HEPES), final pH 7.2), which contains no extra Ca^{2+} in the media. After experiment, cell media was replaced by PBS and ionomycin (2 μM) was added to work as free ion channels in the cell membrane to get the maximum fluorescence intensity of Ca^{2+} (Fmax) for normalization. As shown in Fig. 5-15 (a), cells were firstly exposed by the fs beam at cytosol for 1 s to form a slow release of Ca^{2+} followed by its decrease in duration of around 15 s. One minute rest later, that cell was exposed at nucleus. A slow Ca^{2+} level rise was again observed but the amplitude was much smaller. The calculated fluorescence value (Cell 1) was shown in Fig. 5-15 (c). To prevent that that the second peak in the nucleus is due to the depletion of Ca^{2+} store or fluorescence bleaching after the 1st laser exposure, the fs laser beam expose first to the cell nucleus and then cytosol (Cell 2), as shown in Fig. 5-15 (b). Even though it was the second exposure, the Ca^{2+} rise illuminated at cytosol was still much stronger than at nucleus. Since during this experiment there was no extra Ca^{2+}, it can be concluded that the release of Ca^{2+} in cytosol by fs beam is more than in nucleus. And it can be

suspected that the Ca^{2+} store in cytoplasm is more than in nucleus.

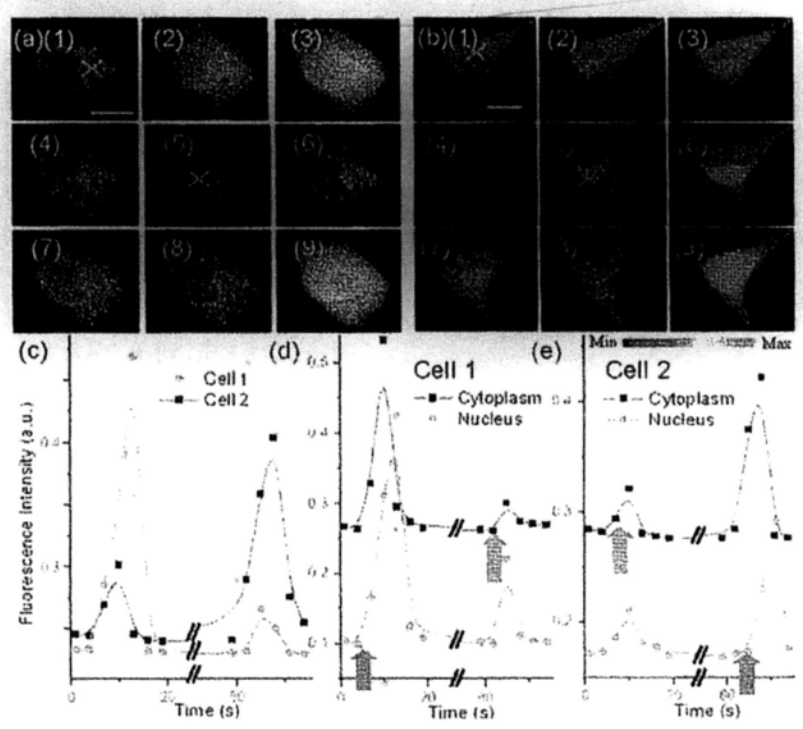

Fig. 5-15. Typical Ca^{2+} fluorescence change of cells after exposure by the fs beam for 1 s at 100 mW in Ca^{2+}-free buffer. (a) Cells were exposed on cytosol first and then on nucleus (cell 1 in (c)). (b) Cells were exposed on cytoplasm first and then on nucleus (cell 2 in (c)). Sections (1-8) were taken at 0, 5, 10, 20, 80, 83, 85, 95 s respectively. Section (9) was the maximum fluorescence by ionomycin treatment. Red cross: fs laser focusing spot. Bar: 10 μm. Calculated fluorescence intensity change of (c) the whole cell, (d) cytosol and nucleus respectively of Cell 1 and (e) Cell 2. Blue arrow: exposure on nucleus. Purple arrow: exposure on cytoplasm.

Fluorescence in nucleus and cytosol was calculated respectively as shown in Fig 5-15 (d) and (e). It can be found the Ca^{2+} level in cytosol was always much higher than in nucleus. It should be noted that when the cytosol was exposed, there

was a delay (2~3 s) between the two Ca^{2+} peaks at cytosol and nucleus. This is due to the diffusion speed of Ca^{2+} from cytosol to nucleus. However, this delay did not show clearly when exposure at nucleus. Possibly it is because the Ca^{2+} diffusion mechanism from cytoplasm to nucleus is quite different with the inverse path, which is modulated by proteins in the nuclear membrane acting as nuclear pore complexes [54].

Next, we tried to explore the role of extracellular Ca^{2+} in the Ca^{2+} response elicited by the fs laser beam by using the Ca^{2+} channel blocker, nifedipine, which can block all the Ca^{2+} channels in the membrane. At first, cells incubated in PBS were exposed under the fs beam for 1 s. According to the mechanism [50], the fs laser could release the intracellular Ca^{2+} store and open the Ca^{2+} channel in cell membrane. Since the Ca^{2+} concentration of PBS is around 2 mM, and inside cells is only 1-100 nM (the high Ca^{2+} concentration in PBS is working for cellular membrane potential), this opening of Ca^{2+} channel would induce an extracellular Ca^{2+} influx into cells. After that, nifedipine was added into the media (100 nM) and incubated for 40 min. The cell was then exposed again but this time the extracellular Ca^{2+} could not diffuse into cells. In the control, cells were exposed twice in PBS without any treatment as a reference.

As shown in Fig. 5-16 (a), with the calculated fluorescence intensity in Fig. 5-16 (c) (the whole cell) and Fig. 5-16 (e) (nuclear and cytosol), the exposure site was cytosol. In the first exposure, the $[Ca^{2+}]$ rise is very similar with the control.

But after the nifedipine treatment, it can be found that the second peak is lower than the control. And that difference (around 0.05-fold of Fmax) responds to the extracellular Ca^{2+}. It is interesting that the duration of the Ca^{2+} peak of the whole cell is around 50 s, much longer than in the Ca^{2+}-free media. Besides, in the Fig. 5-16 (e), the delay between two peaks in cytoplasm and nucleus can be again, around 3 s, and the nucleus showed a faster Ca^{2+} clearing rate than cytoplasm.

Another group of cells were then treated the same way except exposure at nucleus, as shown in Fig. 5-16 (b), (d), and (f). The first peak was still similar to the control, but the second was much lower. That large difference (around 0.2-fold of Fmax) should also responds to the extracellular Ca^{2+}. Compared with the result of exposure on cytosol, it can be expected that the Ca^{2+} store in the nucleus is smaller than that of the cytosol.

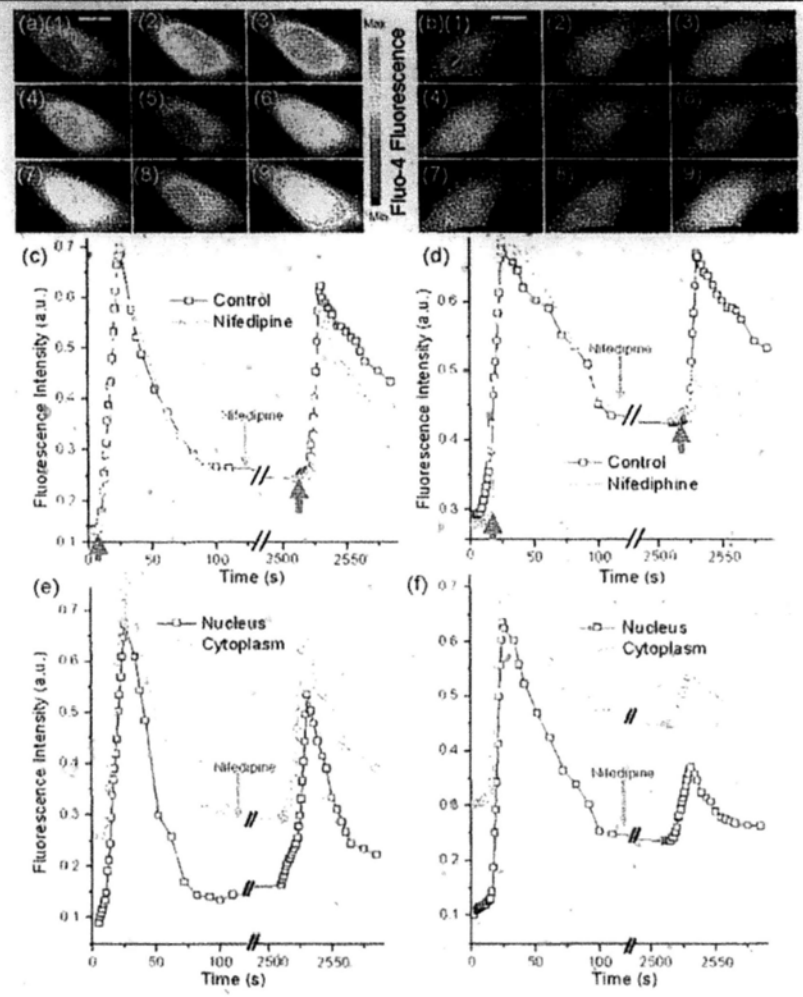

Fig. 5-16. Typical fluorescence of Fluo-4 by confocal scanning with exposure on cytoplasm (a) and on nucleus (b). Sections (1-8) were taken at 0, 15, 30, 45, 2520, 2530, 2540, 2550 s respectively. Section (9) was the maximum fluorescence by ionomycin treatment. Red cross: fs laser focusing spot. Bar: 10 μm. Normalized fluorescence intensity exposed by the fs laser (c) at cytoplasm (n=5) and (d) at nucleus (n=5), and their corresponding fluorescence changes in cytoplasm and nucleus were calculated respectively in (e) and (f). Blue arrow: exposure instant. Orange arrow in (e): peak of the fluorescence.

In conclusion, it was found that the fs beam can induce a slow Ca^{2+} release in

the cell. The extracellular Ca^{2+} plays an important role for the Ca^{2+} rise, especially exposure on nucleus (volume: ~ 0.2–fold of Fmax). The Ca^{2+} store in the nucleus and cytosol are separated or regulated separately, and Ca^{2+} stored in cytoplasm is significantly more than in nucleus. The Ca^{2+} diffusion path inside a cell was record, and due to the diffusion speed, there is a delay between the nucleus and the cytosol reach the Ca^{2+} rise peak. In summary, the fs beam provides a clean, non-invasive, controllable, and precise tool to trigger a slow Ca^{2+} release at sub-cellular level, which makes the observation of intracellular Ca^{2+} dynamics very easy and convenient, compared with traditional chemical methods.

5.5 Summary

Apoptosis is one of the most important processes of cellular activities, and the mechanism is an important fundamental biological research field which is very complicated and remains unclear. Traditional biochemical methods of inducing apoptosis bring chemical side effects. However, since those approaches can not target on a special single cell and the cellular death is totally out of control, people hardly know if the cell is dead, the phase of the process and the start point of apoptosis. In this work, we investigated the effects of fs beams on cells and this optical method should be the potential tool for such research.

We examined the effect of femtosecond (fs) and continuous wave (CW) lasers at near-infrared range on the creation of reactive oxygen species in a human liver cancer cell line. By controlling the mitochondria electron transport chain (ETC), it was found that a major part of the oxidative stress was generated by the laser induced thermal effect on the mitochondria while the remaining part was created by direct free electron liberation by the fs pulses, which could be observed after breaking the ETC. The study helps clarify the major effects produced on animal cells when excited by fs lasers.

It was found that nuclear tubules (NTs) would develop inside the nuclei of HeLa cells when they were irradiated by a femtosecond laser at the wavelength of 1554 nm for 40 s or longer. These NTs provided a pathway for the excess calcium generated by the laser to diffuse from the cytoplasm to the nucleus. Concurrently, the NTs served to spread mitochondria deep inside the nucleus so that they could

initiate DNA fragmentations in regions covered by the NTs in the apoptotic cell. The role of NT as the precursor and passage to apoptosis is firmly established.

Calcium is an important messenger in cells, but its store and diffusion at the subcellular level remains unclear. We induced subcellular Ca^{2+} release by femtosecond laser exposure in Ca^{2+}-free media and PBS with Ca^{2+} channels in cell membrane blocked, and observed its propagation by confocal scanning. It was found Ca^{2+} store volume in cytoplasm is significantly more than in nucleus, and Ca^{2+} will diffuse into nucleus after trigger. Ca^{2+} release inside nucleus can also influence Ca^{2+} in cytoplasm.

In summary, fs pulses can be focused in a sub-cellular region to induce apoptosis. The process can be controlled precisely both in spatial and temporal dimension. The speed of the inducing events of cells can be modulated by the laser power and exposure duration. There is no chemical or biological pollution in this method, and the cells will definitely undergo into apoptosis. People can observe the pre-apoptosis phenomenon and monitor the programmed death using this approach.

References

1. SIMONE FULDA, KLAUS-MICHAEL DEBATIN, Apoptosis Signaling in Tumor Therapy, Annals of the New York Academy of Sciences, 1028, 150 - 156. (2006)
2. Karine F. Ferri and Guido Kroemer, Organelle-specific initiation of cell death pathways, Nature Cell Biology 3, 255 - 263 (2001)
3. M. Lam et al., Proc. Natl. Acad. Sci. U.S.A. 91, 6569 (1994).
4. P. Pinton et al., J. Cell Biol. 148, 857 (2000).
5. R. Foyouzi-Youssefi et al., Proc. Natl. Acad. Sci. U.S.A. 97, 5723 (2000).
6. Martinou, J.-C. & Green, D. R. Breaking the mitochondrial barrier. Nature Rev. Mol. Cell Biol. 2, 63–67 (2001).
7. Zamzami, N. & Kroemer, G. Mitochondria in apoptosis. How Pandora's box opens. Nature Rev. Mol. Cell Biol. 2, 67–71 (2001).
8. M.W. Berns, Sci Am. 278, 62 (1998).
9. Vikram Kohli, Abdulhakem Elezzabi, and Jason Acker, Lasers in Surgery and Medicine 37, 227 (2005).
10. U. K. Tirlapur and K. König, Nature 418, 290 (2002); Hao He, Kit-Ying Lee, Yick-Keung Suen, and Kam Tai Chan, Optics Letters 33, 2961 (2008).
11. Hao He, Kam Tai Chan, Siu Kai Kong, and Kit Ying Lee, Appl. Phys. Lett. 93, 163901 (2008).
12. K. König, Histochem Cell Biol. 114, 79 (2000).
13. S. K. Mohanty, A. Rapp, S. Monajembashi, P.K. Gupta, and K.O. Greulich,

Radiat. Res. 157, 378 (2002).

14. U.K. Tirlapur, K. König, C. Peuckert, R. Krieg, and K. Halbhuber, Experimental Cell Research 263, 88 (2001).
15. G. Saretzki, T. Walter, S. Atkinson, J. Passos, B. Bareth, W.N. Keith, R. Stewart, S. Hoare, M. Stojkovic, L. Armstrong, T. Zglinicki, and M. Lako, Stem Cells 26, 455 (2008).
16. M.D. Jacobson, Trends Biochem Sci. 21, 83 (1996).
17. A. Vogel, J. Noack, G. Hüttman, and G. Paltauf, Applied Physics B: Lasers and Optics 81, 1015 (2005).
18. S.T. Smiley, C. Mottola-Hartshorn, M. Lin, A. Chen, T.W. Smith, G.D. Steele, and L.B. Chen, Proceedings of the National Academy of Sciences of the United States of America 88, 3671 (1991).
19. C. Moore and B.C. Pressman, Biochem. Biophys. Res. Comm. 15, 562 (1964).
20. W. Gorczyca, S. Bruno, R.J. Darzynkiewicz, J Gong, and Z. Darzynkiewicz, Int. J. Oncol. 1, 639 (1992).
21. L.V Keldysh, Sov. Phys. JETP 20, 1307 (1965).
22. Green DR and Kroemer G, The pathophysiology of mitochondrial cell death, Science, 305, 626-629 (2004)
23. Karine F. Ferri and Guido Kroemer, Organelle-specific initiation of cell death pathways, Nature Cell Biology 3, 255 - 263 (2001)
24. Zhou, B.-B. S. & Elledge, S. J. The DNA damage response: putting checkpoints in perspective. Nature 408, 433–439 (2000).

25. M. Fricker, M. Hollinshead, N. White, D. Vaux, Interphase nuclei of many mammalian cell types contain deep, dynamic, tubular membrane-bound invaginations of the nuclear envelope, J. Cell Biol. 136 (1997) 531-544.

26. Lui PP. Kong SK, Kwok TT, Lee CY The nucleus of HeLa cell contains tubular structures for Ca2+ signaling. Biochem Biophys Res Commun 247, 88-93 (1998)

27. Lee RK, Lui PP, Ngan EK, Lui JC, Suen YK, Chan F, Kong SK, The nuclear tubular invaginations are dynamic structures inside the nucleus of HeLa cells. Can J Physiol Pharmacol 84, 477-486 (2006)

28. Uday K. Tirlapur, Karsten König, Christiane Peuckert, Reimar Krieg and Karl-J. Halbhuber, "Femtosecond Near-Infrared Laser Pulses Elicit Generation of Reactive Oxygen Species in Mammalian Cells Leading to Apoptosis-like Death," Experimental Cell Research, 263, 88-97 (2001).

29. Negoescu A, Guillermet C, Lorimier P, Brambilla E, Labat-Moleur F. Biomed Pharmacother. 1998;52(6):252-8

30. Hao He, Siu-Kai Kong, Rebecca Kit-Ying Lee, Yick-Keung Suen, and Kam Tai Chan, Targeted photoporation and transfection in human HepG2 cells by a fiber femtosecond laser at 1554 nm, Optics Letters, 33. 2961-2963 (2008)

31. A. Vogel, J. Noack, G. Hüttman, G. Paltauf, "Mechanisms of femtosecond laser nanosurgery of cells and tissues," Applied Physics B: Lasers and Optics, 81, 1015-1047 (2005)

32. Cossarizza A, Baccarani-Contri M, Kalashnikova G, Franceschi C, A new

method for the cytofluorimetric analysis of mitochondrial membrane potential using the J-aggregate forming lipophilic cation 5,5',6,6'-tetrachloro-1,1',3,3'-tetraethylbenzimidazolcarbocyanine iodide (JC-1). Biochem Biophys Res Commun 197, 40-45 (1993)

33. Manon Carr, Nicolas Andr, Gérard Carles, Hélène Borghi, Laetitia Brichese, Claudette Briand, and Diane Braguer, Tubulin Is an Inherent Component of Mitochondrial Membranes That Interacts with the Voltage-dependent Anion Channel, J. Biol. Chem., 277, 33664-33669. (2002)
34. P. Nicotera, S. Orrenius, Cell Calcium 23, 173 (1998).
35. Nicholas I. Smith, et al. Generation of calcium waves in living cells by pulsed-laser-induced photodisruption, Appl. Phys. Lett. 79, 1208 (2001)
36. Luca Scorrano, et al. BAX and BAK Regulation of Endoplasmic Reticulum Ca2+: A Control Point for Apoptosis. Science 300 : 135-139. 2003
37. Shigeki Iwanaga, et al. Location-dependent photogeneration of calcium waves in HeLa cells, Cell Biochemistry and Biophysics, 45, 167-176 2006
38. María Teresa Alonso, et al. Calcium microdomains in mitochondria and nucleus, Cell Calcium, 40, 513-525, 2006
39. MD Bootman, et al., Nuclear calcium signalling, Cellular and Molecular Life Sciences (CMLS), 57, 371-378. 2000
40. Wihelma Echevarr, et al., Regulation of calcium signals in the nucleus by a nucleoplasmic reticulum, Nature Cell Biology, 5, 440-446, 2003
41. Michael J. Berridge, Martin D. Bootman & Peter Lipp, Nature, 395, 645-648.

1998

42. Karine F. Ferri and Guido Kroemer, Nature Cell Biology, 3, E255. (2001)

43. Wihelma Echevarr, et al. Nature Cell Biology, 5, 440. (2003)

44. Berridge, M. J., Lipp, P. & Bootman, M. D., Nature Rev. Mol. Cell Biol. 1, 11–21 (2000)

45. Luca Scorrano et al., Science, 300, 135-139. (2003)

46. Malviya, A. N., Rogue, P. & Vincendon, G., PNAS USA 87, 9270–9274 (1990).

47. Allbritton, N. L., Oancea, E., Kuhn, M. A. & Meyer, T., PNAS USA 91, 12458–12462 (1994).

48. María Teresa Alonso et al., Cell Calcium, 40, 513. (2006)

49. Yuan Zhao, et al., Optics Express, 17, 1291. (2009)

50. Nicholas I. Smith, et al., Appl. Phys. Lett. 79, 1208 (2001)

51. Shigeki Iwanaga, et al., Cell Biochemistry and Biophysics, 45, 167. (2006)

52. M. C. Wei et al., Science 292, 727 (2001).

53. J. W. Deitmer, A. Verkhratsky, and C. Lohr, "Calcium signalling in glial cells," Cell Calcium 24, 405-416 (1998).

54. K.R. Gee et al., Chemical and physiological characterization of fluo-4 Ca(2+)-indicator dyes, Cell Calcium 27 (2) (2000) 97–106.

55. Martin D. Bootman, et al., Journal of Cell Science, 122, 2337. (2009)

Chapter 6: Conclusions and Future Work

6.1 Conclusions

Biophotonics is an exciting and fast-spreading frontier which involves a fusion of advanced photonics and biology, and has been not only developing a lot of novel methodologies for biomedical researches, but also getting more and more significant results as an independent field. In our works, we build up a system coupled with a femtosecond laser based on an inverted microscope. Human cancer cells can be manipulated on this system by that laser and imaged at real time. The ultra-short pulses can be thus focused in a sub-cellular region while its side effects can be confined in a tiny volume with little harm to the cells. In this thesis, we mainly developed novel approaches of most important operations on cells, including transfection, cell-cell fusion, and apoptosis inducing using the fs laser.

Transfection is a process by which membrane-impermeable molecules such as a DNA sequence can be transmitted across the cell membrane and expressed the corresponding protein by the cell. It is a key technique in cell and molecular biology with many important biochemical applications. We selected a fiber fs laser at 1554 nm, an instrument widely used in optical communication research, as the excitation source. Our results demonstrated that the fs laser could perforate cell membrane and the hole would close in sub-second period after the laser exposure. We tested the safe exposure duration by detected if there was any sign of mitochondrial

depolarization at 1.5 hours after photoporation. Furthermore, the laser had successfully transfected HepG2 cells with a plasmid DNA containing the GFP gene, whose fluorescence could be detected 24 hours after exposure, and the efficiency was as high as 77.3%. Proliferation of the transfected cells have been observed 48 hours after the exposure event, and cells of the new generation can still express GFP.

Cell-cell fusion is a powerful tool for the analysis of gene expression, chromosomal mapping, monoclonal antibody production, and cancer immunotherapy. One of the challenges of *in vitro* cell fusion is to improve the fusion efficiency without adding extra chemicals while maintaining the cells alive and healthy. We show here that targeted human cancer cells could be selected by an optical tweezer and fused by a finely focused fs laser beam at 1550 nm with a high fusion efficiency, which confirmed that human cells could be fused exclusively by fs laser pulses, and this is the first time human cells were fused together all-optically. Mixing of cytoplasm in the fused cells was subsequently observed, and cells from different cell lines were also fused. Based on these, we developed the probable mechanism of optical cell-cell fusion.

Failure in the induction of apoptosis or programmed cell death is one of the major contributions to the development of cancer and autoimmune diseases. Here we used a fs laser as a novel method to provide a precise direct apoptosis trigger at the subcellular level to observe dynamic changes at subcellular level during apoptosis. First, we examined the effect of the fs lasers illuminating cells on the

creation of reactive oxygen species, which can trigger programmed cell death. By controlling the mitochondria electron transport chain (ETC), we developed the mechanism of ROS generation by the fs pulses including thermal effect and direct free electron liberation. Second, we induced apoptosis to targeted cells by the fs laser and found the nuclear envelope (NE) forms tubular or tunnel-like structures inside the nucleus. The average number of NTs in each cell with laser treatment is significantly larger than the control. Besides, by the precise temporal apoptosis trigger, the development of a NT was observed and it was found that the NT was eventually merged with another one to form a larger NT. Meanwhile, mitochondria and tubulin were found inside the NT, and the NT formation always occurs after an upsurge of cellular Ca^{2+} concentration. More DNA fragmentation were also found in the region around the NTs. Based on this, we proposed the mechanism and function of NT formation, which suggests that NTs are developed during apoptosis and mitochondria migrate into the nucleus through the NTs to release death signals to trigger DNA fragmentation. Third, since abnormal Ca^{2+} concentration increase in cells was observed during the apoptosis inducing event, we used the fs laser to trigger Ca^{2+} to get the resource of it. Calcium is an important messenger in cells, but its store and diffusion at the subcellular level remains unclear. We induced subcellular Ca^{2+} release by femtosecond laser exposure in Ca^{2+}-free media and PBS with Ca^{2+} channels in cell membrane blocked, and observed its propagation by confocal scanning. It was found Ca^{2+} store volume in cytoplasm is significantly more than in nucleus, and Ca^{2+} will diffuse into nucleus after trigger. Ca^{2+} release

inside nucleus can also influence Ca^{2+} in cytoplasm.

6.2 Future Works

Based on our researches above, we propose to further our methods for cell engineering, described as following:

6.2.1 Microfluidic System for Optical Cell Engineering

Microfluidics is a very important technology for the manipulation of cells on a massive scale. Cytometry as an example of microfluidics is a well developed and high throughout technique based on single cell flow for cell counting, sorting and sensing purposes. However, cytometry can only acquire optical signals from cells working as cell assays and cannot perform any operation to the cells in the flow [1]. On the other hand, it has been explained in above that the fs laser-induced transfection and fusion techniques can operate on cells either individually or in the form of a paired-up dual with high efficiency and precision. The only problem there is the extremely low throughput. It would make a huge impact to the entire field of cell engineering if we can combine microfluidics with fs laser processing together to develop a system that can perform transfection and cell fusion with extremely high throughput.

The last decade has witnessed revolutionary advances in the manipulation of fluids at small scales [2]. Biological samples have been studied extensively in microfluidic devices. For example, *Zhan et al.* applied the traditional electrical method to transfecting cells in a droplet-based microfluidic chip [3]. In their setup, cells were first encapsulated into aqueous droplets in oil and then the cell-containing droplets would flow downstream inside the chip. The droplets

would pass through a place where a pair of surface microelectrodes had been fabricated and the cells inside would be electroporated by the voltage across the electrodes while passing by at a high flow rate. However, both the transfection efficiency and the cell viability were low, at 11% and 10%, respectively.

We propose to design and fabricate two different microfluidic systems for transfection and cell fusion, respectively, for inclusion in an inverted microscope system coupled with the most suitable fs laser. The microscope system is still the same as the one we are using. The experimental scheme for conducting transfection and cell fusion is described in Fig. 6-1.

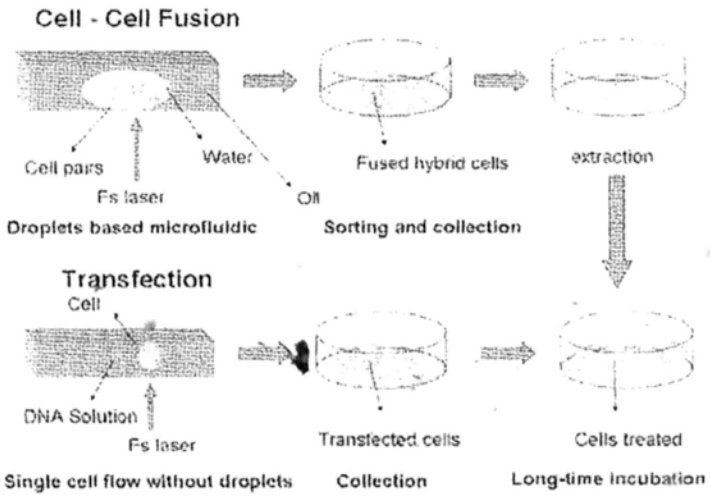

Fig. 6-1. Experimental scheme for cell engineering in a microfluidic system.

Two different types of microfluidic systems will be developed for cell transfection and cell-cell fusion. For cell transfection, three laminar flows will be generated in microfluidic channels as shown in Fig. 6-2a. The only difference between the streams is that the center stream contains cells suspended in an aqueous solution that already has the DNA molecules to be transferred into the cells. This

stream of cell suspension is sandwiched between two buffer streams, and the width of the center stream will be controlled by varying the flow ratios between the three streams [4]. The width of the stream of cell suspension should be controlled to be smaller than twice the cell dimension, so that the cells will flow in a single-lane manner in the center stream. The diffusion of the cells from the center stream to the side stream can be estimated to be $t = x^2/D = (10\ \mu m)^2/10^{-13}\ m^2s^{-1} = 1000$ s. Here x is the half width of the center stream, and D is the diffusion coefficient of E. coli [5], which has a size comparable to that of the cells in our study. As a result, we can safely assume that during the optical transfection procedure, the cells will stay in the center stream. When the cells pass through the focal region of the fs laser at the downstream end of the channel, the cell membrane will be perforated and DNA molecules can enter the cells to achieve transfection. For cell-cell fusion, a droplet-based microfluidic chip will be developed in order to confine two cells tightly together as explained in below. Figure 6-2b shows how aqueous droplets encapsulating single cells are first formed at the junction where the two oil streams pinch off the aqueous flow to generate the droplets. Next, cells to be fused together will be encapsulated in droplets in two parallel microchannels as the one shown in Fig. 3b. The concentration of cells and the flow rate will be controlled so that the droplets in each channel contain either one or no cell. By removing the empty droplets, we can obtain two streams of droplets, each of which contains a single cell [6]. Then the two arrays of droplets merge at a T-junction to form a single array of droplets that contain two cells each by synchronizing the flow of the two arrays of

droplets as shown in Fig. 6-2c [7]. At the downstream end, the fs laser beam will open up the contacting membranes of the cell pair to fuse the two cells together, if the contacting region of the cell pair moves into the focal volume of the laser. An imaging processing software will be developed to control the time gating of laser irradiation.

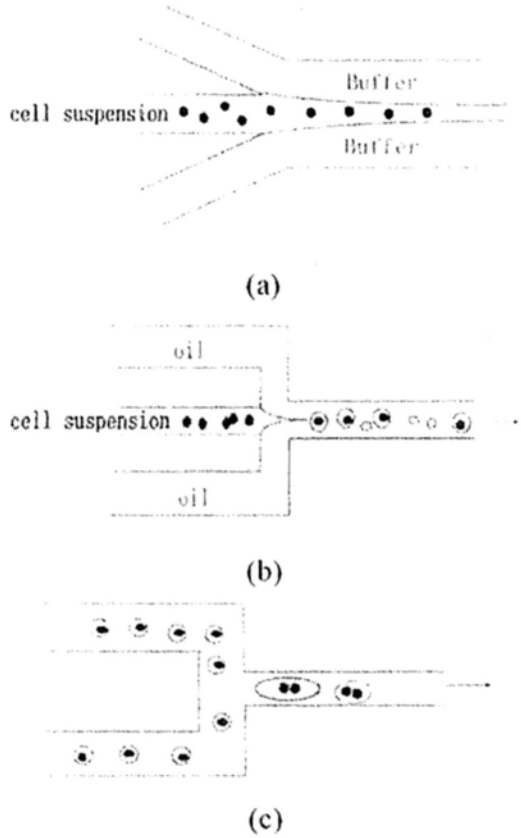

Fig. 6-2. Microfluidic systems for transfection and cell fusion. (a) Three laminar flows will be generated in microfluidic channels for transfection. (b) Cells encapsulated in droplets. (c) Two arrays of droplets merge at a T-junction to form one array of droplets with two cells each for cell-cell fusion.

The cell viability in the system will be tested and the flow velocity will be optimized. The efficiency will be calculated using large sample sizes. After the laser

treatment, cells will be collected and extracted for long-time culture to analyze their proliferation and gene expression.

6.2.2 Transfection and Imaging Aided by Gold Nanorods

Optical transfection by fs laser has shown a lot of advantages and high efficiency. But in such methods, ultra-high photon density for plasma formation is needed, and thus a high N.A. objective and laser power is necessary. The focus size is only around 2 μm and each time only a single cell can be treated. Those critical requirements limit the development and population of the optical transfection method. Hence we propose to use gold nanorods (GNRs) treating with cells to decrease the laser power for transfection, increase the cell number of each exposure time, and maintain other advantages of optical transfection.

C.C. Chen et al. reported their works using fs beam at 800 nm and GNRs for transfection, by connecting DNA molecules with GNRs through the band of -H-S-Au [8]. This band is not easy to break. Thus, after the GNRs diffuse into cells, it needs long time exposure (1 min) of the fs laser to heat the GNRs to make them deform and separate from DNA molecules. The cell viability is then a big problem and the transfection efficiency is quite low, only around 20%. Here we propose to connect the GNRs with DNA molecules simply by electrical charge, and separate them by triggering the surface plasma resonance induced by the fs pulses after the GNRs diffuse into cells with DNA. The electrical connection is very easy to break. And thus the exposure time can be decreased a lot, as short as only some seconds, while the laser power can be only 1 mW for each cell. This enables this optical

transfection method working at high efficiency and low laser power.

Besides, according to the surface enhancement, we also plan to work on the cell membrane imaging and detection aided with GNRs. In our previous works, we found cell membrane has some periodic vibrations [9] (Fig 6-3), and some groups even found this kind of motions at very high frequency band by an AFM [10], as shown in Fig. 6-4.

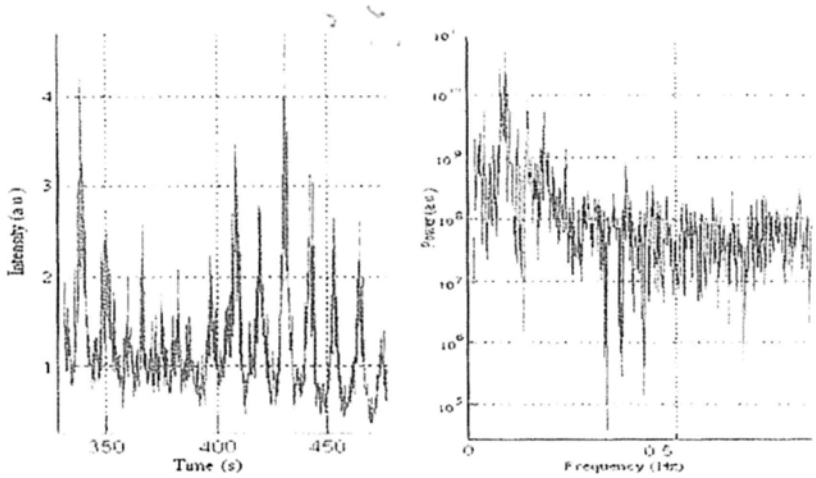

Fig. 6-3 Typical scattering signals of HepG2 cells and the Fast Fourier Transform of the signals.

The advantage of this optical method is the cells are live and health in cell medium. But the fiber collect all the scattering signal from the whole cell and thus the signal can not be localized in a sub-cellular level to get a more precise result..

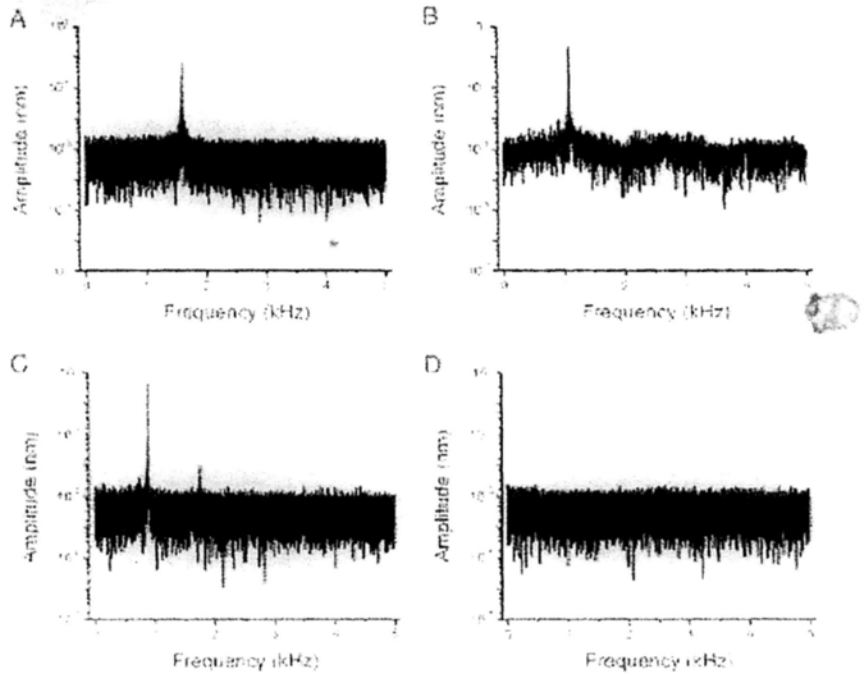

Fig. 6-4. Spectrum of the cellular motion at different temperature. The Fourier transform of the motion at 30°C reveals a prominent peak at 1.634 kHz (A). At 26°C at frequency of 1.092 kHz (B) is observed and at 22°C a frequency of 0.873 kHz (C). Exposure of the cells to sodium azide causes the motion to cease, and only noise is observed (D).

However, in the second work, the yeast cells are put on carbon board, a dry environment. The cellular motion detected is thus influenced by such bad condition a lot. Hence we propose to use the near field microscope for such detection in a liquid environment, where the optical signal will be enhanced by the GNRs. The GNRs attached in cell membrane have been confirmed by TIRF microscopy method (Fig. 6-5) and will be detected by the fiber probe. This can be a live, real time, and quite localized monitor of the motion of cell membrane.

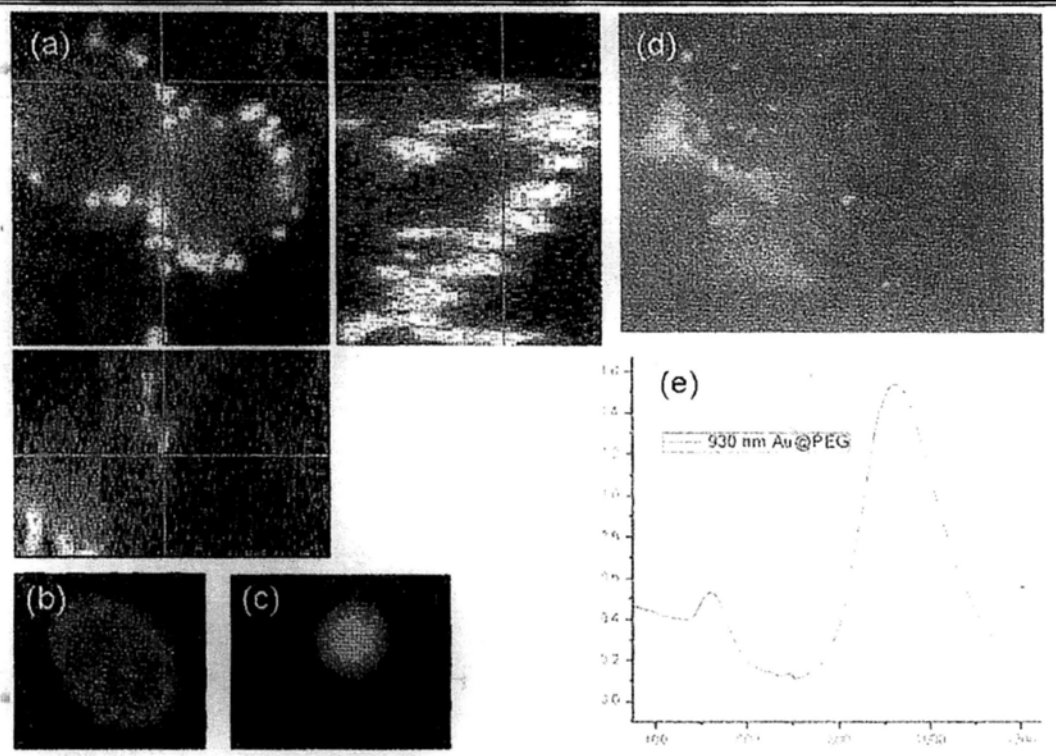

Fig. 6-5. Imaging of GNRs with cells. (a) Confocal scanning of GNRs mixed with propidium iodide attaching in HeLa cell membrane and emitting red fluorescence. (b) Confocal scanning of GNRs attaching with cells directly at 488 nm. (c) Scanning of dry GNRs cluster on a glass slide by white light. (d) Total internal reflection fluorescence microscopy of GNRs in cell membrane (bright spots). (e) The extinction spectrum of pure GNRs. Note the peak is around 930 nm

References

1. H. M. Shapiro, Practical Flow Cytometry, 3rd edition, Wiley-Liss, New York. (1995)
2. G. M. Whitesides, "The origins and the future of microfluidics", Nature London 442, 368 (2006).
3. Yihong Zhan, Jun Wang, Ning Bao, and Chang Lu, "Electroporation of Cells in Microfluidic Droplets", Anal. Chem. 81, 2027–2031 (2009)
4. James B. Knight, Ashvin Vishwanath, James P. Brody, and Robert H. Austin, Hydrodynamic "Focusing on a Silicon Chip: Mixing Nanoliters in Microseconds". Phys. Rev. Lett. 80, 3863 - 3866 (1998)
5. Howard C. Berg, E. Coli In Motion, Springer; 1 edition (Oct 1 2003)
6. Max Chabert and Jean-Louis Viovy. "Microfluidic high-throughput encapsulation and hydrodynamic self-sorting of single cells". PNAS, 105:3191-3196 (2008)
7. Helen Song, Joshua D. Tice, Rustem F. Ismagilov, "A Microfluidic System for Controlling Reaction Networks in Time", Angewandte Chemie International Edition, 42, 768-772 (2003)
8. Chia-Chun Chen, et al., DNA-Gold Nanorod Conjugates for Remote Control of Localized Gene Expression by near Infrared Irradiation, J. AM. CHEM. SOC. 2006, 128, 3709-3715
9. H He, SK Kong, KT Chan, First optical observation of periodic motion of native human cancer cells, CLEO/QELS, 2008

10. Andrew E. Pelling, Sadaf Sehati, Edith B. Gralla, Joan S. Valentine, James K. Gimzewski, "Local Nanomechanical Motion of the Cell Wall of *Saccharomyces cerevisiae*," Science, **305**, 1147-1150 (2004)

Publication List

Journal Paper

1. **Hao He**, S.K. Kong, R.K.Y. Lee, Y.K. Suen, K.T. Chan, "Targeted photoporation and transfection in human HepG2 cells by a fiber femtosecond laser at 1554 nm," **Optics Letters**, vol. 33, page 2961. 2008.
2. **Hao He**, K.T. Chan, S.K. Kong, R.K.Y. Lee, "All-optical human cell fusion by a fiber femtosecond laser," **Applied Physics Letters,** vol. 93, page 163901. 2008.

   (This paper was *highlighted* by "Femtosecond Fusion," **Nature Photonics,** vol. 2, page 709. 2008.)
3. **Hao He**, S. K. Kong, K.T. Chan, "Mechanism of oxidative stress generation in cells by localized near-infrared femtosecond laser excitation," **Applied Physics Letters,** vol. 96, page 173501.2010.

   (This paper was selected for the December 15, 2009 issue of Virtual Journal of Biological Physics Research. (by American Physical Society))
4. **Hao He**, S. K. Kong, K.T. Chan, "Role of nuclear tubule on the apoptosis of HeLa cells induced by femtosecond laser," Accepted by **Applied Physics Letters**. 2010.

   (This paper was selected for the June 15, 2010 issue of Virtual Journal of Biological Physics Research. (by American Physical Society))

5. **Hao He**, S. K. Kong, K.T. Chan, "The source of Ca2+ released by the fs laser," submitted to **Journal of Biomedical Optics**. 2010.

Conferences

1. **H He**, SK Kong, KT Chan, "First optical observation of periodic motion of native human cancer cells," Conference on Lasers and Electro-Optics/Quantum Electronics and Laser Science Conference (CLEO/QELS), Optical Society of America, 2008
2. **H He**, SK Kong, RKY Lee, KT Chan, "Generation of Oxidative Stress in Cells by Localized Laser Radiation," IEEE PhotonicsGlobal@ Singapore, 2008
3. **Hao He**, SK Kong, RKY Lee, KT Chan, "Targeted Transfection in Human HepG2 Cells by Fiber Femtosecond Laser at 1550 nm," The International Conference on Laser Applications in Life Sciences 2008 (LALS 2008), Taipei, Taiwan, 2008.
4. **Hao He**, Siu Kai Kong, Kam Tai Chan, "Location of Subcellular Calcium Store by Femtosecond Laser," Conference on Lasers and Electro-Optics/Quantum Electronics and Laser Science Conference (CLEO/QELS), Optical Society of America, 2010

Appendix: Protocols

Appendix A: Experimental Setup for Transfection and Cell-Cell Fusion

In our setup, the fs laser was coupled to a Nikon TE2000U inverted microscope with a 40X objective lens (N.A.=1.0). The microscope is re-designed to compose with two layers for different laser coupling with dichroic mirrors. The first layer is used for the NIR laser coupling, with a dichroic mirror reflecting NIR beam and transmitting visible light. This mirror was specially designed to get an efficiency of reflecting beams at around 1550 nm more than 85%, while the efficiency of transmitting visible light from 450 nm to 650 nm more than 80%. The second layer is working for the fluorescence excitation. There are several dichroic mirrors for different fluorescence, such as reflecting 488 nm and transmitting 520 nm. Those mirrors are standard fluorescence mirror and should be selected according to the spectrum of different fluorophores. The optical path is shown in Fig. 3-2.

There were 2 lasers in this study. The fs fiber laser had a central wavelength at 1554 nm and a repetition frequency of 20 MHz with a mean power around 100 mW (Calmar, FPL-04). The pulse width was around 170 fs. The diameter of the laser beam focus was around 2um, and thus the peak power was 10^{12} Wcm^{-2} in the focus, which was high enough to perforate the cell membrane. Another laser diode working at 980 nm had a power of 400 mW (Aligent), which was used to trap and

move cells as an optical tweezer. This laser was continuous wave and had no observable influence on the cells. Both lasers are at first collimated by a fiber collimator (Thorlab), and then expended and further collimated by two lenses to couple into the objective. The working distance of the objective is less than 0.22 mm, and thus the bottom of petri dishes we used is 0.17 mm glass slide.

Appendix B: Experimental Setup and Protocols for Apoptosis Inducing and Confocal Scanning

In those experiments with confocal scanning, we used the same setup for the fs laser coupling as in Appendix A. The confocal microscope we used is the Nikon C1 plus, whose body is actually the TE2000U mode. Thus the same double layers design is used in the confocal microscope.

Confocal microscopic scanning was performed with a 510 nm long pass filter when observing JC-1, Tubulin Tracker Green, Fluo-4/AM, and TUNEL assay. JC-1 (final concentration: 1 μg/ml), Tubulin Tracker Green (final concentration: 200 nM), and Fluo-4/AM (final concentration: 10 μM) were mixed with cells for one hour at 37℃ and 5% CO_2. Before observation, cells were washed two times by PBS. After scanning, the voltage of the PMT was turned down until no fluorescence signal was obtained. Then DiOC6(3) (final concentration 100 nM) was added and 5 minutes later confocal scanning was performed again to get the images of NTs. Vertical NTs were also present but they appeared as small dots in the x-y focal plane image and were therefore neglected to avoid error in counting. Hence, the actual number of

NTs generated has been underestimated in our counting method.

Ionomycin stimuli: ionomycin was added into cell solution directly to reach a final concentration of 2 μM in the presence of extracellular Ca^{2+}, and the ionophore caused an increase of Ca^{2+} inside cells due to Ca^{2+} influx. Free Ca^{2+} in the media (concentration: 1-2 mM) diffuses into cells (Ca^{2+} concentration: 1-100 nM) very fast.

Appendix C: Protocols for Optical Transfection

In our experiments, we used the DNA plasmid of GFP for the optical transfection in HeLa and HepG2 cells. The protocol for the transfection is as following:

1. Preparation of cells

Human HepG2 hepatocellular carcinoma cells were cultured in RPMI 1640 medium (Sigma) supplemented with 10% (v/v) fetal calf serum (FCS) (Gibco) or phenol-red free RPMI 1640 medium (Invitrogen) at 37°C and 5% CO_2 for more than 12 hours to attach on the bottom. Cells (3×10^5/ml) were seeded on a 35mm culture dish with a glass slide (0.17mm thick) at the bottom (MatTek).

2. DNA plasmid incubation

The cell medium was at first removed away, and add only 0.5 mL new medium with 20 μg GFP plasmid DNA to get the final concentration of 40 μg/mL. The cells were then incubated for another three hours for the DNA molecules attaching on the membrane of cells.

3. Laser treatment

The cell dish was put on the microscope and only adherent cells on the bottom are randomly selected to be illuminated by the fs laser for 7 s. The focus of the laser should be in the upper-membrane of the exposed cell, which can be adjusted by the lens pair and the objective. The exposure time can be controlled by an electrical or mechanical shutter.

4. Cell incubation

After the laser treatment, 2 mL cell medium was added and cells were incubated for 24 hours at at 37°C and 5% CO_2 for the GFP expression.

Appendix D: Protocols for Cell-Cell Fusion

In the experiment, we used HeLa and HepG2 cells suspension. The protocol for the cell-cell fusion is as following:

1. Preparation of cells

Human HepG2 hepatocellular carcinoma cells were cultured in RPMI 1640 medium (Sigma) supplemented with 10% (v/v) fetal calf serum (FCS) (Gibco) or phenol-red free RPMI 1640 medium (Invitrogen). Cells (3×10^5/ml) were seeded on a 35mm culture dish with a glass slide (0.17mm thick) at the bottom (MatTek) and one dish of cells can be labeled by fluorophores like calcein/AM (Molecular Probes). The cells should be suspended in the medium during this experiment.

2. Cell mixture

The cells with calcein labeled were at first centrifuged and washed two times by PBS and then mixed with the other group without any labeling. The cell mixture can be observed by the fluorescence of calcein.

3. Laser treatment

The cell mixture was then put in the incubator (Nikon) on microscope stage (37°C and 5% CO_2). One cell with calcein labeled was randomly selected and to be trapped by the optical tweezer at 980 nm. It can be moved to contact with another cell without any labeling. After the contacting, the optical tweezer was turned off and the common part of the membrane of the two cells was illuminated by the fs beam for 1-10 s. It should be noted that it would be better if the two cells had similar size and weight, because optical tweezer the fs beam will induce different force to the two cells. If they are quite different, the cell pair will rotate in the vertical direction.

4. Cell incubation

After the laser treatment, the cells were incubated in the incubator for around 4 hours. The cells can be fused together by chance. During this time, the cells would be adherent gradually. It can be observed the diffusion of cytoplasm of the fused cell by the fluorescence of calcein.